TABLE OF CONTENT

Arch Virol (2009) 154:1841–1845
DOI 10.1007/s00705-009-0518-2

BRIEF REPORT

Molecular detection of kobuviruses and recombinant noroviruses in cattle in continental Europe

Axel Mauroy · Alexandra Scipioni · Elisabeth Mathijs · Christine Thys · Etienne Thiry

Received: 7 May 2009 / Accepted: 14 September 2009 / Published online: 9 October 2009

Abstract Two genotypes (Jena and Newbury2) and two intergenotype recombinant strains have been recognized in bovine noroviruses. Several studies have shown an apparent predominance of bovine infection with Newbury2-related (genotype 2) strains. Bovine stool samples were screened with two primer pairs targeting both the polymerase and the capsid genes. Among the predominant genotype 2 sequences, two were genetically related to the recombinant strain Thirsk10. The detection of sequences genetically related to Thirsk10, together with the very low rate of detection of Jena-related sequences, characterized the bovine norovirus population in Belgium, a representative region of continental Europe. Unexpectedly, bovine kobuvirus-related sequences were also amplified, extending their distribution area in Europe.

Noroviruses (NoV) and kobuviruses (KoV), belonging to the family *Caliciviridae*, genus *Norovirus*, and to the family *Picornaviridae*, genus *Kobuvirus*, respectively, both have single-stranded positive-sense RNA genomes, with slight differences in the organization and function of their genes. They both infect the gastrointestinal tract of different animal species including human beings [6, 13, 15, 17]. Two NoV strains and one KoV prototype strains have been already identified in bovine (Bo) species: Jena virus (JV) [1] and Newbury 2 (NB2) [21] for BoNoV; U1 for BoKoV [22]. Five genogroups (G) are described in the genus *Norovirus*, where all BoNoV strains fall into GIII, which is further subdivided into two genotypes. Viruses genetically related to JV and NB2 strains have been assigned to genotype 1 and 2, respectively [8, 12]. Recombination is a common event in NoVs and is usually reported to occur near the overlapping region between open reading frame (ORF) 1 (end of the polymerase gene) and ORF2 (beginning of the single capsid protein gene). Two GIII.1/GIII.2 BoNoV recombinant strains have been described, including the recombinant strain Bo/NoV/Thirsk10/00/UK (Thirsk10), which was identified in the year 2000 in Great Britain [3, 11]. To our knowledge, no other genetically related strains have been reported since.

Bovine KoVs were first identified in cell culture in association with infected cattle serum in Japan [22]. They were detected by RT-PCR in stool samples from healthy calves from Japan [22] and in samples from diarrhoeic calves from Thailand [6], and they were also identified very recently in Europe, namely in Hungary [14].

Bovine NoV prevalence studies performed in different areas have shown the predominance of the GIII.2 genotype [16, 17], but this could reflect a GIII.1 specificity failure in the RT-PCR methods. The aim of this study was to screen cattle stool samples with two primer sets targeting the polymerase and the capsid region. The primer pair targeting the capsid region was designed based on a GIII.1 sequence in order to improve their detection.

A stool bank ($n = 300$) was created with diarrhoeic samples from calves and young stock, received from a Belgian diagnostic laboratory throughout the year 2008. Veterinarians from five provinces in Belgium (Hainaut, Liège, Namur, Luxembourg, and Walloon Brabant)

A. Mauroy · E. Mathijs · C. Thys · E. Thiry (✉)
Laboratory of Virology and Viral Diseases,
Department of Parasitic and Infectious Diseases,
Faculty of Veterinary Medicine, University of Liège,
4000 Liège, Belgium
e-mail: etienne.thiry@ulg.ac.be

A. Scipioni
Federal Agency for Security of the Food Chain,
Bruxelles, 1000 Liége, Belgium

submitted these stool samples to the laboratory for diagnosis of lesions or clinical signs of gastroenteritis. Viral RNA extraction was performed on a 10% w/v stool sample dilution in PBS using a QIAamp kit (Qiagen, Hiden, Germany). One-step RT-PCR was carried out on 2 µl of each viral RNA extraction using a Quick Access kit (Promega, Madison, WI, USA) with CBECu-F/R primers [19] (nucleotide position on JV 4543–4565 and 5051–5074) and a primer pair, named AMG1-F/R, designed from the JV genomic sequence (F—tgtgggaaggtagtcgcgaca, nucleotide position on JV 5012–5032; R—cacatgggggaactgagtggc, 5462–5482). Combined approaches with the CBECu-F and AMG1-R primers, additional internal primers (F2—atgatgccagaggtttcca, position on JV 4727–4745; R2—gcaaaaatccatgggtcaat, 5193–5211) or CBECu-F and a polyTVN-linker were also carried out on some positive samples, attempting to produce longer genomic fragments (including the polymerase and the 5′ part of the capsid gene) in order to detect BoNoV recombinant strains or co-infection. Agarose gel purification was performed on RT-PCR amplicons using a QIAquick purification kit (Qiagen GmbH, Hiden, Germany). RT-PCR products were directly sequenced twice or cloned into pGEMt-Easy plasmid (Promega, Madison, WI, USA) and purified using a Miniprep kit (Invitrogen, Carlsbad, CA, USA) before sequencing. Sequencing of plasmid DNA or RT-PCR products was carried out at the GIGA facilities of the University of Liège using a BigDye terminator kit, version 3.1, and reaction products were resolved using an ABI 3730 automatic capillary sequencer (AppliedBiosystem, Foster City, CA, USA). Nucleotide sequences were analysed using BioEdit Sequence Editor version 7.0 software [2]. Nucleotide similarity with the NCBI genetic database was assessed using the BLAST tool (available at http://www.ncbi.nlm.nih.gov/blast/Blast.cgi). A phylogenetic inference was performed using the MEGA version 4 software package [20] and cross-validated with the Mr Bayes program [5] (available at http://www.phylogeny.fr/). Tree topology was constructed by neighbour-joining analysis with the MEGA4 software (where evolutionary distances were computed using the maximum composite likelihood method with the Tamura and Nei model, confidence values of the internal nodes were calculated by performing 1000 replicate bootstrap values) and checked by Bayesian analysis with the Mr Bayes program (where the 4by4 model was used for substitution and Four Markov Chain Monte Carlo chains were run for 10000 generations, sampled every 10 generations and first 250 sampled trees discarded). Only cloned sequences were submitted to GenBank. Genetic recombination was analysed using a sliding-window genetic diversity plot (Simplot software version 3.5.1 available at http://sray.med.som.jhmi.edu/SCRoftware) and the Recombinant Detection Program (RDP), version 3, available at http://darwin.uvigo.es/rdp/rdp.html) [9].

Twenty-eight positive samples were identified among the 300 samples: 24 and 23 BoNoV sequences with the CBECu and AMG1 primer pairs, respectively, giving a combined apparent molecular prevalence of 9.33% [CI 95% (9.27; 9.38%)]. Using BLAST, three sequences amplified with CBECu-F/R (BV164, BV362, and BV416) were genetically more closely related to the GIII.1 JV and Aba-Z5/02/HUN sequences, and one (BV168) to the recombinant strain Thirsk10. The others were genetically related to GIII.2 BoNoV. All but one of the sequences amplified with AMG1-F/R matched with GIII.2 BoNoV genetically. The AMG1 amplicon of the BV416 sample matched with the recombinant strain Thirsk10. No AMG1 amplicon was obtained for BV362. With the combined primer pair CBECu-F/AMG1-R, no amplicon was obtained for BV164, 168 and 362. However, a 2,410-nucleotide (nt)-long genomic sequence was obtained from BV416 (GenBank accession number FJ946859) with CBECu-F/TVN-linker, which was a recombinant sequence genetically related to the Thirsk10 strain. This result was confirmed by phylogenetic and by Simplot analysis (Figs. 1; 2a). The potential recombination breakpoint of BV416 was located near or within the ORF1/ORF2 overlapping region, depending on the bioinformatic program used (Fig. 2b). Comparison between its different genomic regions and the

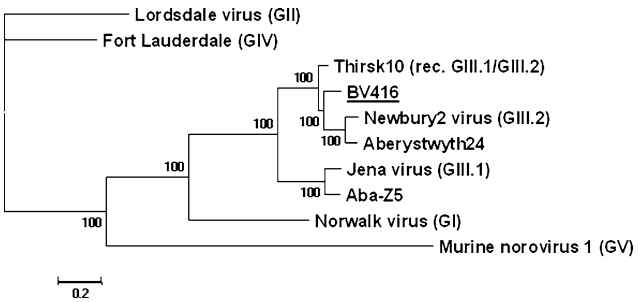

Fig. 1 Phylogenetic tree constructed by Bayesian analysis and based on partial coding region for polymerase, entire capsid protein and small basic protein (2,410 nt) of one of the recombinant bovine norovirus strains identified in this study (*underlined*), bovine norovirus strains, including the reference strains (Jena virus and Newbury Agent 2), and other genogroup representative strains (Norwalk virus, Fort Lauderdale strain and Murine norovirus 1). The tree topology was inferred using the Bayesian method (Mr Bayes program). The *scale bar* represents the phylogenetic distances expressed as units of expected nucleotide substitutions per site. Not all sequences are shown, as not all RT-PCR products were cloned. Accession numbers in GenBank: AF097917 (Bo/NoV/Newbury2/1976/UK); AY126475 (Bo/NoV/Aberystwyth24/2000/UK); AJ011099 (Bo/NoV/Jena/1980/DE); EU360814 (Bo/NoV/Aba-Z5/2002/HUN); AY126468 (Bo/NoV/Thirsk10/2000/UK); M87661 (Hu/NoV/Norwalk 8FIIa/1968/USA); X86557 (Hu/NoV/Lordsdale/1993/UK); AF414426 (Hu/NoV/Fort Lauderdale/560/1998/USA); NC008311 (Mu/NoV/MNV1/2002/USA); FJ946859 (Bo/NoV/BV416/2008/BE)

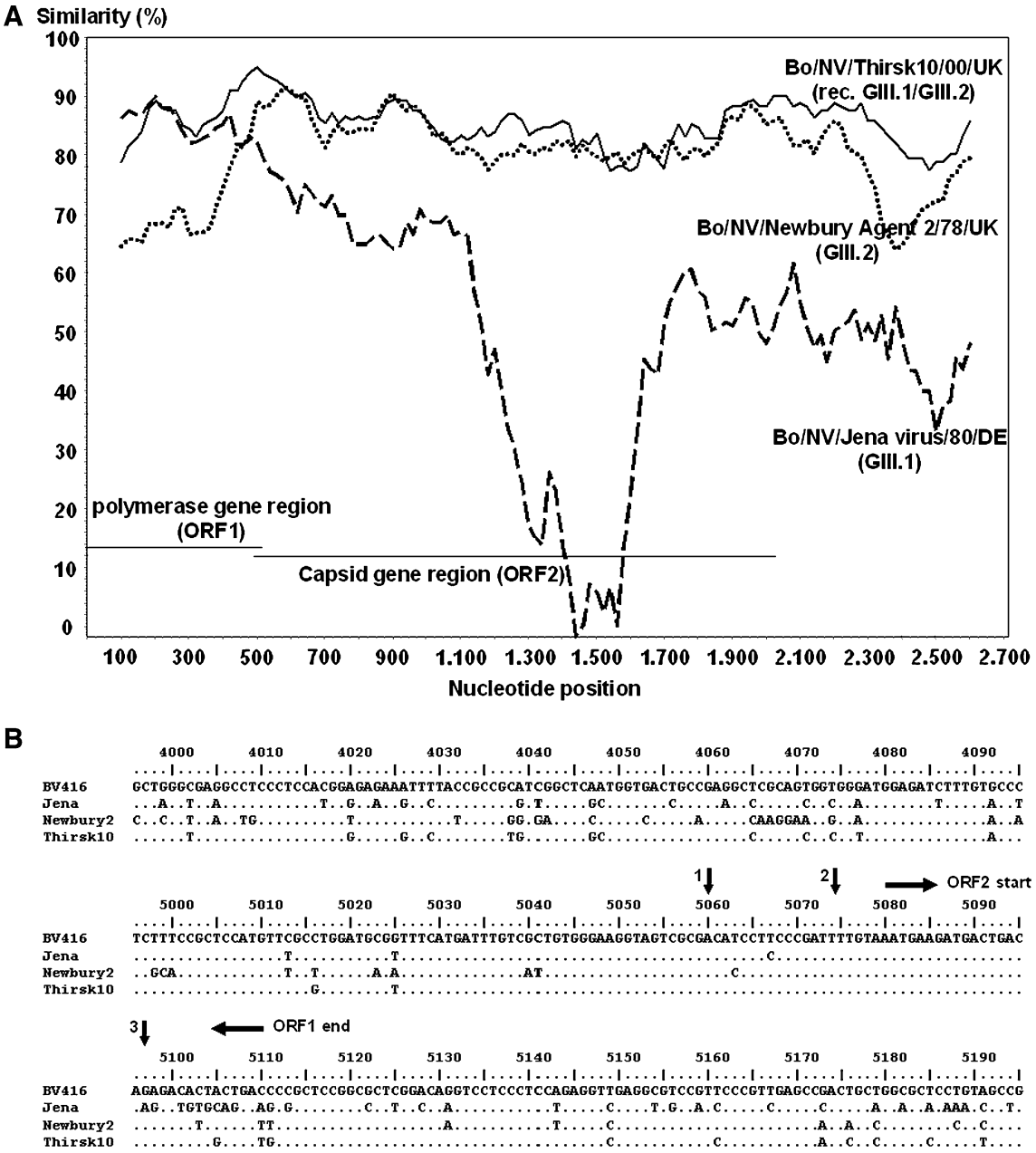

Fig. 2 **a** Nucleotide identity plot of a partial coding region for the RNA-dependent RNA polymerase (3′ end), the entire single capsid protein and the small basic protein of the Bo/NV/BV416/07/BE genome compared with bovine norovirus reference strains Jena and Newbury2 and the recombinant Thirsk10 strain. Nucleotide positions are reported on the *X*-axis and percent similarity on *Y*-axis. **b** Multiple alignment of a 300-nt-long sequence of BV416 in comparison to the corresponding sequences of the Jena (4890–5190 nt), Newbury2 and Thirsk10 genomes and related to the ORF1/ORF2 overlapping region. The *vertical arrows* indicate recombination breakpoints determined by the Bootscan and maximum Chi Square methods (*1*) or by the RDP and Chimaera methods (*2*) in the present study, and by the LARD method (*3*) by Oliver et al. [11]. ORF1 termination codons and ORF2 start codons are shown

JV, Newbury2 and Thirsk10 genomic sequences showed that the polymerase region of BV416 was genetically more closely related to the GIII.1 than to the recombinant strain (Table 1). F2/R2 amplicons from BV164 and BV362 were genetically related to GIII.2 and GIII.1 BoNoV, respectively.

Surprisingly, three amplicons of the expected molecular weight obtained with the combined primer pair CBECu-F/AMG1-R using BoNoV-positive samples did not match genetically with BoNoV but did so with different genomic regions of the BoKoV U1 strain (86, 92 and 93% nucleotide identity by BLAST for BV228, 250 and 253,

Table 1 Nucleotide and amino acid comparison of BV416 with Jena, Newbury2 and Thirsk10 sequences in their three genomic regions

	RdRP gene (ORF1, 3′ end)		Capsid gene (ORF2)		ORF3	
	Nt	AA	Nt	AA	Nt	AA
Jena	88	99	67	69	69	85
Newbury2	77	89	85	95	80	88
Thirsk10	87	96	86	95	86	93

Results are expressed as percent identity

RdRP RNA-dependent RNA polymerase, *ORF* open reading frame, *Nt* nucleotide, *AA* amino acid

respectively, on sequences of about 500–700 nt) [GenBank accession numbers FJ946860 (Bo/KoV/BV228/08/BE); FJ946861 (Bo/KoV/BV250/08/BE), FJ946862 (Bo/KoV/BV253/08/BE)]. Nucleotide identity with the recently characterized porcine KoV strain (S-1-HUN/2007/Hungary) was less important (66, 75 and 73% nucleotide identity by BLAST for BV228, 250 and 253, respectively, on sequences of about 500–700 nt). The BV250 and BV253 amplicons genetically matched with the polymerase region of the U1 strain and BV228 with the VP3-VP1 coding region. The amplification on these genomic sequences was achieved with the sole AMG1-R primer.

Bovine NoV and BoKoV-related sequences were found in stools of calves and young stock suffering from gastroenteritis. The association of these viruses with calf gastroenteritis cases and outbreaks remains to be elucidated because the implication of other aetiological agents cannot be ruled out. However, their detection raises questions about epidemiology, prevalence and the real impact of these newly recognized bovine enteric pathogens. In this study, very few genotype 1 BoNoV were identified (BV362 was the sole GIII.1 sequence obtained in the ORF1/2 overlapping region), confirming results reported in a previous study on BoNoV infection in the same area [10]. Moreover, the detection of genomic sequences with the AMG1 primer pair but not with CBECu one and vice versa highlights the well-known high nucleotide variability in RNA viruses and the difficulty in the development of broad diagnostic methods for these viruses. The recombinant status was clarified for BV416. Co-infection with GIII.1 and GIII.2 BoNoV in the BV164 sample was evident but could not be excluded in the BV168 sample because an overlapping sequence could not be obtained, although genetic analyses related its CBECu-F/R sequence to the Thirsk10 sequence. These results raise issues about genetic characterization using primers targeting either the polymerase region or the capsid region. By exclusion of the potential recombination breakpoint, these primers can lead to the misclassification of strains and to the underestimation of circulation of recombinant strains, as already mentioned by Zheng et al. [23]. To overcome this problem, a primer pair covering both ORF1 and 2 could be used, allowing the detection of recombination events in prevalence/detection studies where genogroup/genotype is specified, but secondary structures located in the ORF1/2 overlapping region [18] might impair the RT-PCR reaction. On the other hand, serological methods were also proposed for the classification of such poorly cultivable viruses following the recent availability of different systems for efficient production of NoV recombinant proteins and virus-like particles. Recombination between the genomic regions coding for the non-structural proteins and the single capsid protein, the latter presumably responsible for all antigenic properties related to neutralization [4], implies that such serological methods could be impaired, allowing a misclassification of strains in the same cluster. In the same way, serological methods could mask a part of the natural evolution of the viral population within the genus *Norovirus*.

Multiple alignment and bioinformatic analysis performed with JV, Aba Z5, NB2, Thirk10 and BV416 sequences has suggested a recombination breakpoint for BV416 located near the ORF1/ORF2 overlapping region and one quite similar to those determined for the Thirsk10 strain [11]. Nevertheless, the greater similarity of BV416 to the Jena and Aba Z5 viruses in the polymerase region and the exact localization of the recombination breakpoint suggest a different origin or genetic evolution than that of the Thirsk10 strain. The identification, in geographically and temporally different samples, of a relatively large proportion of sequences (about 7%, 2 out of the 28 BoNoV-positive samples) that could be genetically related to the recombinant Thirsk10 strain suggests at least that Thirsk10-related strains circulate in the northern European cattle population. Furthermore, the low detection rate of GIII.1 BoNoV could reflect an evolution of the viral population pattern to the benefit of the Thirsk10-related and genotype 2 strains in the studied region. This situation could be compared to the contemporaneous dominance of the GII.4-related strains with regard to other human genogroups and genotypes by emergence of recombinants and antigenic drift in human NoV gastroenteritis outbreaks [7]. Thirsk10 and the genotype 2 strains were shown to share high amino acid identities in their capsid protein sequences. As this is the primary structure involved in receptor binding, it could suggest a better adaptation of such strains to their hosts.

To date, BoKoV-related sequences have very rarely been identified, and in only three countries (namely Japan, Thailand and Hungary) [4, 22]. Their detection in another European country suggests their wider distribution, making them at least emerging bovine viruses in the studied region. BoKoV-related sequences were not systematically found in

all BoNoV-positive samples, but their association with these viruses in stools of calves suffering from enteritis raises interesting questions on the *primum movens* and the diversity of enteric pathogens.

In conclusion, prevalence studies on BoNoV using RT-PCR assays, even targeting relatively well-conserved genomic regions, need to take into account in their protocols both their high genetic variability and their relative genetic proximity to other viruses in order to maximize sensitivity and specificity. This study also showed that recombination events could lead to emerging strains in the BoNoV population, as already found for HuNoV. The molecular detection of bovine kobuvirus-related sequences in the studied area extends the distribution of these viruses in Europe.

Acknowledgments This study was funded by the Federal Public Service of Health, Food Chain Safety and Environment (RF6185), the Belgian policy "Science for a Sustainable Development" (SD/AF/01) and by the Région Wallonne (415701). The authors thank the Association Régionale de Santé et d'Identification Animales (ARSIA) for accessing stool samples and also thank Dominique Ziant for his excellent technical assistance.

References

1. Deng Y, Batten CA, Liu BL, Lambden PR, Elschner M, Gunther H, Otto P, Schnurch P, Eichhorn W, Herbst W, Clarke IN (2003) Studies of epidemiology and seroprevalence of bovine noroviruses in Germany. J Clin Microbiol 41:2300–2305
2. Hall TA (1999) BioEdit: a user-friendly biological sequence alignment editor and analysis program for Windows 95/98/NT. Nucleic Acids Symp Ser 41:95–98
3. Han MG, Smiley JR, Thomas C, Saif LJ (2004) Genetic recombination between two genotypes of genogroup III bovine noroviruses (BoNVs) and capsid sequence diversity among BoNVs and Nebraska-like bovine enteric caliciviruses. J Clin Microbiol 42:5214–5224
4. Hardy ME (2005) Norovirus protein structure and function. FEMS Microbiol Lett 253:1–8
5. Huelsenbeck JP, Ronquist F (2001) MRBAYES: Bayesian inference of phylogenetic trees. Bioinformatics 17:754–755
6. Khamrin P, Maneekarn N, Peerakome S, Okitsu S, Mizuguchi M, Ushijima H (2008) Bovine kobuviruses from cattle with diarrhea. Emerg Infect Dis 14:985–986
7. Lindesmith LC, Donaldson EF, Lobue AD, Cannon JL, Zheng DP, Vinje J, Baric RS (2008) Mechanisms of GII.4 norovirus persistence in human populations. PLoS Med 5:e31
8. Liu BL, Lambden PR, Gunther H, Otto P, Elschner M, Clarke IN (1999) Molecular characterization of a bovine enteric calicivirus: relationship to the Norwalk-like viruses. J Virol 73:819–825
9. Martin DP, Williamson C, Posada D (2005) RDP2: recombination detection and analysis from sequence alignments. Bioinformatics 21:260–262
10. Mauroy A, Scipioni A, Mathijs E, Saegerman C, Mast J, Bridger JC, Ziant D, Thys C, Thiry E (2009) Epidemiological study of bovine norovirus infection by RT-PCR and a VLP-based antibody ELISA. Vet Microbiol 137:243–251
11. Oliver SL, Brown DW, Green J, Bridger JC (2004) A chimeric bovine enteric calicivirus: evidence for genomic recombination in genogroup III of the Norovirus genus of the Caliciviridae. Virology 326:231–239
12. Oliver SL, Asobayire E, Charpilienne A, Cohen J, Bridger JC (2007) Complete genomic characterization and antigenic relatedness of genogroup III, genotype 2 bovine noroviruses. Arch Virol 152:257–272
13. Reuter G, Biro H, Szucs G (2007) Enteric caliciviruses in domestic pigs in Hungary. Arch Virol 152:611–614
14. Reuter G, Egyed L (2009) Bovine kobuviruses in Europe. Emerg Infect Dis 15:822–823
15. Sasaki J, Kusuhara Y, Maeno Y, Kobayashi N, Yamashita T, Sakae K, Takeda N, Taniguchi K (2001) Construction of an infectious cDNA clone of Aichi virus (a new member of the family Picornaviridae) and mutational analysis of a stem-loop structure at the 5′ end of the genome. J Virol 75:8021–8030
16. Scipioni A, Mauroy A, Mathijs E, Ziant D, Daube G, Thiry E (2009) Molecular analysis of contemporaneous human and bovine noroviruses in Belgium (Submitted)
17. Scipioni A, Mauroy A, Vinje J, Thiry E (2008) Animal noroviruses. Vet J 178:32–45
18. Simmonds P, Karakasiliotis I, Bailey D, Chaudhry Y, Evans DJ, Goodfellow IG (2008) Bioinformatic and functional analysis of RNA secondary structure elements among different genera of human and animal caliciviruses. Nucleic Acids Res 36:2530–2546
19. Smiley JR, Hoet AE, Traven M, Tsunemitsu H, Saif LJ (2003) Reverse transcription-PCR assays for detection of bovine enteric caliciviruses (BEC) and analysis of the genetic relationships among BEC and human caliciviruses. J Clin Microbiol 41:3089–3099
20. Tamura K, Dudley J, Nei M, Kumar S (2007) MEGA4: molecular evolutionary genetics analysis (MEGA) software version 4.0. Mol Biol Evol 24:1596–1599
21. Woode GN, Bridger JC (1978) Isolation of small viruses resembling astroviruses and caliciviruses from acute enteritis of calves. J Med Microbiol 11:441–452
22. Yamashita T, Ito M, Kabashima Y, Tsuzuki H, Fujiura A, Sakae K (2003) Isolation and characterization of a new species of kobuvirus associated with cattle. J Gen Virol 84:3069–3077
23. Zheng DP, Ando T, Fankhauser RL, Beard RS, Glass RI, Monroe SS (2006) Norovirus classification and proposed strain nomenclature. Virology 346:312–323

Journal of Virological Methods 161 (2009) 247–253

Contents lists available at ScienceDirect

Journal of Virological Methods

journal homepage: www.elsevier.com/locate/jviromet

Multiplex real-time RT-PCR for simultaneous detection of GI/GII noroviruses and murine norovirus 1

Ambroos Stals[a,*], Leen Baert[b], Nadine Botteldoorn[c], Hadewig Werbrouck[a], Lieve Herman[a], Mieke Uyttendaele[b], Els Van Coillie[a]

[a] Flemish Government, Institute for Agricultural and Fisheries Research (ILVO), Technology and Food Sciences Unit, Brusselsesteenweg 370, 9090 Melle, Oost-Vlaanderen, Belgium
[b] Ghent University, Faculty of Bioscience Engineering, Department of Food Safety and Food Quality, Laboratory of Food Microbiology and Food Preservation. Coupure Links 653, 9000 Ghent, Oost-Vlaanderen Belgium
[c] Belgian Scientific Institute of Public Health, Department of Microbiology, Division of Bacteriology, Juliette Wytsmanstraat 14, 1050 Brussels, Belgium

Article history:
Received 3 February 2009
Received in revised form 14 June 2009
Accepted 21 June 2009
Available online 27 June 2009

Keywords:
Internal amplification control
Norovirus
Murine norovirus 1
Multiplex real-time RT-PCR

A B S T R A C T

A quantitative two-step multiplex real-time reverse transcriptase (RT-) PCR assay for the simultaneous detection of genogroup I (GI) and genogroup II (GII) noroviruses (NoVs) is described below. A murine norovirus 1 (MNV-1) real-time PCR detection assay described recently was integrated successfully into the multiplex assay, making it possible to detect GI and GII NoVs and MNV-1 in one reaction tube with MNV-1 plasmid DNA as real-time PCR internal amplification control (IAC).

The results showed a nearly complete concordance between the multiplex assay and the corresponding single-target PCRs. Analysis of competition between the individual reactions within the multiplex real-time PCR assay showed that GI and GII NoV plasmid DNAs mixed at equimolar concentrations were detected reproducibly and quantitatively, while a 4 log excess between GI and GII plasmid DNAs hindered amplification of the target with the lowest concentration. High concentrations of the real-time PCR IAC (MNV-1 plasmid DNA) also interfered with the possibility of the developed multiplex real-time RT-PCR assay to detect quantitatively and simultaneously the presence of GI and GII NoVs within one sample.

The specificity of the multiplex assay was evaluated by testing a NoV RNA reference panel containing nine GI, eight GII, and one GIV in vitro synthesized RNA fragment, plus 16 clinical samples found positive for GI and GII NoVs previously. In addition, a collection of bovine NoVs and other (non-NoV) enteric viruses were found to be negative, and no cross-amplification between genogroups was observed.

1. Introduction

Noroviruses (NoVs) are recognized as the single most common cause of gastroenteritis in people of all age groups worldwide (Koopmans and Duizer, 2004). NoV infections result frequently from person-to-person transmission in cruise ships (Chimonas et al., 2008; Depoortere and Takkinen, 2006) and hospitals (Gallimore et al., 2008). Other causes of infection are ingestion of contaminated food (De Wit et al., 2007; Gallimore et al., 2005; Johansson et al., 2002) and water (Craun et al., 2005; Schvoerer et al., 1999). The *Norovirus* genus belongs to the *Caliciviridae* family and can be subdivided into five genogroups (GI, GII, GIII, GIV, and GV), of which GI, GII, and GIV NoVs are infectious to humans (Koopmans et al., 2002). However, only a small number of outbreaks due to genogroup IV NoVs have been reported (Fankhauser et al., 2002; Koopmans, 2008). Genogroup III consists of bovine NoVs (van der Poel et al., 2003) and genogroup V contains the MNV-1 murine norovirus 1 (Wobus et al., 2006).

There is no reliable culture method available to detect NoVs (Duizer et al., 2004), although efforts have been made recently (Asanaka et al., 2005; Straub et al., 2007). Currently, (real-time) reverse transcriptase (RT-) PCR is considered to be the gold standard for detection of NoVs in clinical, food and environmental samples (Baert et al., 2007; Jothikumar et al., 2005; Park et al., 2008; Wolf et al., 2007). Recently, several (multiplex) real-time RT-PCR assays for detection of GI and GII NoVs in clinical samples (Pang et al., 2005) and in different food matrices such as shellfish (De Medici et al., 2004; Jothikumar et al., 2005) and raspberries (Le Guyader et al., 2004) have been published. However, only a limited number of (real-time) RT-PCR based norovirus detection assays include a PCR internal amplification control (Dreier et al., 2005; Escobar-Herrera et al., 2006; Rolfe et al., 2007; Scipioni et al., 2008). The use of an appropriate (real-time) PCR internal amplification control (IAC) is an absolute requirement to avoid false-negative results due to malfunction of the thermal cycler, incorrect PCR mixture, poor DNA polymerase activity or, importantly, the presence of

* Corresponding author. Tel.: +32 09 272 30 26; fax: +32 09 272 30 01.
E-mail address: Ambroos.Stals@ilvo.vlaanderen.be (A. Stals).

0166-0934/$ – see front matter © 2009 Elsevier B.V. All rights reserved.
doi:10.1016/j.jviromet.2009.06.019

inhibitory substances in the sample matrix (Hoorfar et al., 2004; Malorny et al., 2003; Niesters, 2002). Only a few assays have been reported where a (real-time) PCR IAC was included in NoV detection assays. These assays used two types of DNA: either DNA originating from NoV surrogates, such as the MS2 bacteriophage (Dreier et al., 2005; Rolfe et al., 2007) and a genetically modified cultivable mengovirus (Comelli et al., 2008), or nucleotide fragments containing NoV-specific primer binding sites (Escobar-Herrera et al., 2006; Scipioni et al., 2008). In this study, the use of MNV-1 plasmid DNA as real-time PCR IAC was based on the ease of cultivation and quantitation of this virus (Wobus et al., 2006), making it also possible to use MNV-1 virus particles as process control when detecting NoVs from clinical, food and environmental samples. In addition, recent studies demonstrated that MNV-1 virus particles behave more like human NoVs than other NoV surrogates, such as MS2 bacteriophage, feline calicivirus and poliovirus (Bae and Schwab, 2008).

This study describes the optimization of a multiplex real-time RT-PCR assay for the detection of human GI and GII NoVs with the successful integration of MNV-1 as real-time PCR IAC. This assay combined available primers and probes for the detection of the majority of the human infective GI and GII NoV strains, designed by the CEN/TC/WG6/TAG4 research group (Loisy et al., 2005; Svraka et al., 2007), and primers and probes for the detection MNV-1 (Baert et al., 2008) in a multiplex real-time RT-PCR assay. MNV-1 plasmid DNA was used as PCR internal amplification control when testing GI and GII NoV positive (clinical) samples.

2. Materials and methods

2.1. Clinical specimens and norovirus reference panel

Five GI and eleven GII NoV samples were obtained from clinical specimens submitted to the Belgian Scientific Institute of Public Health (IPH; Brussels, Belgium) and the Rega Institute for Medical Research (Leuven, Belgium) during a 6-year period (2002–2008).

An RNA NoV reference panel designed by the Dutch National Institute for Public Health and the Environment (RIVM; Bilthoven, the Netherlands) was tested in this study. The reference panel contained in vitro synthesized RNA fragments covering genomic regions A, B and C (Vinje et al., 2004) of nine GI, eight GII and one GIV NoV. In addition, seven RNA preparations from other enteric viruses (rotavirus, astrovirus types 1 and 4, sapovirus, feline calicivirus, canine calicivirus and hepatitis A virus), kindly provided by the RIVM, and cDNA from four bovine GIII NoVs, kindly provided by Liège University (Ulg; Mauroy et al., 2008), were included in this study. An overview of all tested samples/ RNA fragments is shown in Table 1.

Table 1
Overview of all tested samples/RNA fragments.

Virus type/NoV genotype	Sample type	Source	Ct GI	Ct GII	Ct MNV-1
GI.?	Faeces	IPH[a]	38.46	Undet	27.89
GI.1 (Norwalk)	RNA fragment	RIVM[b]	29.01	Undet	Undet
GI.2 (Whiterose)	RNA fragment	RIVM	20.52	Undet	Undet
GI.2	Faeces	REGA[c]	29.79	Undet	27.70
GI.2	Faeces	REGA	28.07	Undet	27.69
GI.2 (Southhampton)	RNA fragment	RIVM	20.83	Undet	Undet
GI.3 (Birmingham)	RNA fragment	RIVM	19.09	Undet	Undet
GI.4 (Malta)	RNA fragment	RIVM	19.33	Undet	Undet
GI.4	VTM[d]	REGA	26.04	Undet	27.56
GI.5 (Musgrove)	RNA fragment	RIVM	39.12	Undet	Undet
GI.6 (Mikkeli)	RNA fragment	RIVM	19.62	Undet	Undet
GI.7 (Winchester)	RNA fragment	RIVM	17.54	Undet	Undet
GI.8	Faeces	REGA	22.76	Undet	27.32
GI.10 (Boxer)	RNA fragment	RIVM	19.34	Undet	Undet
GII.1 (Hawaii)	RNA fragment	RIVM	Undet	19.46	Undet
GII.2 (Melksham)	RNA fragment	RIVM	Undet	18.66	Undet
GII.2	Faeces	REGA	Undet	29.92	27.76
GII.3 (Toronto)	RNA fragment	RIVM	Undet	21.78	Undet
GII.4 (Grimsby)	RNA fragment	RIVM	Undet	18.26	Undet
GII.4	Vomit	REGA	Undet	28.95	27.83
GII.4	Faeces	REGA	Undet	22.90	27.82
GII.4	Faeces	REGA	Undet	21.63	28.78
GII.?	Faeces	IPH	Undet	28.92	27.79
GII.?	Faeces	IPH	Undet	26.30	27.41
GII.?	Faeces	IPH	Undet	33.57	27.89
GII.?	Faeces	IPH	Undet	25.72	27.37
GII.?	Faeces	IPH	Undet	26.28	27.61
GII.?	Faeces	IPH	Undet	27.05	27.58
GII.6 (Seacroft)	RNA fragment	RIVM	Undet	22.07	Undet
GII.7	Faeces	IPH	Undet	21.48	Undet
GII.10 (Erfurt)	RNA fragment	RIVM	Undet	18.49	Undet
GIIb (GGIIb)	RNA fragment	RIVM	Undet	19.05	Undet
GIIc (GGIIc)	RNA fragment	RIVM	Undet	19.21	Undet
GIV (Alphatron)	RNA fragment	RIVM	35.87	Undet	Undet
GIII (Bovine)	Faeces	Ulg[e]	Undet	Undet	Undet
GIII (Bovine)	Faeces	Ulg	Undet	Undet	Undet
GIII (Bovine)	Faeces	Ulg	Undet	Undet	Undet
GIII (Bovine)	Faeces	Ulg	Undet	Undet	Undet
Rotavirus	Faeces	RIVM	Undet	Undet	Undet
Astrovirus type 1	Faeces	RIVM	Undet	Undet	Undet
Astrovirus type 4	Faeces	RIVM	Undet	Undet	Undet
Sapovirus	Faeces	RIVM	Undet	Undet	Undet
Feline calicivirus	Faeces	RIVM	Undet	Undet	Undet
Canine calicivirus	Faeces	RIVM	Undet	Undet	Undet
Hepatitis A virus	Faeces	RIVM	Undet	Undet	Undet

[a] IPH: Belgian Scientific Institute of Public Health.
[b] RIVM: Dutch National Institute for Public Health and the Environment.
[c] REGA: Rega Institute for Medical Research.
[d] VTM: viral transport medium.
[e] Ulg: Liège University.

2.2. Viral RNA extraction

Viral RNA was extracted from 100 μl clinical samples (10% diluted in PBS) by using the RNeasy Mini kit (Qiagen, Hilden, Germany), according to the RNA Cleanup protocol, or by using the Viral RNA mini kit (Qiagen) according to the manufacterer's instructions, then stored at −20 °C.

2.3. Reverse transcription

A pre-reaction mix consisting of extracted/ in vitro synthesized RNA and random hexamers (Applied Biosystems, Foster City, CA, USA), in a final volume of 11.5 μl, was heated to 95 °C during 2 min, then cooled on ice during 2 min (thus avoiding the presence of secondary structures in the RNA and allowing the full hybridization of the RNA with the random hexamers). This first pre-reaction mix was then mixed with a second pre-reaction mix of 8.5 μl to obtain a final 20 μl RT-mastermix containing 2.5 μM random hexamers (Applied Biosystems), 25 U of Multiscribe reverse transcriptase (Applied Biosystems), 20 U of RNase inhibitor (Applied Biosystems), 5 mM $MgCl_2$ (Applied Biosystems), 1× PCR buffer II (10 mM Tris HCl, pH 8.3, 50 mM KCl; Applied Biosystems), 0.1 mM dNTPs (GE Healthcare; Diegem, Belgium) and extracted/in vitro synthesized RNA. Reverse transcription was carried out in a GeneAmp® PCR System 9700 (Applied Biosystems) with the following temperature profile: 22 °C for 10 min, 42 °C for 15 min, 99 °C for 5 min and 5 °C for 5 min. All cDNA was stored at −20 °C.

2.4. Real-time PCR

2.4.1. Generation of plasmid standards

To obtain representative positive control standards, the previously described plasmid p20.3 was used for the quantification of MNV-1 (Baert et al., 2008), while plasmids containing primers-probe binding sites were constructed for GI and GII

Table 2
Overview of primers and probes used for real-time RT-PCR.

Primers/probes	Sequence (5′–3′)[a]	Polarity[b]	Position[c]	Final conc.	Fluorophore[d] (5′)/Quencher (3′)
NoV GI					
QNIF4	CGCTGGATGCGNTTCCAT	+	5291–5308	500 nM	
NV1LCR	CCTTAGACGCCATCATCATTTAC	–	5354–5376	900 nM	
NVGG1p	TGGACAGGAGAYCGCRATCT	+	5321–5340	100 nM	6-FAM/BHQ-1
NoV GII					
QNIF2	ATGTTCAGRTGGATGAGRTTCTCWGA	+	5012–5038	500 nM	
COG2R	TCGACGCCATCTTCATTCACA	–	5100–5080	900 nM	
QNIFS	AGCACGTGGGAGGGCGATCG	+	5042–5061	250 nM	Texas Red/BHQ-1
MNV-1					
FW-ORF1/ORF2	CACGCCACCGATCTGTTCTG	+	4972–4991	200 nM	
RV-ORF1/ORF2	GCGCTGCGCCATCACTC	–	5064–5080	200 nM	
MGB-ORF1/ORF2	CGCTTTGGAACAATG	+	5001–5015	200 nM	NED/MGBNFQ

[a] Mixed bases in degenerate primers and probes are as follows: Y, C or T; R, A or G; N, any.
[b] +, virus sense; –, anti-virus sense.
[c] Corresponding nucleotide position of Norwalk/68 virus (accession nr. M87661) for NoV GI, Lorsdale virus (accession nr. X86557) for NoV GII or murine norovirus 1 clone CW1 (accession nr. DQ285629).
[d] BHQ-1: Black Hole Quencher – 1, MGBNFQ: Minor Groove Binding Non-Fluorescent Quencher.

NoVs. For GI NoVs, a 100 bp PCR amplicon (ATGCCATGTTCCGCTGGATGCGCTTCCATGACCTCGGATTGTGGACAGGAGATCGCGATCTTCTGCCCGAATTCGTAAATGATGATGGCGTCTAAGGAAT) covering the primers-probe binding sites (underlined) was cloned into the pMOS Blue vector (Amersham Biosciences, Saclay, France), resulting in the pGI plasmid. For GII NoVs, a 102 bp PCR amplicon (TTCAAGAGTCAATGTTTAGGTGGATGAGATTCTCAGATCTGAGCACGTGGGAGGGCGATCGCAATCTGGCTCCCAGCTTTGTGAATGAAGATGGCGTCGATT) covering the primers-probe binding sites (underlined) was cloned into the pGEM-T-Easy vector (Promega, Leiden, the Netherlands), resulting in the pGII plasmid. Plasmid DNA was purified by using a Plasmid Midi Kit (Qiagen). The plasmid concentration was determined by photospectroscopy at 260 nm using the NanoDrop® ND-1000 UV-Vis Spectrophotometer (NanoDrop Technologies, Wilmington, DE, USA). Ten-fold serial dilutions ranging from 10^7 to 10 copies of all three positive control plasmids were used to prepare the standard curves.

2.4.2. Primers and probes

Primers and probes for the individual quantitation of GI and GII NoVs were designed by the CEN/TC/WG6/TAG4 research group (Loisy et al., 2005; Svraka et al., 2007). The primers and probe for the individual quantification of MNV-1 were designed by Baert et al. (2008). An overview of the primers and probes sequences is shown in Table 2. All primers and probes were purchased from Eurogentec (Liège, Belgium), except the NED-labeled Minor Groove Binding (MGB) TaqMan probe, which was purchased from Applied Biosystems.

2.4.3. Real-time PCR assay

Quantitative real-time PCR was carried out in a 25 μl reaction mix containing 1 μl of template DNA and 12.5 μl of TaqMan Universal PCR Master Mix (Applied Biosystems), which contains dUTP and uracyl N-glycosylase (UNG). Primers and probes were used in the concentrations given in Table 2. In some cases, 10^3 copies of plasmid p20.3 were added to this reaction mix as real-time PCR IAC. Real-time quantitation was performed on the Lightcycler LC480 real-time PCR instrument (Roche Diagnostics, Mannheim, Germany) under the following conditions: incubation at 50 °C for 2 min to activate UNG, initial denaturation/activation at 95 °C for 10 min, followed by 50 cycles of amplification with denaturation at 95 °C for 15 s and annealing and extension at 60 °C for 1 min. Amplification data were collected and analyzed with the LC480 instruments' software. The amplification efficiency (E) was calculated from the plasmid standard curves using the equation $E = (10^{(-1/\text{slope})} - 1) \times 100$. To minimize cross-talk between the different channels of the real-time PCR instrument, a minimal wavelength difference of 25 nm was taken between both excitation and emission maxima of the different fluorescent labels. Eventual cross-talk was minimized by applying the color compensation as described in the LC480 manual.

3. Results

3.1. Singleplex real-time PCR assays for GI and GII NoVs and MNV-1

Plasmids pGI, pGII and p20.3 – containing primers-probe binding sites of GI and GII NoVs and MNV-1, respectively – were each diluted 10-fold serially in water and subjected to the singleplex real-time PCR assays. Fig. 1 shows the standard curves of these three singleplex assays. Analysis of the parameters of the standard curves of replicates of two independent runs showed that the three singleplex assays (GI, GII and MNV-1) are sensitive (detection limits of 10 copies) and efficient (PCR efficiencies of 91.6%, 87.3% and 94.2%, respectively). Standard deviations were small (with a maximum of 0.92 Ct), and the square regression coefficient (R^2) value was ≥0.998 for all three singleplex assays in the concentration range tested. Lastly, all intercepts were within a 2.9 Ct range.

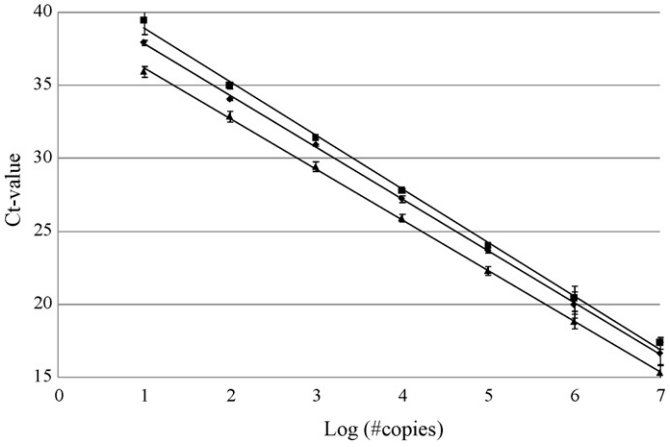

Fig. 1. Standard curves for the three singleplex GI, GII and MNV-1 real-time PCR detection assays using 10-fold serially diluted plasmid standards of pGI (series ♦), pGII (series ■) and p20.3 (series ▲), respectively, ranging from 10^7 to 10 copies.

3.2. Multiplex real-time PCR for the simultaneous detection of GI/GII NoVs and MNV-1

To examine the possible competition between the three individual PCR reactions within the multiplex real-time assay, plasmids pGI, pGII and p20.3 were mixed in equimolar amounts ranging from 10^7 to 10 copies. A comparison of parameters of the standard curves of duplicates of five independent multiplex runs (shown in Fig. 2) with those of the singleplex runs (shown in Fig. 1) showed that Ct values are in accordance with each other, with a maximum difference of less than one Ct. Furthermore, all parameters of the standard curves of the individual GI, GII and MNV-1 reactions within the multiplex PCR indicated that these individual reactions were sensitive (detection limit of 10 copies) and efficient (PCR efficiencies of 96.1%, 93.8% and 93.1%). Again, standard deviations were small (with a maximum of less than 1 Ct), and the R^2-value was $\geq$0.999 for all three individual PCRs within the multiplex assay in the concentration range tested. Lastly, all intercepts were within a 1.5 Ct range. These data suggest that reliable quantitative detection of the GI/GII NoVs and MNV-1 within the same sample is possible on the LC480 instrument using the multiplex real-time PCR assay.

The competitive effect between the individual PCR reactions within the multiplex assay was tested further by preparing all possible combinations of quantities of 0, 10, 10^3 and 10^5 copies of pGI, pGII and p20.3 and submitting these combinations to the multiplex assay. The resulting Ct values are shown in Fig. 3. In particular, this analysis focused on competitive effects between the GI and GII reactions (to examine the possibility of detecting both GI and GII NoVs within one sample), as well as the competition between the MNV-1 reaction and both the GI and GII reactions (to examine the possibility of using MNV-1 as real-time PCR IAC), all within the multiplex assay.

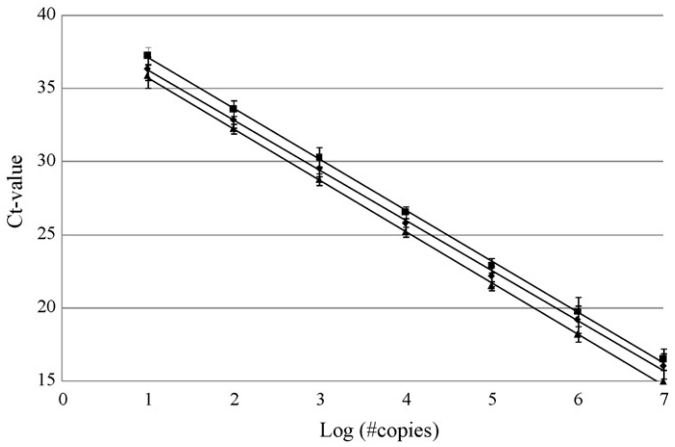

Fig. 2. Standard curves for the three individual GI, GII and MNV-1 real-time PCR reactions within the multiplex real-time PCR detection assays using 10-fold serially diluted plasmid standards of pGI (series ♦), pGII (series ■) and p20.3 (series ▲), respectively, ranging from 10^7 to 10 copies.

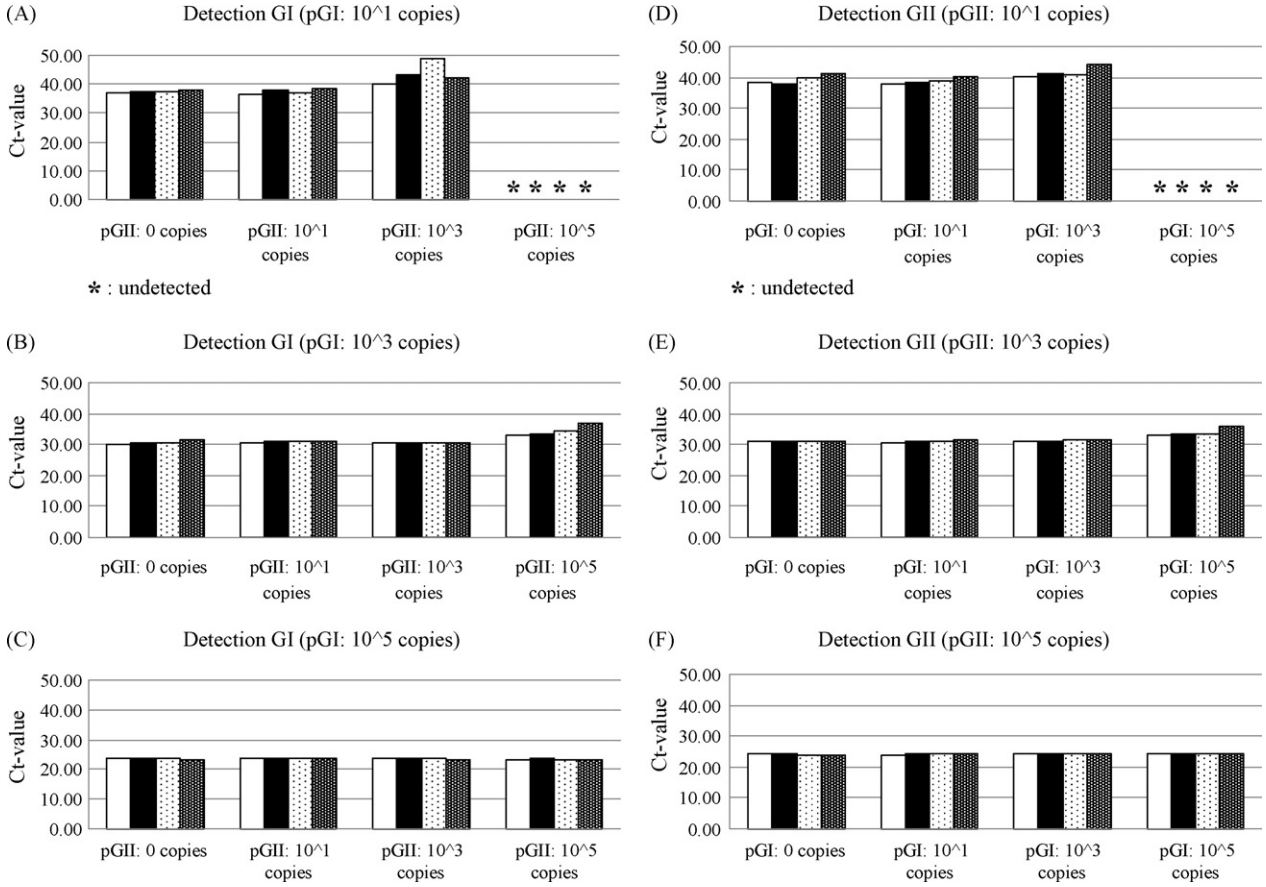

Fig. 3. (A–C) The effect of the presence of GII on Ct values (vertical axis) of the GI reaction within the multiplex real-time PCR assay. Different copy numbers (0, 10, 10^3 and 10^5 copies) of pGII (horizontal axis) are combined with 10 (Fig. 3A), 10^3 (Fig. 3B) and 10^5 (Fig. 3C) copies of pGI. (D–F) The effect of the presence of GI on Ct values (vertical axis) of the GII reaction within the multiplex real-time PCR assay. Different copy numbers (0, 10, 10^3 and 10^5 copies) of pGI (horizontal axis) are combined with 10 (Fig. 3A), 10^3 (Fig. 3B) and 10^5 (Fig. 3C) copies of pGII. The effect of the presence of MNV-1 on the GI and GII reactions within the multiplex real-time PCR assay was also included in Fig. 3. Copy numbers of 0 (series □), 10 (series ■), 10^3 (series ⬚) and 10^5 (series ▩) of p20.3 were combined with any combination of copy numbers of pGI and pGII. All Ct values are means of duplicates.

The effect of the presence of GII on the GI reaction within the multiplex assay was not negligible (Fig. 3A–C). 10^5 copies of plasmid pGI were detected at the expected Ct value in the presence of 10, 10^3 and 10^5 copies of pGII (Fig. 3A). 10^3 copies of pGI were detected at the expected Ct value in the presence of 10 or 10^3 copies of pGII, while a 2.8 Ct increase was observed in the presence of 10^5 copies of pGII (Fig. 3B). Ten copies of pGI were detected at the expected Ct value in the presence of 10 copies of pGII. However, a 2.9 Ct-shift was noticeable in the presence of 10^3 copies of pGII while these ten copies of pGI could not be detected (Ct > 50) in the presence of 10^5 copies of pGII (Fig. 3C).

Similarly, the presence of GI affected the GII reaction within the multiplex assay when high amounts (10^5 and 10^3 copies) of pGII were combined with any copy number (0, 10, 10^3 and 10^5 copies) of pGI (Fig. 3D and E). Similarly, a 2.2 Ct-shift was noticeable when 10^3 copies of pGII were detected in the presence of 10^5 copies of pGI (Fig. 3E). Ten copies of pGII were detected as expected in the presence of 10 copies of pGI. However, a 1.8 Ct-shift was noticeable in the presence of 10^3 copies of pGI while ten copies of pGII could not be detected (Ct > 50) in the presence of 10^5 copies of pGI (Fig. 3F).

Overall, the effect of the MNV-1 reaction on the GI and GII reactions within the multiplex assay was limited when pGI or pGII were solitarily present, as only a 4 log excess (10^5 copies) of plasmid p20.3 over pGI or pGII (10 copies) caused a Ct-shift ranging from 0.9 to 2.7 Cts (Fig. 3A and D). On the other hand, the effect of the MNV-1 reaction on the GI and GII reactions within the multiplex assay was not negligible when pGI and pGII were both present in one sample. When 10 and 10^3 copies of pGI were combined with 10^3 and 10^5 copies of pGII, respectively, Ct-shifts ranging from 2.1 to 8.9 and 1.6 to 3.8, respectively, were caused by the presence of 10^3 or 10^5 copies of p20.3. Similarly, when 10 and 10^3 copies of pGII were combined with 10^3 and 10^5 copies of pGI, respectively, Ct-shifts ranging from 0.5 to 3.8 and 0.2 to 3.8, respectively, were caused by the presence of 10^3 or 10^5 copies of p20.3.

3.3. Analysis of the specificity of the multiplex real-time RT-PCR

The specificity of the multiplex assay was analyzed by subjecting a norovirus RNA reference panel containing in vitro synthesized RNA fragments covering genomic regions A, B and C (Vinje et al., 2004) of nine GI, eight GII and one GIV NoV and 16 clinical GI/GII NoV samples to this assay (Table 1). All tested genotypes in the norovirus RNA reference panel were detected specifically, all clinical samples found positive for GI (5 samples) or GII (11 samples) NoVs previously were confirmed and no cross-amplification between the different GI, GII and GIV genotypes was observed. The seven alternative virus strains and the bovine GIII NoVs were not detected. 10^3 copies of the p20.3 plasmid used as real-time PCR internal amplification control were detected at expected Ct value (~28), suggesting that no PCR inhibitory components were present in the cDNA preparations of the clinical samples.

4. Discussion

The current study describes the successful combination of three singleplex real-time PCR assays for detection of GI/GII NoVs and MNV-1 into one multiplex real-time RT-PCR assay. Primers and probes in all three singleplex assays target the ORF1-ORF2 junction regions, which are considered to be the most conserved region of the NoV genome (Kageyama et al., 2003; Nishida et al., 2003).

All singleplex PCR reactions proved to be sensitive, with detection limits of 10 copies of the pGI, pGII and p20.3 plasmids (containing the primers-probe binding sites of GI/GII NoVs and MNV-1, respectively). Other authors reported similar detection limits ranging between 1 and 10 genomic copies (Jothikumar et al., 2005; Pang et al., 2005; Wolf et al., 2007). This low detection limit is necessary (1) because of the low viral concentration in environmental and food samples and (2) because of the low infectious dose of NoVs; it is reported that only 10 virions could be enough to infect a healthy adult (Hutson et al., 2004).

The combination of these three singleplex reactions into a multiplex assay requires similar PCR kinetics (Molenkamp et al., 2007; Persson et al., 2005). PCR efficiencies of all singleplex assays were within a 9% range and intercepts differed less than 2.9 Cts.

When equally mixed amounts of the pGI, pGII and p20.3 plasmids were detected with the multiplex assay, only a negligible loss in sensitivity was observed in comparison to the singleplex reactions.

When pGI, pGII and p20.3 plasmids were mixed in different concentrations, a mutual competitive effect was noticeable between the individual GI and GII reactions within the multiplex assay. This competitive effect became clear when a 2 log concentration difference (10^5/10^3 copies and 10^3/10 copies) was present between the two targets (pGI and pGII), resulting in Ct-shifts between 1.8 and 2.9 Cts for the target present in the lowest concentration. Additionally, when a 4 log concentration difference (10^5/10 copies) was present between the 2 targets (pGI/pGII), the target with the lowest concentration could not be detected (Ct > 50).

The effect of the MNV-1 reaction on the GI and GII reactions within the multiplex assay was limited when pGI or pGII were solitarily present. However, the presence of 10^3 and 10^5 copies of p20.3 did cause additional Ct-shifts when both pGI and pGII were present in one sample.

This analysis showed the limits of the multiplex assay for the detection of low amounts of one NoV genotype (GI/GII) in the presence of high amounts of another NoV genotype (GII/GI) in the same sample. These results also indicated that the use of the MNV-1 reaction as real-time PCR internal amplification control (IAC) is achievable. To avoid (1) competitive effects and (2) the loss of the quantitative properties of the multiplex assay (especially when detecting low virus concentrations), no more than 10^2 to 10^3 copies of plasmid p20.3 should be added to the real-time PCR reaction as real-time PCR IAC when detecting GI/GII NoVs.

A previous study of competitive effects between individual reactions within a multiplex PCR assay designed to simultaneously detect 4 virus types did not report analogous Ct-shifts (Molenkamp et al., 2007), but in this study only a 3 log difference between the target DNAs was investigated. However, the results of the current experiments support another multiplex real-time RT-PCR study (Candotti et al., 2004), in which Ct-delays (2–3 Cts) were reported when low concentrations of viral genome (50 to 10^3 genomic RNA copies) were detected simultaneously with another abundant viral genome (10^4 to 10^6 genomic RNA copies). Competition of individual PCR reactions within a multiplex (real-time) PCR is a known problem (Cook et al., 2002) and the results of the current study show that this issue should not be neglected during the design and optimization of quantitative multiplex real-time PCR assays, especially when detecting low-concentration DNA targets. Nevertheless, a well-optimized multiplex (real-time) PCR assay has benefits, including reduced expense of reagents and preparation time, combined with the possibility to include a (real-time) PCR IAC (Edwards and Gibbs, 1994).

Specificity of the multiplex assay was analyzed by testing a wide range of human GI, GII and GIV NoV genotypes, bovine GIII NoV genotypes and alternative virus strains. Specific detection of human NoV genotypes by real-time RT-PCR has been demonstrated before in other studies (Menton et al., 2007; Wolf et al., 2007). However, the Alphatron (GIV) NoV genotype was only included in a limited number of studies (Jothikumar et al., 2005; Trujillo et al., 2006) and to our knowledge, this is the first study to include the GIIb (a new emerging NoV genotype (Phan et al., 2006; Reuter et al., 2005)) and GIIc NoV genotypes.

Multiplex real-time RT-PCR assays for the simultaneous detection of GI and GII NoVs have been reported before (Jothikumar et al., 2005; Kageyama et al., 2003; Pang et al., 2005) and many authors have suggested the use of a PCR IAC to detect possible false-negative results due to inhibition when detecting genomic material (Hoorfar et al., 2004; Reiss and Rutz, 1999; Scipioni et al., 2008). This inhibition of (real-time) PCR assays is a known problem when detecting pathogens in faecal samples (Lantz et al., 1997; Monteiro et al., 1997), sewage samples (Guy et al., 2003) and food matrices (Rijpens and Herman, 2002). Therefore, a cultivable MS2 bacteriophage (Dreier et al., 2005; Rolfe et al., 2007), a genetically modified cultivable mengovirus (Comelli et al., 2008) and a cDNA fragment (whether or not NoV-related) flanked by primer binding sites (Escobar-Herrera et al., 2006; Scipioni et al., 2008) have recently been used as (multiplexed) PCR IAC. The use of DNA originating from a cultivable surrogate as (multiplexed real-time) PCR IAC is favored above the use of a cDNA fragment flanked by primer binding sites, as these cultivable surrogate organisms can also be utilized as (quantifiable) process control for the full extraction procedure when detecting GI and GII NoVs in clinical, environmental and food samples.

A comparison between several cultivable NoV surrogates for the detection of human NoVs in water favored the use of MNV-1 compared to other candidates such as MS2 bacteriophage, feline calicivirus (Bidawid et al., 2003) and poliovirus (Bae and Schwab, 2008). In addition, the similar biological properties of MNV-1 and human GI and GII NoVs (Cannon et al., 2006; Wobus et al., 2006) make it a preferred process control in human NoV detection assays. Therefore, 10^3 copies of plasmid p20.3 (MNV-1 positive control plasmid) were used as real-time PCR IAC in the multiplex assay developed. Detection of this PCR IAC at expected Ct values suggested absence of PCR inhibitory compounds in the cDNA preparations of the tested clinical samples.

This study describes the design of a multiplex real-time RT-PCR assay for detection of human GI and GII NoVs in clinical samples, with the successful use of MNV-1 plasmid DNA as real-time PCR IAC. This multiplex real-time PCR assay can be used as a rapid method for the detection of NoVs in environmental and food samples, although the robustness of this assay should be examined further for these types of samples.

Acknowledgements

This work was supported by the Belgian Science Policy Area – Science for a Sustainable Development (SSD–NORISK–SD/AF/01). Clinical (Noro)virus samples and the norovirus RNA reference panel were kindly provided by Prof. Marc Van Ranst and Dr. Elke Wollants of the Rega Institute for Medical Research (Leuven, Belgium), Dr. Katelijne Dierickx and Dr. Nadine Botteldoorn of the Belgian Scientific Institute of Public Health (Brussels, Belgium), Dr Axel Mauroy and Elisabeth Matthijs of the University of Liège (Belgium) and Prof. Marion Koopmans and Dr. Erwin Duizer of the National Institute for Public Health and the Environment (Bilthoven, the Netherlands). Finally, the authors would like to thank Miriam Levenson (Institute for Agricultural and Fisheries Research (ILVO)) for the critical reading of this article.

References

Asanaka, M., Atmar, R.L., Ruvolo, V., Crawford, S.E., Neill, F.H., Estes, M.K., 2005. Replication and packaging of Norwalk virus RNA in cultured mammalian cells. Proc. Natl. Acad. Sci. U.S.A. 102, 10327–10332.

Bae, J., Schwab, K.J., 2008. Evaluation of murine norovirus, feline calicivirus, poliovirus, and MS2 as surrogates for human norovirus in a model of viral persistence in surface water and groundwater. Appl. Environ. Microbiol. 74, 477–484.

Baert, L., Uyttendaele, M., Debevere, J., 2007. Evaluation of two viral extraction methods for the detection of human noroviruses in shellfish with conventional and real-time reverse transcriptase PCR. Lett. Appl. Microbiol. 44, 106–111.

Baert, L., Wobus, C.E., Van Coillie, E., Thackray, L.B., Debevere, J., Uyttendaele, M., 2008. Detection of murine norovirus 1 by using plaque assay, transfection assay, and real-time reverse transcription-PCR before and after heat exposure. Appl. Environ. Microbiol. 74, 543–546.

Bidawid, S., Malik, N., Adegbunrin, O., Sattar, S.A., Farber, J.M., 2003. A feline kidney cell line-based plaque assay for feline calicivirus, a surrogate for Norwalk virus. J. Virol. Methods 107, 163–167.

Candotti, D., Temple, J., Owusu-Ofori, S., Allain, J.P., 2004. Multiplex real-time quantitative RT-PCR assay for hepatitis B virus, hepatitis C virus, and human immunodeficiency virus type 1. J. Virol. Methods 118, 39–47.

Cannon, J.L., Papafragkou, E., Park, G.W., Osborne, J., Jaykus, L.A., Vinje, J., 2006. Surrogates for the study of norovirus stability and inactivation in the environment: a comparison of murine norovirus and feline calicivirus. J. Food Prot. 69, 2761–2765.

Chimonas, M.A., Vaughan, G.H., Andre, Z., Ames, J.T., Tarling, G.A., Beard, S., Widdowson, M.A., Cramer, E., 2008. Passenger behaviors associated with norovirus infection on board a cruise ship—Alaska, May to June 2004. J. Travel Med. 15, 177–183.

Comelli, H.L., Rimstad, E., Larsen, S., Myrmel, M., 2008. Detection of norovirus genotype I.3b and II.4 in bioaccumulated blue mussels using different virus recovery methods. Int. J. Food Microbiol. 127, 53–59.

Cook, R.F., Cook, S.J., Li, F., Montelaro, R.C., Issel, C.J., 2002. Development of a multiplex real-time reverse transcriptase-polymerase chain reaction for equine infectious anemia virus (EIAV). J. Virol. Methods 105, 171–179.

Craun, G.F., Calderon, R.L., Craun, M.F., 2005. Outbreaks associated with recreational water in the United States. Int. J. Environ. Health Res. 15, 243–262.

De Medici, D., Croci, L., Suffredini, E., Toti, L., 2004. Reverse transcription-booster PCR for detection of noroviruses in shellfish. Appl. Environ. Microbiol. 70, 6329–6332.

De Wit, M.A.S., Widdowson, M.A., Vennema, H., de Bruin, E., Fernandes, T., Koopmans, M., 2007. Large outbreak of norovirus: the baker who should have known better. J. Infect. 55, 188–193.

Depoortere, E., Takkinen, J., 2006. Coordinated European actions to prevent and control norovirus outbreaks on cruise ships. Eur. Surveill. 11, E061018.

Dreier, J., Stormer, M., Kleesiek, K., 2005. Use of bacteriophage MS2 as an internal control in viral reverse transcription-PCR assays. J. Clin. Microbiol. 43, 4551–4557.

Duizer, E., Schwab, K.J., Neill, F.H., Atmar, R.L., Koopmans, M.P.G., Estes, M.K., 2004. Laboratory efforts to cultivate noroviruses. J. Gen. Virol. 85, 79–87.

Edwards, M.C., Gibbs, R.A., 1994. Multiplex PCR—advantages, development, and applications. PCR Methods Appl. 3, S65–S75.

Escobar-Herrera, J., Cancio, C., Guzman, G.I., Villegas-Sepulveda, N., Estrada-Garcia, T., Garcia-Lozano, H., Gomez-Santiago, F., Gutierrez-Escolano, A.L., 2006. Construction of an internal RT-PCR standard control for the detection of human caliciviruses in stool. J. Virol. Methods 137, 334–338.

Fankhauser, R.L., Monroe, S.S., Noel, J.S., Humphrey, C.D., Bresee, J.S., Parashar, U.D., Ando, T., Glass, R.I., 2002. Epidemiologic and molecular trends of "Norwalk-like viruses" associated with outbreaks of gastroenteritis in the United States. J. Infect. 186, 1–7.

Gallimore, C.I., Pipkin, C., Shrimpton, H., Green, A.D., Pickford, Y., McCartney, C., Sutherland, G., Brown, D.W.G., Gray, J.J., 2005. Detection of multiple enteric virus strains within a foodborne outbreak of gastroenteritis: an indication of the source of contamination. Epidemiol. Infect. 133, 41–47.

Gallimore, C.I., Taylor, C., Gennery, A.R., Cant, A.J., Galloway, A., Xerry, J., Adigwe, J., Gray, J.J., 2008. Contamination of the hospital environment with gastroenteric viruses: comparison of two paediatric wards over a winter season. J. Clin. Microbiol. 46 (9), 3112–3115.

Guy, R.A., Payment, P., Krull, U.J., Horgen, P.A., 2003. Real-time PCR for quantification of Giardia and Cryptosporidium in environmental water samples and sewage. Appl. Environ. Microbiol. 69, 5178–5185.

Hoorfar, J., Malorny, B., Abdulmawjood, A., Cook, N., Wagner, M., Fach, P., 2004. Practical considerations in design of internal amplification controls for diagnostic PCR assays. J. Clin. Microbiol. 42, 1863–1868.

Hutson, A.M., Atmar, R.L., Estes, M.K., 2004. Norovirus disease: changing epidemiology and host susceptibility factors. Trends Microbiol. 12, 279–287.

Johansson, P.J.H., Torven, M., Hammarlund, A.C., Bjorne, U., Hedlund, K.O., Svensson, L., 2002. Food-borne outbreak of gastroenteritis associated with genogroup I calicivirus. J. Clin. Microbiol. 40, 794–798.

Jothikumar, N., Lowther, J.A., Henshilwood, K., Lees, D.N., Hill, V.R., Vinje, J., 2005. Rapid and sensitive detection of noroviruses by using TaqMan-based one-step reverse transcription-PCR assays and application to naturally contaminated shellfish samples. Appl. Environ. Microbiol. 71, 1870–1875.

Kageyama, T., Kojima, S., Shinohara, M., Uchida, K., Fukushi, S., Hoshino, F.B., Takeda, N., Katayama, K., 2003. Broadly reactive and highly sensitive assay for Norwalk-like viruses based on real-time quantitative reverse transcription-PCR. J. Clin. Microbiol. 41, 1548–1557.

Koopmans, M., von Bonsdorff, C.H., Vinje, J., De Medici, D., Monroe, S., 2002. Foodborne viruses. FEMS Microbiol. Rev. 26, 187–205.

Koopmans, M., Duizer, E., 2004. Foodborne viruses: an emerging problem. Int. J. Food Microbiol. 90, 23–41.

Koopmans, M., 2008. Progress in understanding norovirus epidemiology. Curr. Opin. Infect. Dis. 21, 544–552.

Lantz, P.G., Matsson, M., Wadstrom, T., Radstrom, P., 1997. Removal of PCR inhibitors from human faecal samples through the use of an aqueous two-phase system for sample preparation prior to PCR. J. Microbiol. Methods 28, 159–167.

Le Guyader, F.S., Mittelholzer, C., Haugarreau, L., Hedlund, K.O., Alsterlund, R., Pommepuy, M., Svensson, L., 2004. Detection of noroviruses in raspberries associated with a gastroenteritis outbreak. Int. J. Food Microbiol. 97, 179–186.

Loisy, F., Atmar, R.L., Guillon, P., Le Cann, P., Pommepuy, M., Le Guyader, F.S., 2005. Real-time RT-PCR for norovirus screening in shellfish. J. Virol. Methods 123, 1–7.

Malorny, B., Tassios, P.T., Radstrom, P., Cook, N., Wagner, M., Hoorfar, J., 2003. Standardization of diagnostic PCR for the detection of foodborne pathogens. Int. J. Food Microbiol. 83, 39–48.

Mauroy, A., Scipioni, A., Matthijs, E., Miry, C., Ziant, D., Thys, C., Thiry, E., 2008. Noroviruses and sapoviruses in pigs in Belgium. Arch. Virol. 153 (10), 1927–1931.

Menton, J.F., Kearney, K., Morgan, J.G., 2007. Development of a real-time RT-PCR and reverse line probe hybridisation assay for the routine detection and genotyping of noroviruses in Ireland. Virol. J. 4, 86–94.

Molenkamp, R., van der, Ham, A., Schinkel, J., Beld, M., 2007. Simultaneous detection of five different DNA targets by real-time Taqman PCR using the Roche LightCycler480: application in viral molecular diagnostics. J. Virol. Methods 141, 205–211.

Monteiro, L., Bonnemaison, D., Vekris, A., Petry, K.G., Bonnet, J., Vidal, R., Cabrita, J., Megraud, F., 1997. Complex polysaccharides as PCR inhibitors in feces: *Helicobacter pylori* model. J. Clin. Microbiol. 35, 995–998.

Niesters, H.G., 2002. Clinical virology in real time. J. Clin. Virol. 25 (Suppl. 3), S3–S12.

Nishida, T., Kimura, H., Saitoh, M., Shinohara, M., Kato, M., Fukuda, S., Munemura, T., Mikami, T., Kawamoto, A., Akiyama, M., Kato, Y., Nishi, K., Kozawa, K., Nishio, O., 2003. Detection, quantitation, and phylogenetic analysis of noroviruses in Japanese oysters. Appl. Environ. Microbiol. 69, 5782–5786.

Pang, X.L.L., Preiksaitis, J.K., Lee, B., 2005. Multiplex real time RT-PCR for the detection and quantitation of norovirus genogroups I and II in patients with acute gastroenteritis. J. Clin. Virol. 33, 168–171.

Park, Y., Cho, Y.H., Jee, Y., Ko, G., 2008. Immunomagnetic separation combined with real-time reverse transcriptase PCR assays for detection of norovirus in contaminated food. Appl. Environ. Microbiol. 74, 4226–4230.

Persson, K., Hamby, K., Ugozzoli, L.A., 2005. Four-color multiplex reverse transcription polymerase chain reaction—overcoming its limitations. Anal. Biochem. 344, 33–42.

Phan, T.G., Kuroiwa, T., Kaneshi, K., Ueda, Y., Nakaya, S., Nishimura, S., Yamamoto, A., Sugita, K., Nishimura, T., Yagyu, F., Okitsu, S., Muller, W.E.G., Maneekarn, N., Ushijima, H., 2006. Changing distribution of norovirus genotypes and genetic analysis of recombinant GIIb among infants and children with diarrhea in Japan. J. Med. Virol. 78, 971–978.

Reiss, R.A., Rutz, B., 1999. Quality control PCR: a method for detecting inhibitors of Taq DNA polymerase. Biotechniques 27, 920/2–924/6.

Reuter, G., Krisztalovics, K., Vennema, H., Koopmans, M., Szucs, G., 2005. Evidence of the etiological predominance of norovirus in gastroenteritis outbreaks—emerging new-variant and recombinant noroviruses in Hungary. J. Med. Virol. 76, 598–607.

Rijpens, N.P., Herman, L.M.F., 2002. Molecular methods for identification and detection of bacterial food pathogens. J. AOAC Int. 85, 984–995.

Rolfe, K.J., Parmar, S., Mururi, D., Wreghitt, T.G., Jalal, H., Zhang, H., Curran, M.D., 2007. An internally controlled, one-step, real-time RT-PCR assay for norovirus detection and genogrouping. J. Clin. Virol. 39, 318–321.

Schvoerer, E., Bonnet, F., Dubois, V., Rogues, A.M., Gachie, J.P., Lafon, M.E., Fleury, H.J., 1999. A hospital outbreak of gastroenteritis possibly related to the contamination of tap water by a small round structured virus. J. Hosp. Infect. 43, 149–154.

Scipioni, A., Mauroy, A., Ziant, D., Saegerman, C., Thiry, E., 2008. A SYBR Green RT-PCR assay in single tube to detect human and bovine noroviruses and control for inhibition. Virol. J. 5, 94–102.

Straub, T.M., Bentrup, K.H.Z., Orosz-Coghlan, P., Dohnalkova, A., Mayer, B.K., Bartholomew, R.A., Valdez, C.O., Bruckner-Lea, C.J., Gerba, C.P., Abbaszadegan, M., Nickerson, C.A., 2007. In vitro cell culture infectivity assay for human noroviruses. Emerg. Infect. Dis. 13, 396–403.

Svraka, S., Duizer, E., Vennema, H., de Bruin, E., van der Veer, B., Dorresteijn, B., Koopmans, M., 2007. Etiological role of viruses in outbreaks of acute gastroenteritis in the Netherlands from 1994 through 2005. J. Clin. Microbiol. 45, 1389–1394.

Trujillo, A.A., McCaustland, K.A., Zheng, D.P., Hadley, L.A., Vaughn, G., Adams, S.M., Ando, T., Glass, R.I., Monroe, S.S., 2006. Use of TaqMan real-time reverse transcription-PCR for rapid detection, quantification, and typing of norovirus. J. Clin. Microbiol. 44, 1405–1412.

van der Poel, W.H., Van der, H.R., Verschoor, F., Gelderblom, H., Vinje, J., Koopmans, M.P., 2003. Epidemiology of Norwalk-like virus infections in cattle in the Netherlands. Vet. Microbiol. 92, 297–309.

Vinje, J., Hamidjaja, R.A., Sobsey, M.D., 2004. Development and application of a capsid VP1 (region D) based reverse transcription PCR assay for genotyping of genogroup I and II noroviruses. J. Virol. Methods. 116, 109–117.

Wobus, C.E., Thackray, L.B., Virgin, H.W., 2006. Murine norovirus: a model system to study norovirus biology and pathogenesis. J. Virol. 80, 5104–5112.

Wolf, S., Williamson, W.M., Hewitt, J., Rivera-Aban, M., Lin, S., Ball, A., Scholes, P., Greening, G.E., 2007. Sensitive multiplex real-time reverse transcription-PCR assay for the detection of human and animal noroviruses in clinical and environmental samples. Appl. Environ. Microbiol. 73, 5464–5470.

Journal of Microbiological Methods 77 (2009) 72–76

Contents lists available at ScienceDirect

Journal of Microbiological Methods

journal homepage: www.elsevier.com/locate/jmicmeth

Laboratory efforts to eliminate contamination problems in the real-time RT-PCR detection of noroviruses

Ambroos Stals [a,*], Hadewig Werbrouck [a], Leen Baert [b], Nadine Botteldoorn [c], Lieve Herman [a], Mieke Uyttendaele [b], Els Van Coillie [a]

[a] Flemish Government, Institute for Agricultural and Fisheries Research, Unit Technology and Food, Brusselsesteenweg 370, 9090 Melle, Belgium
[b] Department of Food Safety and Food Quality, Laboratory of Food Microbiology and Food Preservation, Faculty of Bioscience Engineering, Ghent University, Belgium
[c] Belgian Scientific Institute of Public Health, Department of Microbiology, Division of Bacteriology, Juliette Wytsmanstraat 14, 1050 Brussels, Belgium

ARTICLE INFO

Article history:
Received 17 September 2008
Received in revised form 20 December 2008
Accepted 12 January 2009
Available online 30 January 2009

Keywords:
Contamination
False-positive
Norovirus
Real-time RT-PCR

ABSTRACT

In the current study, laboratory efforts to prevent the presence of positive NTCs (no template controls) during the optimization of a quantitative real-time reverse transcriptase PCR assay for detection of Noroviruses (NoVs) are described. Two DNA types (single-stranded (ss)DNA fragments and plasmid DNA) were used to generate a real-time PCR standard and a high frequency of positive NTCs was noticed in the case of ssDNA fragments. To investigate our suspicion of well-to-well migration of DNA during real-time PCR runs as possible cause of the positive NTCs, an "evaporation-experiment" was set up in which the evaporation of water and the possible co-evaporation of DNA were measured as a function of the DNA type (ssDNA-fragments, plasmid DNA and genomic DNA), the reaction plate seal type (adhesive film or 8-cap strips) and the use of 7 µl of mineral oil as cover layer. Results of this experiment indicated that evaporation of water occurred during real-time PCR runs regardless of the DNA type, the seal type and whether or not 7 µl of mineral oil was used as cover layer. Data from this experiment also suggested co-evaporation of DNA, with an apparent negative correlation between the size of the DNA type and the extent of this co-evaporation. The use of 7 µl of mineral oil as cover layer seemed to prevent to some extent co-evaporation of DNA. The use of plasmids as standard combined with 7 µl of mineral oil as cover layer in the real-time PCR setup resulted in a complete absence of positive NTCs while only minor effects were noticed on the performance of the real-time PCR. In general, our results showed that the high sensitivity of an optimized real-time PCR assay should be considered as – besides a great advantage – a potential risk factor for obtaining false-positive results when using this technique.

1. Introduction

PCR has become an established method for detection of food borne bacterial (Abubakar et al., 2007) and viral agents (Love et al., 2008; Rutjes et al., 2006; Wolf et al., 2007). It is being increasingly used in surveillance studies and end product testing for detection of pathogens as it provides a rapid and sensitive tool for the screening of large numbers of clinical and environmental samples (Lampel et al., 2000). Since cultivation of human NoV strains require a complex cell system to grow (Asanaka et al., 2005; Straub et al., 2007), for now (real-time) reverse transcriptase PCR is considered as the gold standard for detection of NoVs (Houde et al., 2006). The introduction of real-time PCR, the technological improvement of PCR machines and the use of optimized buffers and enzymes greatly increased the PCR sensitivity. If optimized well, real-time PCR assays have the possibility to detect less than 10 copies, corresponding often to cycle threshold (Ct) values of 36–40 (Klein, 2002; Peters et al., 2004; Reynisson et al., 2006). A drawback of (real-time) PCR is that it is prone to contamination, leading to false-positive results (Borst et al., 2004; Niesters, 2002). This is particularly important when detecting NoVs as there is no possibility yet to confirm positive PCR test results by culture (in contradiction to most bacterial pathogens). False-positives can result from sample-to-sample contamination and from carryover DNA originating from previous amplification of the same target (Speers, 2006). The introduction of real-time PCR combined with the use of enzymatic systems (Uracil N-Glycosidase (UNG)) has to a great extent dealt with the latter (carryover-) contamination issue (Kleiboeker, 2005; Pang et al., 1992). To avoid false positive results from sample-to-sample contamination (Borst et al., 2004; Kwok and Higuchi, 1989; Rijpens and Herman, 2002) a constant need remains to respect

* Corresponding author. Mailing address: Institute for Agricultural and Fisheries Research, Unit Technology and Food — Product Quality and Food Safety, Brusselsesteenweg 370, 9090 Melle, Belgium. Tel.: +32 9 272 30 26; fax: +32 9 272 30 01.
E-mail address: Ambroos.Stals@ilvo.vlaanderen.be (A. Stals).

0167-7012/$ – see front matter © 2009 Elsevier B.V. All rights reserved.
doi:10.1016/j.mimet.2009.01.018

dedicated environmental conditions (separate working areas, UV decontamination, dedicated pipettes, mineral oil, no template controls) if real-time PCR and conventional PCR are applied in the microbiological lab.

Positive NTCs (no template controls) are a frequent observation in many labs when setting up or optimizing PCR protocols or executing PCR testing on a routine basis. Especially when manipulating high concentrations of target DNA in setting up real-time PCR standard curves or as positive control templates the risk of false-positive results increases (Espy et al., 2006). Although no guidelines have been published on this matter, attempts to interpret the occurrence of positive NTCs have been made (Bustin and Nolan, 2004). When amplification occurs in NTCs, high Ct values are often noticed, indicating contamination of only few copies of DNA in the NTC.

In the present manuscript the hypothesis is raised if the occurrence of positive NTCs could be due to evaporation of water during the PCR run also enabling co-evaporation of templating DNA and thus transfer to NTC's providing occasionally high Ct values for the NTC reactions.

2. Materials and methods

2.1. Quantitative real-time PCR

The real-time quantitative PCR was carried out in a volume of 25 µl. The reaction mix contained 5 µl of target DNA, 12.5 µl of TaqMan Universal PCR Master Mix (Applied Biosystems, Foster City, CA, USA) containing dUTP and UNG, 500 nM of the QNIF2-forward primer (5′-ATGTTCAGRTGGATGAGRTTCTCWGA-3′; Eurogentec, Liège, Belgium), 900 nM of the COG2R-reverse primer (5′-TCGACGCCATCTTCATTCACA-3′; Eurogentec) and 250 nM of the QNIFS TaqMan-probe for Norovirus GGII detection (YakimaYellow-5′-AGCACGTGGGAGGGCGATCG-3′-BHQ1; Eurogentec). The QNIF2 and COG2R primers and the QNIFS probe were designed by the CEN/TC275/WG6/TAG4 research group and ordered at Eurogentec (Liège, Belgium). PCR amplification was performed with a ABI Prism® 7000 Sequence Detection System (Applied Biosystems) under the following conditions: incubation at 50 °C for 2 min to activate UNG, initial denaturation at 95 °C for 10 min, followed by 50 cycles of amplification with denaturation at 95 °C for 15 s and annealing and extension at 60 °C for 1 min.

Ten-fold serial dilutions of both (1) a 102 nucleotide synthetic ssDNA fragment "ssGII" (Eurogentec, Liège, Belgium) based on the NoV GII real-time RT-PCR protocol designed by Jothikumar et al. (2005) and (2) the "pGII" plasmid (size: 3117 bp) being a pGEM-T-easy vector (Promega, Wisconsin, USA) with an insert of 102 bp containing the primers-probe binding sites, served as standard positive controls in the real-time PCR. When ssGII and pGII were used as template DNA, respectively an 89 bp and a 93 bp real-time PCR amplicon were generated. Sequence details are shown in Table 1. Negative template controls (NTCs) consisted of the real-time PCR reaction mix without DNA added, but instead with 5 µl of sterile HPLC-grade water. The number of NTCs per real-time PCR run varied between 4 and 18.

Both the MicroAmp™ Optical 8-Cap Strip and the MicroAmp™ Optical Adhesive Film (Applied Biosystems) were used as seal for the 96 well real-time PCR reaction plate (Applied Biosystems). In some cases, 7 or 30 µl of mineral oil (Sigma-Aldrich, St. Louis, USA) was used as cover layer on top of the 25 µl real-time PCR reaction mixtures.

Amplification data were collected and analysed with the ABI Prism® 7000 SDS software version 1.0 (Applied Biosystems). Sensitivity of the real-time PCR assay was analysed by evaluating Ct-values, while the reproducibility was examined on the basis of the square regression coefficient (R^2-value) of the obtained real-time PCR standard curves.

To visualise and to measure the size of the real-time PCR amplicons present in the negative control (NTC) wells, agarose gel electrophoration was performed for 30 min at 100 V on a 4% (w/v) NuSieve® 3:1 Agarose (Lonza, Verviers, Belgium) in 0.5×TAE buffer containing 400 mM Tris-acetate and 10 mM EDTA (Invitrogen Ltd., Paisley, UK). As a size marker, the 1 kb DNA ladder (Invitrogen Ltd.) was used. The agarose gels were visualised after staining with ethidium bromide (2 µg/ml), and photographed on a UV transillumination table with a Polaroid MP4 Land Camera (Polaroid Corp., Cambridge, MA, USA) using type 667 film.

2.2. Evaporation experiment

2.2.1. Different DNA types

A 104 nucleotide ssDNA-fragment (5′-TTGCACCACACAGCTGAA TAGTTTGGCTCACT GGATTTTGACCCTTTGTGCAATGGTTGAGGTAACCC GAGTTGACCCTGACATTGTGATGCAAGAATCTGATT-3′) was purchased at Eurogentec, a pGEM-T-easy vector (Promega) containing an 81 bp insert (5′-TGATGCGATTCCATGACGATTGTGGGACAG GAGATCGCGATCTTCTGCG GATCCGAATTCGTAAATGATGATGGCGTCTAA-3′) and with a total plasmid size of ~3,1 kb was isolated by the alkaline lysis method of Birnboim and Doly (1979) and genomic DNA (size: ~4,6 mb) was extracted from DH5α *Escherichia coli* cells grown overnight at 37 °C in Luria Broth Base medium (GIBCO BRL, Eggenstein, Germany) by the method of Flamm et al. (1984). The three DNA types (ssDNA, plasmid DNA and genomic DNA) were diluted in sterile HPLC-grade water to a final concentration of approximately 200 ng/µl. The precise concentration of the DNA was determined using the NanoDrop® ND-1000 UV–Vis Spectrophotometer (NanoDrop Technologies, Wilmington, DE, USA).

2.2.2. Plate setup

Two 96-well reaction plates were prepared with identical setups: 25 µl solutions of each of the 3 DNA types (ssDNA fragments, plasmid DNA and genomic DNA) at the respective final concentrations (178.92, 281.94 and 236.00 ng/µl) were pipetted into respectively 12 different wells of each plate. No real-time PCR components were added to any of the solutions. Wells 1 to 12 contained ssDNA fragments, wells 13 to 24 contained plasmid DNA and wells 25 to 36 contained genomic DNA.

Seven µl of mineral oil (Sigma-Aldrich, St. Louis, Missouri) was used as cover layer on the DNA solutions in wells 1 to 3, 7 to 9, 13 to 15, 19 to 21, 25 to 27 and 31 to 33.

Moreover, each of the three DNA types was combined with two different seal types: the MicroAmp™ Optical 8-Cap Strip and the MicroAmp™ Optical Adhesive Film (Applied Biosystems). Wells 1 to 6, 13 to 18 and 25 to 30 were closed by the 8-cap strip, while wells 7 to 12, 19 to 24 and 31 to 36 were closed by the adhesive film. In summary, three replicates were taken for each of the 12 combinations (DNA type – with or without 7 µl of mineral oil – seal type).

One of the plates underwent a single real-time PCR thermal cycling program as described above, the other plate underwent 5 identical subsequent real-time PCR thermal cycling programs.

Table 1
Sequences of ssGII and insert of pGII

Positive control (length)	Sequence (5′–3′)
Synthetic ssDNA fragment "ssGII" (102 nucleotides)	TTCAAGAGTCATTGTTTAGGTGGATGAGATTCTCAGATCTGAGCACGTGGGAGGGCGATCGCAATCTGGCTCCCAGCTTTGTGAATGAAGATGGCGTCGATT
Insert of "pGII" (102 bp)	AGCTTTGTTCAGATGGATGAGATTCTCAGATCTGAGCACGTGGGAGGGCGATCGCAATCTGGCTCGGATCCAGCTTTGTGAATGAAGATGGCGTCGAAGCTT

Primer and probe binding sites are underlined.

2.2.3. Statistics

All statistical analyses were done using the Statistica 8.0 software (StatSoft, Tulsa, OK, USA). Data from the "evaporation"-experiment were analysed using a two-factor analysis of variance (ANOVA), with factor one the DNA type and factor two the combination of seal type and eventual use of 7 µl mineral oil as cover layer.

3. Results

A comparison between the use of a ssDNA fragment (ssGII) and plasmid DNA (pGII), both containing the primer-probe binding sites, as standard in the quantitative real-time PCR showed that both assays were sensitive (detection limits of 10 copies with intercepts of 42.79 (ssGII) and 43.92 (pGII)), reproducible (R^2-value ≥ 0.99) and efficient (slope = −3.13 (ssGII) or −3.36 (pGII), corresponding to PCR efficiencies of 108.7% and 98.5% respectively).

Although the parameters of both standard curves showed that with both DNA types reliable standard curves were obtained, amplification was noticed in all 10 NTCs in 3 independent real-time PCR runs with ssGII as target DNA, with Ct-values ranging between 38.15 and 40.32, corresponding to an initial presence of about 10 copies of the target DNA. No amplification occurred in any of the NTCs when pGII was used as standard positive control. Agarose gel electrophoresis of the real-time PCR products of the NTCs showed the presence of a DNA-fragment with the same size of the amplicon in the positive controls (data not shown).

To avoid future problems, the cause of these positive NTCs was investigated. This investigation included a study of the possibility of well-to-well transfer of target DNA during the real-time PCR run as possible cause and the influence of both the reaction plate seal type and the eventual use of mineral oil as vapour barrier on the presence of the positive NTCs.

The effect of 3 DNA types frequently used as template for real-time PCR standards and with 3 different size magnitudes (ssDNA — 104 nucleotides, plasmid DNA — ~3.1 kb and genomic DNA — ~4.6 mb) and the seal type (8-cap strip/adhesive film and with or without 7 µl of mineral oil) on the relative increase of the DNA concentration as an indication for co-evaporation of DNA with water after 1 and 5 real-time PCR runs is shown in Figs. 1 and 2.

After 1 run (Fig. 1) a relative increase in the DNA concentration in all wells was noticed, regardless of the DNA type. However, this increase was significantly higher in wells with genomic DNA (15.11%) in comparison to wells with ssDNA (10.93%) and plasmid DNA (10.38%). These observations suggest that evaporation of water occurred in all wells. The differences in the relative increase of the DNA concentration suggest the co-evaporation of DNA, to a lesser degree in wells with genomic DNA and to a greater extent in wells with ssDNA and plasmid DNA. After 5 runs (Fig. 1) similar observations were noticed, but as expected the relative increase of DNA concentrations in all wells was higher than after 1 run. Although the relative increase in the DNA concentration was again highest in wells with genomic DNA (27.64%), there was also a significant difference between the ssDNA fragments (20.50%) and the plasmid DNA (24.47%). An apparent correlation between the size of the DNA and the increase of the DNA concentration was noticeable.

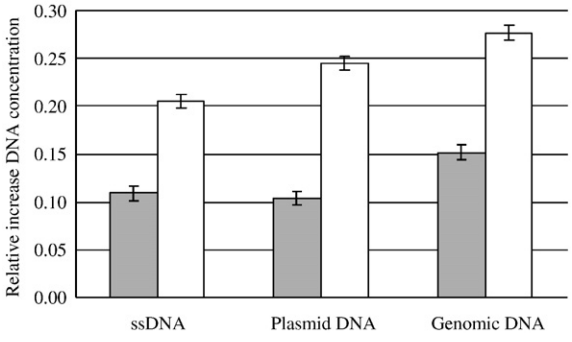

Fig. 1. Effect of the DNA type (horizontal axis) on the relative increase ((final concentration − initial concentration) × 100 / initial concentration; vertical axis) of the DNA concentration after (■) 1 run and after (□) 5 runs. Each DNA type in the horizontal axis represents all possible combinations of (1) a specific DNA type (ssDNA, plasmid DNA, genomic DNA) with (2) all combinations of two seal types (8-cap strip or adhesive film) and whether or not 7 µl of mineral oil was used. Vertical error bars denote the 95% confidence intervals.

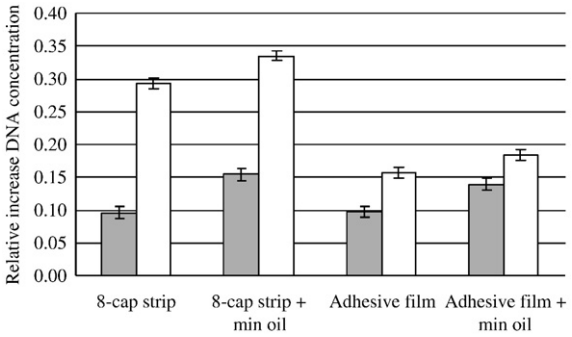

Fig. 2. Effect of the seal type (horizontal axis) on the relative change ((final concentration − initial concentration) × 100 / initial concentration; vertical axis) of the DNA concentration after (■) 1 run and after (□) 5 runs. Each seal type in the horizontal axis represents all possible combinations of (1) the combinations of a seal type (8-cap strip or adhesive film) and whether or not 7 µl of mineral oil was used with (2) the three DNA types (ssDNA, plasmid DNA and genomic DNA). Vertical error bars denote the 95% confidence intervals.

Regardless of the seal type and whether or not 7 µl of mineral oil was used as cover on the DNA solution, a relative increase in the DNA concentration in all wells was noticed after 1 run (Fig. 2). A significantly higher relative increase in DNA concentration in all wells covered by the mineral oil was noticed (15.40% and 13.90% vs. 9.54% and 9.72%). This may suggest that mineral oil, although permitting the evaporation of water may have prevented to some extent the co-evaporation of DNA as such resulting in the increased DNA concentration in the well. After 5 runs (Fig. 2) a significantly higher relative increase in DNA concentration was noticed in wells sealed by the 8-cap strip (29.30% and 33.48%) in comparison to the wells sealed by the adhesive film (15.73% and 18.30%). Although the increase in DNA concentration was consistently higher in wells where mineral oil was used, this difference was not significant.

Given the results of the "evaporation-experiment", the effect of different amounts (7 and 30 µl) of mineral oil as vapour barrier on the efficiency of real-time PCR reactions was tested in comparison to when no mineral oil was used. A real-time PCR amplification was performed in which duplicates of a 10-fold serial diluted series of the ssGII fragment were taken as standard positive control. This real-time PCR was run twice independently and parameter values of the standard curves are shown in Table 2. Seven µl of mineral oil did not cause a considerable reduction of the sensitivity, reproducibility and efficiency of the real-time PCR assay, while this was not the case when 30 µl was used.

To verify the effect of the seal type (8-cap strip and adhesive film) on the occurrence of positive NTCs, two independent real-time PCR runs as described above were performed, with duplicates of a 10-fold

Table 2
Parameter values of the standard curves when different amounts of mineral oil were used as cover layer

Volume mineral oil	Detection limit (Ct)	Slope (PCR-efficiency)	R^2-value
0 µl	10 copies (40.38)	−3.36 (98.5%)	0.99
7 µl	10 copies (39.51)	−3.64 (88.3%)	1.00
30 µl	10 copies (42.5)	−2.01 (214.4%)	0.432

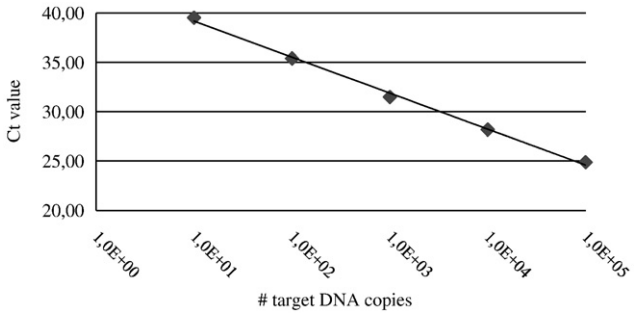

Fig. 3. Standard curve for the real-time PCR assay using following setup: (1) 10-fold serial diluted pGII plasmid was used as standard ranging from 10^5 to 10^1 copies, (2) the real-time PCR reaction plate was sealed using an adhesive film and (3) 7 µl of mineral oil was used as cover layer on top of the real-time PCR reaction mix.

diluted standard series of ssGII as standard positive control and with either the 8-cap strip or the adhesive film as seal type. The use of the 8-cap strip seemed to reduce number of positive NTCs (1/16) compared to when the adhesive film was used (all 4 NTCs positive, with Ct values corresponding to an original concentration of 10 copies). However, the 8-cap strip seemed to reduce the reproducibility of the assay, resulting in a low R^2-value (0.834). The use of the adhesive film resulted in a higher R^2-value (0.997).

The GII NoV real-time PCR was then carried out by using pGII as 10-fold diluted standard positive control (10^5–10 copies), an adhesive film as seal type and 7 µl of mineral oil as cover layer on top of the PCR reaction mixtures (Fig. 3). An efficient (PCR-efficiency of 101.78%), reproducible (R^2-value = 1) and sensitive (detection limit of 10 copies) real-time PCR assay was observed while no amplification occurred in any of the 18 NTCs. A standard curve with a detection limit of 10 copies (with intercept 42.82), a R^2-value of 1 and a slope of −3.28 (corresponding to a PCR-efficiency of 101.78%) indicated that the chosen setup does not have a negative influence on the performance of the real-time PCR assay.

In summary, the above results show that it is recommended to use larger DNA molecules, such as plasmids instead of ssDNA fragments to generate standard curves as positive control in real-time PCR. Moreover, 7 µl of mineral oil on top of the real-time PCR reaction mix attributed to prevent positive NTCs. Since the reduced reproducibility of the real-time PCR assay did not compensate for the reduced number of positive NTCs when the 8-cap strip was applied as seal type, the adhesive film was chosen as the preferred seal type.

4. Discussion

DNA contamination is a reported drawback of conventional and real-time PCR (Josefsson et al., 1999). It has been stated that the risk of DNA contamination has decreased by real-time PCR, due to the closed system which avoids the necessity for the post-PCR handling of amplified material (Klein, 2002; Mackay et al., 2002). Additional systems such as UNG are known methods to prevent carryover contamination of (real-time) PCR amplified material (Pang et al., 1992; Pruvost et al., 2005). However, our results show that these systems do not solve all contamination issues.

A frequent occurrence of positive NTCs was noticed when a ssDNA fragment (ssGII) was used as real-time PCR standard. In contrast, no amplification occurred in any of the NTCs when a plasmid (pGII) was used as standard positive control. Only minor differences in sensitivity were noticed when ssDNA fragments or plasmid DNA were used as real-time PCR standard, confirming previous studies (Moriya et al., 2006). The hypothesis of the positive NTCs being caused by co-evaporation of DNA with water resulting in well-to-well migration of DNA during the real-time PCR was raised and investigated.

Data obtained from the "evaporation-experiment" indicated that evaporation of water and co-evaporation of DNA occurred during a real-time PCR run regardless of the DNA type, seal type (adhesive film and 8-cap strip) or the use of 7 µl of mineral oil as cover layer. An apparent negative correlation between the size of the DNA and the extent of the co-evaporation of the DNA was also noticeable, suggesting the use for larger DNA molecules, such as plasmids instead of ssDNA fragments as standard in real-time PCR.

The higher relative increase in DNA concentration observed when mineral oil was used as cover layer suggests that the mineral oil prevented to some extent the co-evaporation of DNA. A similar conclusion – although to a lesser degree – can be drawn when 8-cap strips were used as seal type.

Given the results of the "evaporation"-experiment, the effect of 2 seal types (adhesive film and 8-cap strip) on the occurrence of positive NTCs was examined. Furthermore, the effect of different amounts of mineral oil on the performance of the real-time PCR was tested. The use of mineral oil and paraffin wax has been suggested before when trying to prevent false-positive PCR results (Rijpens and Herman, 2002; Sparkman, 1992).

The great sensitivity of optimized real-time PCR formats is responsible for the increasing number of detection assays using this technique (Valasek and Repa, 2005). Nevertheless, this high sensitivity should also be considered as a potential risk in the use of high-sensitive techniques because a minor contamination results in positive NTCs (Mobius et al., 2008).

Therefore, we can conclude that it remains necessary to take appropriate measures to obtain reliable results from real-time PCR assays, as different factors can influence the outcome of real-time PCR experiments (Botteldoorn et al., 2006; Werbrouck et al., 2007). A constant awareness should also be focused on the persons executing PCR and in the interpretation of results. These measures can be especially important if PCR is set in routine control or in surveillance studies.

Acknowledgements

This work was supported by Belgian Science Policy — Science for a Sustainable Development (SSD-NORISK-SD/AF/01). The authors would like to thank Ann Vanhee and Jessy Claeys for the excellent technical assistance and Dr. Winy Messens for the statistical analysis of the "evaporation experiment"-data.

References

Abubakar, I., Irvine, L., Aldus, C.M., Wyatt, G.M., Fordham, R., Schelenz, S., Shepstone, L., Howe, A., Peck, M., Hunter, P.R., 2007. A systematic review of the clinical, public health and cost-effectiveness of rapid diagnostic tests for the detection and identification of bacterial intestinal pathogens in faeces and food. Health Technol. Assess. 11, 1–216.

Asanaka, M., Atmar, R.L., Ruvolo, V., Crawford, S.E., Neill, F.H., Estes, M.K., 2005. Replication and packaging of Norwalk virus RNA in cultured mammalian cells. Proc. Natl. Acad. Sci. U. S. A. 102, 10327–10332.

Birnboim, H.C., Doly, J., 1979. Rapid alkaline extraction procedure for screening recombinant plasmid DNA. Nucleic Acids Res. 7, 1513–1523.

Borst, A., Box, A.T.A., Fluit, A.C., 2004. False-positive results and contamination in nucleic acid amplification assays: suggestions for a prevent and destroy strategy. Eur. J. Clin. Microbiol. Infect. Dis. 23, 289–299.

Botteldoorn, N., Van Coillie, E., Grijspeerdt, K., Werbrouck, H., Haesebrouck, F., Donne, E., D'Haese, E., Heyndrickx, M., Pasmans, F., Herman, L., 2006. Real-time reverse transcription PCR for the quantification of the *mntH* expression of *Salmonella enterica* as a function of growth phase and phagosome-like conditions. J. Microbiol. Methods 66, 125–135.

Bustin, S.A., Nolan, T., 2004. Pitfalls of quantitative real-time reverse-transcription polymerase chain reaction. J. Biomol. Tech. 15, 155–166.

Espy, M.J., Uhl, J.R., Sloan, L.M., Buckwalter, S.P., Jones, M.F., Vetter, E.A., Yao, J.D.C., Wengenack, N.L., Rosenblatt, J.E., Cockerill, F.R., Smith, T.F., 2006. Real-time PCR in clinical microbiology: applications for a routine laboratory testing. Clin. Microbiol. Rev. 19, 165–256.

Flamm, R.K., Hinrichs, D.J., Thomashow, M.F., 1984. Introduction of Pam-beta-1 into *Listeria Monocytogenes* by conjugation and homology between native L-monocytogenes plasmids. Infect. Immun. 44, 157–161.

Houde, A., Leblanc, D., Poitras, E., Ward, P., Brassard, J., Simard, C., Trottier, Y.L., 2006. Comparative evaluation of RT-PCR, nucleic acid sequence-based amplification

(NASBA) and real-time RT-PCR for detection of noroviruses in faecal material. J. Virol. Methods 135, 163–172.
Josefsson, A., Livak, K., Gyllensten, U., 1999. Detection and quantitation of human papillomavirus by using the fluorescent 5′ exonuclease assay. J. Clin. Microbiol. 37, 490–496.
Jothikumar, N., Lowther, J.A., Henshilwood, K., Lees, D.N., Hill, V.R., Vinje, J., 2005. Rapid and sensitive detection of noroviruses by using TaqMan-based one-step reverse transcription-PCR assays and application to naturally contaminated shellfish samples. Appl. Environ. Microbiol. 71, 1870–1875.
Kleiboeker, S.B., 2005. Quantitative assessment of the effect of uracil-DNA glycosylase on amplicon DNA degradation and RNA amplification in reverse transcription-PCR. Virol. J. 2, 29.
Klein, D., 2002. Quantification using real-time PCR technology: applications and limitations. Trends Mol. Med. 8, 257–260.
Kwok, S., Higuchi, R., 1989. Avoiding false positives with PCR. Nature 339, 237–238.
Lampel, K.A., Orlandi, P.A., Kornegay, L., 2000. Improved template preparation for PCR-based assays for detection of food-borne bacterial pathogens. Appl. Environ. Microbiol. 66, 4539–4542.
Love, D.C., Casteel, M.J., Meschke, J.S., Sobsey, M.D., 2008. Methods for recovery of hepatitis A virus (HAV) and other viruses from processed foods and detection of HAV by nested RT-PCR and TaqMan RT-PCR. Int. J. Food Microbiol. 126, 221–226.
Mackay, I.M., Arden, K.E., Nitsche, A., 2002. Real-time PCR in virology. Nucleic Acids Res. 30, 1292–1305.
Mobius, P., Hotzel, H., Rassbach, A., Kohler, H., 2008. Comparison of 13 single-round and nested PCR assays targeting IS900, ISMav2, f57 and locus 255 for detection of *Mycobacterium avium* subsp. *paratuberculosis*. Vet. Microbiol. 126, 324–333.
Moriya, Y., Nakamura, T., Okamura, N., Sakaeda, T., Horinouchi, M., Tamura, T., Aoyama, N., Kasuga, M., Okumura, K., 2006. Comparison of synthetic DNA templates with authentic cDNA templates in terms of quantification by real-time quantitative reverse transcription polymerase chain reaction. Biol. Pharm. Bull. 29, 535–538.
Niesters, H.G., 2002. Clinical virology in real time. J. Clin. Virol. 25 (Suppl 3), S3–S12.
Pang, J., Modlin, J., Yolken, R., 1992. Use of modified nucleotides and uracil-DNA glycosylase (Ung) for the control of contamination in the PCR-based amplification of RNA. Mol. Cell. Probes 6, 251–256.
Peters, I.R., Helps, C.R., Hall, E.J., Day, M.J., 2004. Real-time RT-PCR: considerations for efficient and sensitive assay design. J. Immunol. Methods 286, 203–217.
Pruvost, M., Grange, T., Geigl, E.M., 2005. Minimizing DNA contamination by using UNG-coupled quantitative real-time PCR on degraded DNA samples: application to ancient DNA studies. BioTechniques 38, 569–575.
Reynisson, E., Josefsen, M.H., Krause, A., Hoorfar, J., 2006. Evaluation of probe chemistries and platforms to improve the detection limit of real-time PCR. J. Microbiol. Methods 66, 206–216.
Rijpens, N.P., Herman, L.M.F., 2002. Molecular methods for identification and detection of bacterial food pathogens. J. AOAC Int. 85, 984–995.
Rutjes, S.A., Lodder-Verschoor, F., van der Poel, W.H.M., van Duijnhoven, Y.T.H.P., Husman, A.M.D., 2006. Detection of noroviruses in foods: a study on virus extraction procedures in foods implicated in outbreaks of human gastroenteritis. J. Food Prot. 69, 1949–1956.
Sparkman, D.R., 1992. Paraffin wax as a vapor barrier for the PCR. PCR Methods Appl. 2, 180–181.
Speers, D.J., 2006. Clinical applications of molecular biology for infectious diseases. Clin. Biochem. Rev. 27, 39–51.
Straub, T.M., Bentrup, K.H.Z., Orosz-Coghlan, P., Dohnalkova, A., Mayer, B.K., Bartholomew, R.A., Valdez, C.O., Bruckner-Lea, C.J., Gerba, C.P., Abbaszadegan, M., Nickerson, C.A., 2007. *In vitro* cell culture infectivity assay for human noroviruses. Emerg. Infect. Dis. 13, 396–403.
Valasek, M.A., Repa, J.J., 2005. The power of real-time PCR. Adv. Physiol. Educ. 29, 151–159.
Werbrouck, H., Botteldoorn, N., Uyttendaele, M., Herman, L., Van Coillie, E., 2007. Quantification of gene expression of *Listeria monocytogenes* by real-time reverse transcription PCR: optimization, evaluation and pitfalls. J. Microbiol. Methods 69, 306–314.
Wolf, S., Williamson, W.M., Hewitt, J., Rivera-Aban, M., Lin, S., Ball, A., Scholes, P., Greening, G.E., 2007. Sensitive multiplex real-time reverse transcription-PCR assay for the detection of human and animal noroviruses in clinical and environmental samples. Appl. Environ. Microbiol. 73, 5464–5470.

Journal of General Virology (2010), **91**, 2723–2733 DOI 10.1099/vir.0.024109-0

Experimental evidence of recombination in murine noroviruses

Elisabeth Mathijs, Benoît Muylkens,† Axel Mauroy, Dominique Ziant, Thomas Delwiche and Etienne Thiry

Department of Infectious and Parasitic Diseases, Virology and Viral Diseases, Faculty of Veterinary Medicine, University of Liège, 4000 Liège, Belgium

Correspondence
Etienne Thiry
etienne.thiry@ulg.ac.be

Based on sequencing data, norovirus (NoV) recombinants have been described, but no experimental evidence of recombination in NoVs has been documented. Using the murine norovirus (MNV) model, we investigated the occurrence of genetic recombination between two co-infecting wild-type MNV isolates in RAW cells. The design of a PCR-based genotyping tool allowed accurate discrimination between the parental genomes and the detection of a viable recombinant MNV (Rec MNV) in the progeny viruses. Genetic analysis of Rec MNV identified a homologous-recombination event located at the ORF1–ORF2 overlap. Rec MNV exhibited distinct growth curves and produced smaller plaques than the wild-type MNV in RAW cells. Here, we demonstrate experimentally that MNV undergoes homologous recombination at the previously described recombination hot spot for NoVs, suggesting that the MNV model might be suitable for *in vitro* studies of NoV recombination. Moreover, the results show that exchange of genetic material between NoVs can generate viruses with distinct biological properties from the parental viruses.

Received 1 June 2010
Accepted 5 August 2010

INTRODUCTION

Noroviruses (NoVs) are an important cause of acute gastroenteritis in humans worldwide. Since the first description of NoVs in humans in 1968, NoV infections have also been detected in domestic and captive wild animals (Scipioni *et al.*, 2008). The genus *Norovirus* belongs to the family *Caliciviridae*. NoVs are non-enveloped viruses with a single-stranded, positive-sense, polyadenylated RNA genome composed of around 7500 nt. Three overlapping ORFs encode the non-structural (ORF1) and structural (ORF2 and ORF3) viral proteins. The ORF1-encoded polyprotein is cleaved further by the viral proteinase into six mature products with the gene order N-term, NTPase, p18–20/22, genome-linked virus protein (VPg), proteinase and polymerase (Sosnovtsev *et al.*, 2006). NoVs are divided into five genogroups (GI–V) based on their genomic composition (Zheng *et al.*, 2006). Human NoVs are classified into GI, GII and GIV, whereas bovine and murine NoVs (MNVs) cluster respectively into GIII and GV. Other NoVs detected in animals constitute distinct genotypes in GII and GIV: porcine NoVs belong to GII and NoVs detected in a lion cub and young dogs cluster into GIV (Martella *et al.*, 2007, 2008).

Little is known about human NoV biology, due to the lack of a regular cell-culture system or small-animal model for human NoVs. MNVs constitute a substitute for the *in vitro* study of human and other animal NoVs (Wobus *et al.*, 2006), as it is possible for them to be grown in murine macrophages and dendritic cell lines. Viruses can evolve rapidly due to small-scale mutations and recombination. Genetic recombination enables the creation of new combinations of genetic materials, generating more dramatic genomic changes than point mutations. This phenomenon has been described for a large number of RNA viruses (Lai, 1992). Predictive recombination tools together with similarity plots between putative recombinant genomes and the suspected parental genomes have suggested recombination at breakpoints within ORF2 in several MNV genomes (Thackray *et al.*, 2007). Although numerous human and animal recombinant NoVs have been described by phylogenetic analysis (Bull *et al.*, 2007), there is no formal or prospective evidence of recombination occurring in co-infection experiments with two NoV strains, either *in vitro* or *in vivo*.

The aim of this study was to provide experimental evidence of NoV recombination between two genetically related, cultivable MNV isolates, selected as parental isolates.

†Present address: Department of Veterinary Sciences, Physiology, Embryology and Anatomy, Faculty of Sciences, FUNDP, 5000 Namur, Belgium.

The GenBank/EMBL/DDBJ accession number for the consensus nucleotide sequence obtained for Rec MNV covering the ORF1–ORF2 junction is HM044221.

A supplementary table showing primers and probes used in the TaqMan-based discriminative PCR distinguishing between MNV-1 and WU20 is available with the online version of this paper.

Discriminative assays were set up to differentiate between the parental viruses at three loci spanning the entire genome. These assays were further used to analyse the progeny viruses recovered from different co-infections in cell culture. The biological features of the MNV recombinant generated were assessed further *in vitro* in comparison with those of the parental viruses.

RESULTS

Selection of distinguishable parental MNV isolates

Despite their biological diversity, MNV isolates described hitherto cluster into a single genogroup (Thackray *et al.*, 2007). In order to be selected as accurate MNV parental strains involved in co-infection experiments, MNV isolates should: (i) be grown in RAW cells; (ii) induce an obvious cytopathic effect in RAW cell monolayers, enabling a plaque-picking procedure for virus isolation; (iii) be related genetically to each other in order to favour homologous recombination; and (iv) bear sufficient genetic variability for discrimination. Based upon these characteristics, previously published MNV isolates MNV-1.CW1 (MNV-1) and WU20 were selected here for the study of recombination. MNV-1 is the reference MNV strain with pathogenic properties described previously in a mouse model (Karst *et al.*, 2003). WU20 is a field isolate for which pathogenic properties have not yet been determined (Thackray *et al.*, 2007). The two isolates share 87 % nucleotide sequence similarity in their complete genomes, and alignment of their full-length genomes showed maximum sequence similarity at the ORF1–ORF2 junction (Fig. 1a). To determine genetic markers enabling discrimination between MNV-1 and WU20, five RT-PCR fragments were amplified and sequenced (Table 1) from the genes encoding the N-term (locus 1), p18/VPg (locus 2), polymerase (locus 3), major capsid (locus 4) and minor capsid (locus 5) proteins (Fig. 1a). When assembled, these five fragments spanned 26.7 % of the entire genome. Alignment of respective genomic stretches obtained for MNV-1 and WU20 revealed a minimum of 11 point mutations that were used further to differentiate the virus isolates at each selected locus (Fig. 1b). Each discriminative substitution was confirmed by the alignment of five sequences of RT-PCR products obtained independently. Stability of the mutations was further established by sequencing RT-PCR fragments of MNV-1 and WU20 RNA obtained after four successive passages in cell culture (Table 1). Genetic markers were shown to be stable, as only two discriminative mutations (of the 195 detected) between MNV-1 and WU20 were lost after four passages in cell culture.

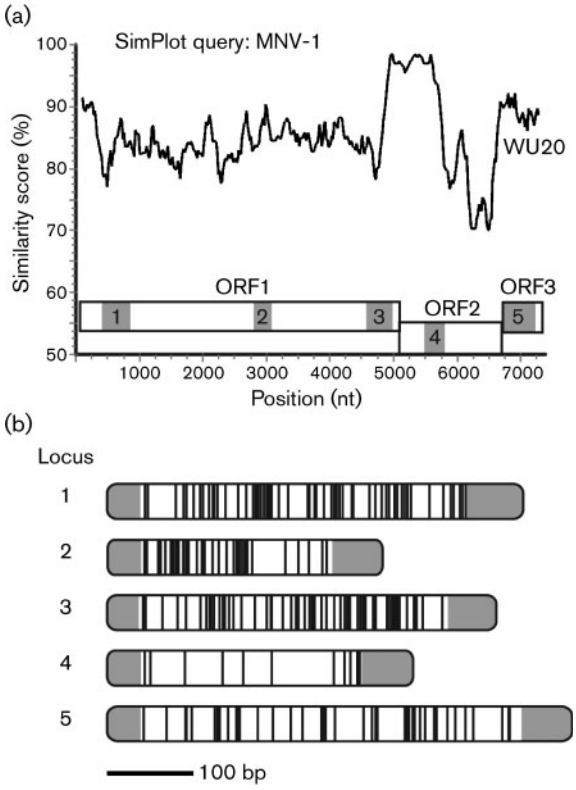

Fig. 1. Similarity plot of full-length genomes from the two parental MNV strains and genetic markers based upon point mutations. (a) SimPlot analysis. Query sequence, MNV-1; window size, 200 bp; step, 20 bp. The ordinate indicates the similarity score between MNV-1 (GenBank accession no. AY228235) and WU20 (EU004665) parental strains and the abscissa indicates the nucleotide positions. A schematic diagram drawn to scale showing the organization of MNV genome and location of the five fragments amplified by RT-PCR is shown. (b) RT-PCR sequencing assays of five amplicons accurately discriminated the two parental strains along the complete genome. Polymorphisms differentiating MNV-1 from WU20 were identified within genes encoding non-structural proteins (ORF1; N-terminal protein, p18/VPg and RNA-dependent RNA polymerase) and structural proteins (ORF2 and ORF3; major and minor capsid protein, respectively). Bars are drawn to scale and represent the five RT-PCR amplicons obtained for each genomic locus. Vertical black lines within the bars indicate the position of the nucleotide polymorphisms between MNV-1 and WU20. Areas filled in grey represent the absence of reliable sequence information due to unidirectional direct sequencing and primer sequences.

Multilocus discrimination between MNV-1 and WU20 by SYBR green- and TaqMan-based PCR assays

Isolates were genotyped at three regions across the genome: two located at the 5′ (N-term locus) and 3′ (ORF3 locus) ends of the genome and one at the polymerase region. Loci 1, 3 and 5 have been chosen for the genotyping assays, despite the fact that slight instability has been observed after four passages in regions 3 and 5. Locus 5 was preferred over locus 4 to allow the detection of potential crossovers within ORF2 or between ORF2 and ORF3. Locus 3 allowed discrimination by melt-curve analysis in SYBR green assays, as the difference in G+C content between parental viruses was sufficient (Table 1). A SYBR green genotyping assay

Table 1. Primers used for the detection of stable genetic markers in the study of recombination between two parental MNV strains, MNV-1 and WU20

The GenBank accession no. for MNV-1 is AY228235. F, Forward; R, reverse. Mixed bases in primers are as follows: Y=C or T; R=A or G.

Locus	Primer sequence (5′–3′)*	Product length (bp) (position in MNV-1)	|ΔG + C content| MNV-1−WU20 (mol%)	Nucleotide conservation after four serial passages (%)	
				MNV-1	WU20
1	**TGTAAAACGACGGCCAGT**TGAGTGGGAGGAGAGGAAG (F)	482 (260–708)	2.01	100.0	100.0
	CAGGAAACAGCTATGACCCCCTCTTCAGCCAGGTGTC (R)				
2	**TGTAAAACGACGGCCAGT**CTCCATTGATGAYTACCTCGC (F)	320 (2735–3018)	2.11	100.0	100.0
	CAGGAAACAGCTATGACCGCACAACACGGGACCAGAT (R)				
3	**TGTAAAACGACGGCCAGT**TAACCCGAGTTGACCCTGAC (F)	452 (4516–4932)	3.60	100.0	99.7
	CAGGAAACAGCTATGACCAGACACGGGAAGCCACAGT (R)				
4	**TGTAAAACGACGGCCAGT**ATTTTTCCCAARGGGTCACTC (F)	356 (5444–5763)	0.44	100.0	100.0
	CAGGAAACAGCTATGACCCTGTATCACGGGCARGTCG (R)				
5	**TGTAAAACGACGGCCAGT**CAAGCCCAGAAGGATCTCAC (F)	469 (6828–7260)	0.46	99.8	100.0
	CAGGAAACAGCTATGACCTCGTGTAGGTGCCTTGAGTC (R)				

*Sequences of standard sequencing primers (−21M13 for F and ReverseM13 for R) are indicated in bold type.

offers the advantage of being more cost-effective and easier to implement than a TaqMan-based assay. For MNV-1, the melt-curve analysis yielded a characteristic sharp peak at 90.2 °C (variation range, 89.8–90.6 °C), whereas the peak melting temperature for WU20 was 88.4 °C (variation range, 88.0–88.6 °C) (Fig. 2a). A 100 % concordance between results of DNA sequencing and T_m-shift genotyping was observed. For the N-term and ORF3 loci, two duplex TaqMan RT-PCR assays were set up for discrimination between MNV-1 and WU20. Each genome-specific probe, designed for hybridization to MNV-1 or WU20 parental viruses, was labelled at the 5′ end with a different fluorescent reporter dye (FAM and Texas red/Cy3, respectively) (see Supplementary Table S1, available in JGV Online). End-point reading of the fluorescence generated during PCR amplification demonstrated that the TaqMan assays were efficacious at discriminating MNV-1 and WU20 specifically at both loci, as shown in Fig. 2(b). DNA sequencing showed a 100 % concordance with the TaqMan PCR assay results. All real-time reactions were shown to be specific by the absence of signal when cDNAs from mock-infected RAW cells were submitted to the discriminative PCR assays. Up to 100-fold dilutions of cDNAs obtained from viral suspension titres of 10^4 p.f.u. ml^{-1} were detected successfully, showing the sensitivity of the PCRs.

Analysis of progeny viruses after MNV-1/WU20 co-infections *in vitro*

Five experiments of co-infection between MNV-1 and WU20 were performed. At least 30 progeny viruses were analysed for each co-infection scenario and were each characterized as either a parental or a recombinant virus by discriminative real-time PCR (Fig. 3a–e). Although differences in the proportion of parental genomes for progeny viruses were observed, none of the MNV-1/WU20 co-infections generated recombinant progeny viruses (Fig. 3a–e). Despite variations in the m.o.i. or the delay of infection, co-inoculation of RAW cells did not allow us to identify recombinant viruses, thereby questioning the ability of MNV-1 and WU20 to recombine in RAW cells. As a basic requirement for the exchange of genetic material between viruses is that both viruses infect a single cell simultaneously, this point was investigated further for MNV-1 and WU20 in RAW cells.

Recombinant virus detection from a co-infected cell by infectious-centre assay

An infectious-centre assay was used (i) to verify that the two virus strains were able to co-infect the same host cell, (ii) to allow further analysis of the progeny virions from a co-infected cell and (iii) to avoid the issue of dominance of one parental virus over the other. Infectious centres were selected randomly in RAW cell monolayers inoculated with a dilution of suspended RAW cells that had previously been co-inoculated by MNV-1 and WU20 at a total m.o.i. of 100 (50 each). RNA extracts from each infectious centre were

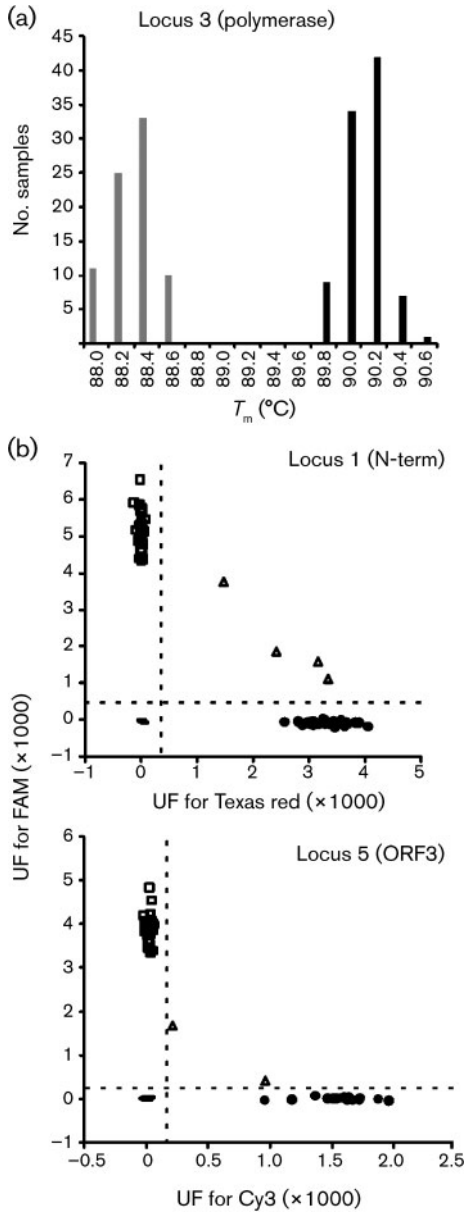

Fig. 2. SYBR green- and TaqMan-based PCR assays discriminating between MNV-1 and WU20. (a) Melt-curve analysis of SYBR green-labelled PCR products, enabling the distinction between MNV-1 (grey bars) and WU20 (black bars) genomes in the polymerase region (locus 3). Mean melting temperatures (T_m) for MNV-1 and WU20 were 90.1 ± 0.15 and 88.3 ± 0.18 °C, respectively. (b) End-point reading of the fluorescence emitted during PCR amplification of loci 1 and 5 discriminating between MNV-1 (□) and WU20 (●). Intensities of Cy3/Texas red and FAM fluorescent signals originating from WU20- and MNV-1-specific probes are plotted on the *x*- and *y*-axes, respectively. UF, Units of fluorescence; △, mixed RNA; –, non-template control and RNA extracted from mock-infected cells.

analysed further for the presence of parental genomes by the TaqMan genotyping assay targeting ORF3. In 13 of the 20 (65 %) infectious centres analysed, both MNV parental genomes were detected, indicating that single, suspended RAW cells were co-infected by MNV-1 and WU20 (Figs 3f and 4a). A total of 122 progeny viruses plaque-purified from a co-infected cell were submitted to the PCR genotyping assays at the three genomic locations described above. One virus showed discordant genotyping at the three loci (Fig. 4b–d). The WU20 signature was detected in the N-term and polymerase regions, whereas the MNV-1 signature was found in the ORF3 region. According to these observations, this progeny virion was generated following recombination occurring between loci 3 and 5 of the MNV genomes.

Genetic and phenotypic characterization of the recombinant virus

In order to confirm that recombination had occurred, the predicted recombination breakpoint of the potential recombinant MNV isolate (Rec MNV) and its parental viruses was sequenced. Alignment of the Rec MNV consensus sequence with the MNV-1 and WU20 sequences showed that the recombination breakpoint is located at the ORF1–ORF2 junction in the region of 123 bp where complete sequence identity was observed between the parental isolates (Fig. 5). Sequences of all five loci were obtained by direct sequencing for the recombinant virus and showed 100 % sequence identity to sequences from the parental viruses, being identical to WU20 for the three loci in ORF1 and to MNV-1 for loci in ORF2 and ORF3 (data not shown). Viability and sequence identities of Rec MNV were maintained during rounds of plaque purification and amplification by three serial passages in RAW cells, indicating that this study was able to generate a viable and stable recombinant virus.

In order to investigate the effect of the recombination event on viral fitness, phenotypic characteristics of Rec MNV were investigated in cell culture. Single-step growth kinetics of the recombinant and parental strains were established from three independent series. Whilst the three viruses showed similar growth curves when total and extracellular virus titres were analysed, differences were observed for intracellular virus production (Fig. 6a). For the parental viruses, intracellular virions constituted the majority of their total virus titres up to 18 h post-infection (p.i.) before extracellular titres exceeded the intracellular titres, probably due to lysis of the infected cells. In contrast, intracellular Rec MNV titres were maintained at a high level up to 24 h p.i. (Fig. 6a). Phenotypic characterization of Rec MNV was completed by plaque-size assays. In order to determine the relevance of the differences in plaque size, a non-parametric statistical method that would take into account the variation in plaque size for each virus was chosen and data were analysed with the Kolmogorov–Smirnov statistic. Results obtained from 64 randomly selected plaques for each virus indicated that Rec MNV produced significantly smaller plaques than the parental isolates, with *P*-values <0.05 (Fig. 6b, c). Taken together,

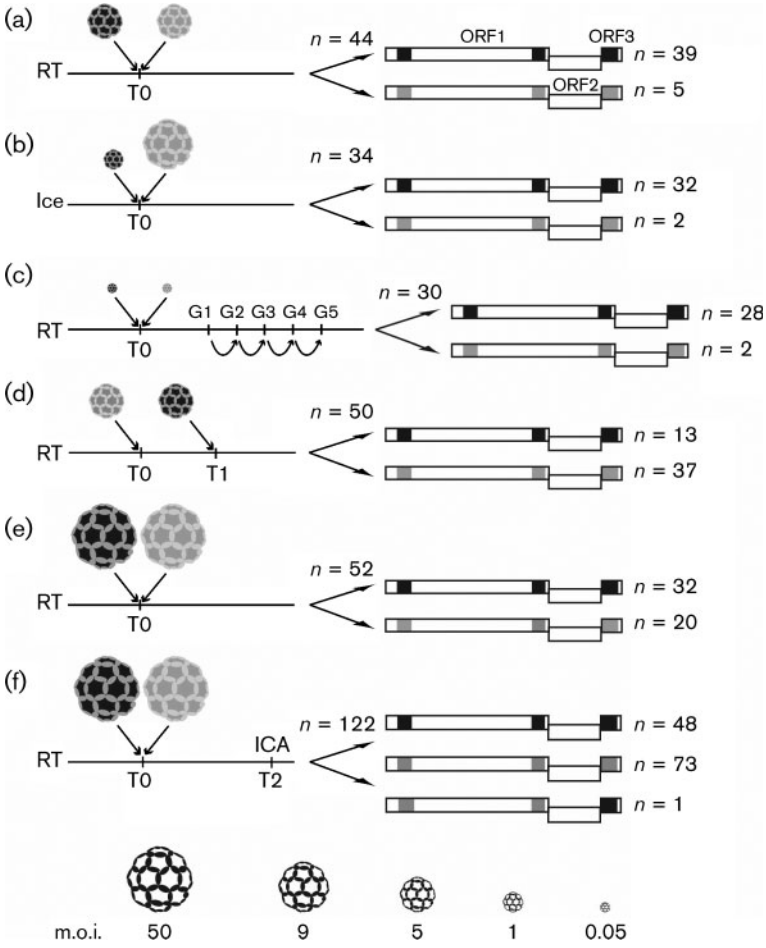

Fig. 3. Experimental schedule of MNV-1 (black)/WU20 (grey) co-infections and results of the screening of the progeny viruses based upon discriminative real-time PCR at three loci of the MNV genome. Numbers indicated above arrows are the total number of progeny viruses screened for each scenario. T0, Time zero. (a) RAW cell monolayer co-infected at an m.o.i. of 10 with an equal proportion of MNV-1 and WU20 (5/5) at room temperature (RT). (b) RAW cells co-infected at an m.o.i. of 10 (MNV-1/WU20, 1/9) on ice. (c) Co-infection at an m.o.i. of 0.1 (0.05/0.05) at RT; progeny viruses were analysed at generation 5 (G5). (d) RAW cells were infected at RT with WU20 at an m.o.i. of 5 followed 1 h later (T1) by superinfection with MNV-1 at an m.o.i. of 5. (e) Co-infection at RT at an m.o.i. of 100 (50/50). (f) Co-infection at RT at an m.o.i. of 100 (50/50) followed by an infectious-centre assay (ICA) at T2. In all scenarios, progeny viruses were analysed from whole-flask lysates at the first generation (G1) except in (c), where progeny viruses were analysed at G5, and (f), where progeny viruses were analysed from a co-infected infectious-centre lysate.

these results indicate that, although similar total virus titres were obtained for all three viruses, Rec MNV seemed to be sequestered longer inside the cell before release. This longer cell association may reduce the spread of Rec MNV to neighbouring cells, thus explaining the smaller plaques.

DISCUSSION

Although phylogenetic analyses have suggested genetic recombination in NoVs (Bull *et al.*, 2007), NoV recombinants have not been identified previously from co-infected cultured cells. Here, using the MNV model, we provide the first experimental evidence of MNV-1 recombination by co-inoculation of two distinguishable parental MNV isolates in RAW cells. Similarly to what has been observed previously for field NoV recombinant viruses (Bull *et al.*, 2005), the crossover region identified in Rec MNV was mapped to a homologous region between the parental MNV-1 and WU20 genomes located at the ORF1–ORF2 junction. Furthermore, our data show that a NoV recombination event yielded a recombinant virus exhibiting biological properties that differ from the parental ones.

In order to provide experimental evidence of recombination between two MNV isolates, we developed a new protocol based on PCR genotyping assays targeting three regions across the entire MNV genome. This tool constitutes a highly sensitive, specific, rapid and robust method for discrimination between the parental viral genomes. Single nucleotide polymorphism (SNP) genotyping assays have recently been validated for use as reliable recombination markers for the study of recombination between two closely related DNA viruses (Muylkens *et al.*, 2009). Here, their use enabled the detection of a recombinant MNV generated *in vitro* and this type of assay would therefore be suitable for *in vivo* MNV recombination studies.

In this study, a chimeric WU20–MNV-1 virus was recovered from one of six permissive co-infection assays in which a total of 332 plaque-isolated progeny viruses were analysed. At an initial m.o.i. of 100 with equal proportions of parental MNV genomes, in contrast to results for whole-flask lysate, analysis by genotyping of viruses from a co-infected infectious-centre lysate allowed the detection of a recombinant virus. Thus, the use of an infectious-centre assay may be required for the detection of recombinant MNVs. Recombination frequencies estimated for other RNA viruses need to be interpreted with care, as there are great disparities between experimental set-ups of *in vitro* RNA recombination studies, and rates vary between

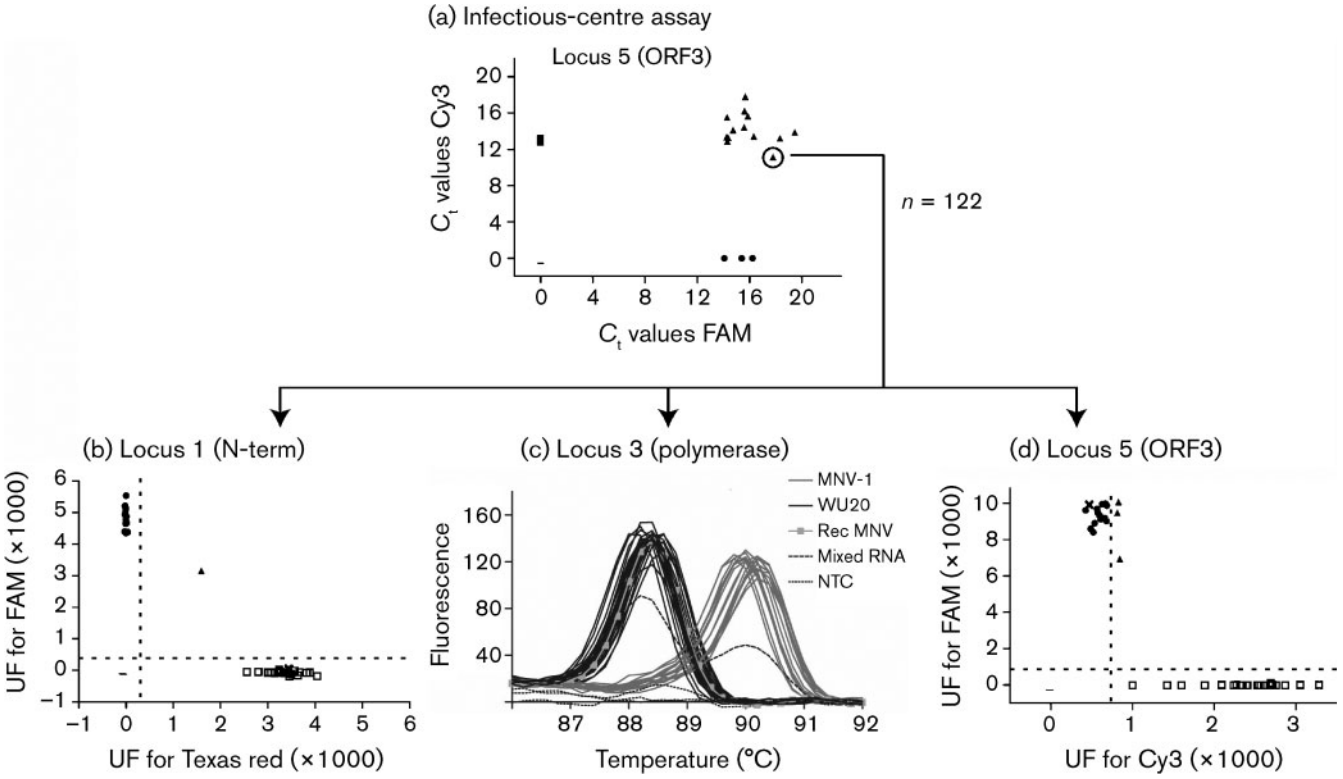

Fig. 4. Detection of a recombinant MNV from a co-infected cell determined by an infectious-centre assay. (a) Twenty infectious centres were selected randomly from RAW cell monolayers previously co-infected by MNV-1 (●) and WU20 (■) at a total m.o.i. of 100 (50 each). ▲, Mixed RNA; NTC, non-template control (–). Both parental genomes could be detected in 13 of 20 infectious centres. Of 122 progeny viruses from one co-infection scenario that were genotyped by PCR in three genomic regions [N-term (b), polymerase (c) and ORF3 (d)], only one virus (Rec MNV; ×) showed discordant genotyping in the three regions. C_t, Threshold cycle; UF, units of fluorescence.

0.13 and 2 % for picornaviruses (Cooper, 1968; Kirkegaard & Baltimore, 1986; McCahon & Slade, 1981). Also, most recombination experiments performed with RNA positive-strand viruses have been designed under extreme positive selection (e.g. with temperature-sensitive, guanidine-resistant or poorly replicative viruses being used as parental viruses) to allow the detection of rare recombination events *in vitro* (Giraudo *et al.*, 1988; Spann *et al.*, 2003). In our study, the MNV recombination frequency obviously exceeded reversion rates and was sufficiently high for the detection of a recombinant genome in the absence of selection pressure. Therefore, NoV recombination rates could be higher than those of other positive-sense RNA viruses. This finding is consistent with the great amount of data available for field NoV recombinant strains based upon sequence analysis (Ambert-Balay *et al.*, 2005; Bull *et al.*, 2007; Jiang *et al.*, 1999; Martella *et al.*, 2009; Mauroy *et al.*, 2009). We are aware that our results might not reflect the actual frequency of crossover between the parental genomes because our method relies upon multiple virus-amplification steps, which only enable the identification of replication-effective recombinants. Moreover, homologous recombination involves genomic transfer between viruses with significant sequence similarity (Kirkegaard & Baltimore, 1986; Meurens *et al.*, 2004), indicating that co-infections of MNV genomes with higher nucleotide identities than the parental genomes used in the present study might yield more recombinant viruses. All in all, on the proviso that the method is optimized further for the generation of recombinants, MNV constitutes a valuable study model for *in vitro* and *in vivo* NoV recombination.

Homologous recombination has been described for a wide range of RNA and DNA viruses (Lai, 1992; Spann *et al.*, 2003; Thiry *et al.*, 2005). A copy-choice mechanism in which the viral RNA polymerase switches templates during RNA synthesis seems to account for the majority of RNA virus recombinants (Lai, 1992). In the present study, the recombination crossover for Rec MNV has been shown to lie near the ORF1–ORF2 junction, but we were unable to define the point more precisely due to the perfect identity between parental strains across 123 bp in this region. Recombination hot spots have also been found in other RNA viruses, including poliovirus, brome mosaic virus and retroviruses (Fan *et al.*, 2007; Nagy & Simon, 1997; Tolskaya *et al.*, 1987). Such hot spots are either sequence-dependent

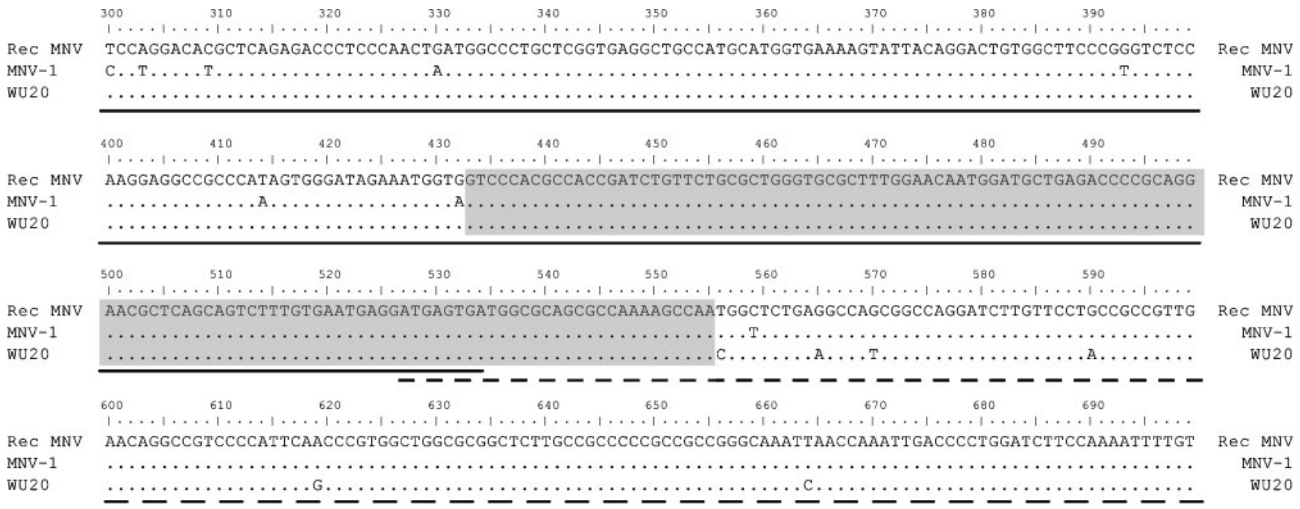

Fig. 5. Sequence alignment of a 1530 bp fragment covering the ORF1–ORF2 junction of MNV recombinant (Rec MNV) and parental (MNV-1 and WU20) viruses. Nucleotide identities with the upper sequence are represented by dots. The boxed grey area represents the region (123 bp) that potentially served as breaking point in the RNA recombination event. Sequences corresponding to the 3′ end of ORF1 and the 5′ end of ORF2 are indicated by a continuous and a dashed line, respectively.

or associated with RNA secondary structures. Sequence analysis of field NoV, sapovirus and feline calicivirus recombinants has stipulated the ORF1–ORF2 junction to be a preferential breakpoint for recombination (Bull *et al.*, 2005; Coyne *et al.*, 2006; Hansman *et al.*, 2005). Indeed, this region has been shown to exhibit a marked suppression of synonymous variability that coincides precisely with stem–loop RNA secondary structures on the anti-genomic strand upstream of a subgenomic transcript within each genus of the family *Caliciviridae*, including MNV (Simmonds *et al.*, 2008). In the present study, when the anti-genomic RNA sequence of the homologous region, including the crossover point between MNV-1 and WU20, was submitted for RNA secondary-structure prediction, a similar stem–loop structure was observed (data not shown). This suggests that viral RNA secondary structures in this region may enhance RNA recombination in MNV, as they are predicted either to hold recombination sites in close proximity, acting as a 'handle' for the RNA-dependent RNA polymerase to grab the acceptor strand, or to contribute to polymerase pausing. Thus, our data provide some experimental evidence in support of the recombination model for NoVs proposed by Bull *et al.* (2005). Phylogenetic shifts, probably due to recombination events, have been described previously in MNV genomes (Thackray *et al.*, 2007). In contrast to our observation, most of the predicted crossover sites were located in ORF2 or at the ORF2–ORF3 junction. One explanation for this discrepancy could be that recombination hot spots might differ depending on experimental or field conditions. Also, convergent evolution could be responsible for phylogenetic disagreement among MNV sequences. Additional experimental and field data will be needed to identify MNV recombination hot spots.

RNA recombination is thought to be a major driving force in virus evolution (Worobey & Holmes, 1999). In this study, phenotypic characteristics of Rec MNV were investigated in cell culture in order to understand the biological benefits caused by recombination. Plaque-size analysis together with intracellular growth-curve kinetics of Rec MNV, in comparison with those of the parental viruses, indicated a reduction in fitness *in vitro*, probably due to less efficient virus egress. However, an effect due to a different cell-passage history could not be ruled out because changes in virus phenotypes have previously been observed throughout subsequent cell passaging (Wobus *et al.*, 2004). The altered phenotype of Rec MNV could be explained by the fact that viral processes could be influenced by suboptimal interactions between the non-structural proteins and the structural proteins acquired from each parental virus. Evidence based on recombinants generated from a small, ssDNA virus, maize streak virus, demonstrated that fragments of genetic material only function optimally if they reside within genomes similar to those in which they evolved (Martin *et al.*, 2005). Observations made for field NoV recombinants may indicate that shifts between NoV genomic materials could generate viruses with increased virulence in hosts. From 2000 to 2002, sporadic cases as well as outbreaks of gastroenteritis were linked with recombinant NoV GIIb variants throughout Europe (Ambert-Balay *et al.*, 2005; Reuter *et al.*, 2006). Later, GIIb recombinants were identified in a wide range of countries, indicating their widespread distribution across continents (Bruggink & Marshall, 2009; Fukuda *et al.*, 2008; Gomes *et al.*, 2007). It is possible that recombination was able to give rise to novel NoV strains capable of epidemic spread in human

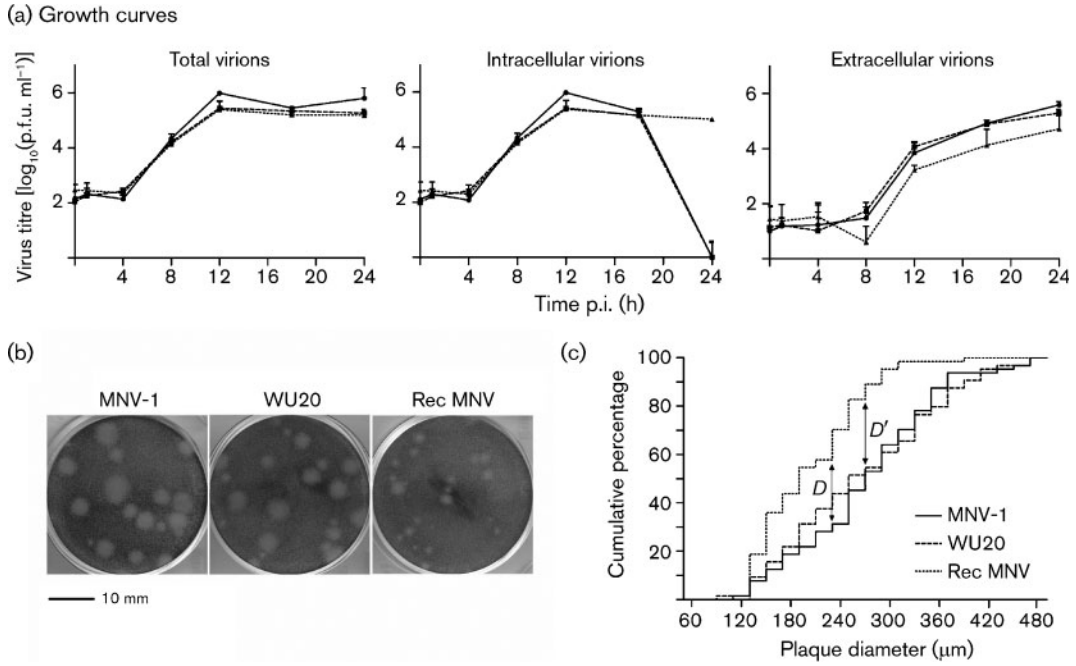

Fig. 6. *In vitro* growth properties of Rec MNV. (a) Single-step growth kinetics of MNV-1 (●), WU20 (■) and Rec MNV (▲). Data for total, intracellular and extracellular MNV virions were obtained after infection of RAW 264.7 cells at an m.o.i. of 5. Virus titres, expressed as p.f.u., are means + SD of triplicates. (b) RAW cell monolayers were infected with dilutions of MNV-1, WU20 and Rec MNV (passages 5, 4 and 3, respectively) and processed by plaque assay. Cells were fixed by adding 4 % formaldehyde and plaques were visualized with crystal violet staining. Pictures were taken of wells with dilutions showing individual plaques. (c) Plaque sizes of Rec MNV were compared with the parental ones by Kolmogorov–Smirnov statistic. From a total of 64 randomly selected plaques measured in each virus population, the cumulative percentage of plaques within increasing diameter ranges was calculated. Data were plotted with the diameter values of plaque size on the *x*-axis and the cumulative percentage on the *y*-axis. Rec MNV was compared with its parental strains by calculating maximum absolute difference (D_{max}) between the cumulative percentage of Rec MNV and its parental strains MNV-1 and WU20 (referred to as *D* and *D′*, respectively). Two-tailed *P*-values were used to determine the level of significance between the compared populations (Muylkens *et al.*, 2006). The *D* calculated for Rec MNV/MNV-1 gave a *P*-value <0.0001, and the *D′* for Rec MNV/WU20 gave a *P*-value <0.0011. For MNV-1/WU20, the D_{max} value gave a *P*-value of 0.9497.

populations. This study provides experimental proof for the acquisition of novel biological properties of an MNV that had undergone recombination. The effect of recombination upon the virulence of recombinant viruses needs be evaluated through *in vivo* studies in mice, the natural host of MNV.

In conclusion, a recombinant virus was generated by co-inoculation of RAW cells with two distinguishable MNV isolates in the absence of selection markers. The MNV model appears to be suitable for the study of NoV recombination in cell culture in the absence of available culture systems for human NoVs. Additional *in vitro* and *in vivo* studies would enable further insights into NoV genetic-diversifying mechanisms such as recombination.

METHODS

Viruses and cells. MNV isolates [MNV-1.CW1 and WU20 (Thackray *et al.*, 2007)] were propagated in RAW 264.7 cells (ATCC TIB-71) grown in Dulbecco's modified Eagle's medium (Invitrogen) complemented (DMEMc) with 10 % heat-inactivated FCS (BioWhittaker), 2 % penicillin (5000 U ml^{-1}) and streptomycin (5000 μg ml^{-1}) (PS; Invitrogen) and 1 % HEPES buffer (1 M; Invitrogen).

Virus stocks were produced by infection of RAW cells at an m.o.i. of 0.05. Two days p.i., cells and medium were harvested and clarified by centrifugation for 20 min (1000 ***g***) after two freeze/thaw cycles. Supernatants were purified by ultracentrifugation on a 30 % sucrose cushion in an SW28 rotor (Beckman Coulter) at 25 000 r.p.m. for 4 h at 4 °C. Pellets were resuspended in PBS, aliquotted and frozen at −80 °C.

Plaque assay and plaque purification of MNV isolates. Titres of each virus production were determined by plaque assay as described by Hyde *et al.* (2009). MNV isolates were plaque-purified three times following a plaque-picking method adapted from the plaque-assay method.

Co-infection experiments. Monolayers of RAW cells prepared in 25 cm^2 flasks (6.5×10^6 cells) were infected by MNV-1, WU20 or both viruses at an m.o.i. of 10. Further co-infections were performed under different conditions. Briefly, co-infections were carried out

either at room temperature or on ice. Different m.o.i.s of each parental virus for co-infection were used and supernatants were collected for analysis either after 24 h or after five serial passages. Finally, superinfection of MNV-1 upon WU20 with a 1 h delay was performed. After 1 h infection, inocula were removed and cells were washed thoroughly with sterile PBS before the addition of fresh medium. Forty-eight hours after infection, cells and medium were harvested and clarified after two freeze/thaw cycles.

Isolation and screening of progeny viruses. A plaque assay for virus isolation was set up by modifying the protocol described by Hyde *et al.* (2009). Briefly, RAW 264.7 monolayers cultured in six-well plates (1.5×10^6 cells per well) were infected with 1 ml of the appropriate dilution per well at room temperature. After 1 h, the inoculum was removed and cells were overlaid with 2 ml medium containing 70 % DMEM-Glutamax (4.5 g glucose l^{-1} and 15 mM sodium hydrogen carbonate), 2.5 % FCS, 2 % PS, 1 % HEPES and 0.7 % SeaPlaque agarose (Lonza). After 2 days incubation at 37 °C with 5 % CO_2, cells were stained for visualization by adding 2 ml minimum essential medium (Invitrogen)/1 % low-melting-point agarose containing 0.01 % neutral red. Individual plaques were picked and propagated by inoculation onto RAW cells grown in 24-well plates. After 72 h (a time corresponding to the cytopathic effect generated by plaque-purified isolates), supernatants were collected and frozen at −80 °C before further analysis.

Infectious-centre assay. In order to determine whether RAW cells were infected by both MNV strains, an infectious-centre assay was carried out with a 50 : 50 mixture of MNV-1 and WU20 at an m.o.i. of 100 as described by Chuang & Chen (2009). After 2 days, viruses from infectious centres (plaques) were isolated and virus infection was verified by genome amplification by a discriminative TaqMan-based PCR as described below.

Viral RNA preparation, RT-PCR and sequencing. Viral RNA from parental and progeny viruses was extracted from 100 µl supernatant of MNV-infected RAW cells with an RNeasy mini kit (Qiagen) according to the manufacturer's instructions. RNA extracts were stored at −80 °C until use. Five fragments of 300–600 bp were amplified with hybrid primers, specific to the viral sequence and harbouring the sequence of the M13 forward and reverse primers at their 5′ end (Vende *et al.*, 1995) (Table 1). First-stranded cDNA was generated by an iScript cDNA Synthesis kit (Bio-Rad). PCRs were carried out on 3 µl cDNA in 50 µl nuclease-free water containing 300 nM of both forward and reverse primers, 0.1 mM dNTPs, 2.5 % DMSO, 20 mM Tris/HCl, 10 mM $(NH_4)_2SO_4$, 10 mM KCl, 2 mM $MgSO_4$, 0.1 % Triton X-100 and 1 U *Taq* DNA Polymerase (New England Biolabs). Two successive PCR-amplification cycles with distinct annealing temperatures were performed as described by Vende *et al.* (1995). Amplicons were visualized by electrophoresis and purified by ethanol precipitation. Direct sequencing of PCR products was carried out by GATC Biotech sequencing facilities (Konstanz, Germany) with reverse primer M13 using an ABI 3730xl DNA Analyzer (Applied Biosystems). In order to obtain sequences covering the ORF1–ORF2 junction, PCR was performed with the forward primer from locus 3 and the reverse primer from locus 4 in order to amplify a 1578 bp long fragment. The reaction was carried out with iProof High Fidelity DNA polymerase (Bio-Rad) on 2 µl cDNA in a reaction volume of 50 µl according to the manufacturer's instructions. After purification, fragments were cloned into a pGEM-T Easy cloning vector (Promega) before being sequenced in both directions at GATC Biotech sequencing facilities (Konstanz, Germany).

Virus discrimination. For locus 3, a SYBR green assay with the hybrid primer pair 3 in the polymerase region was implemented (Table 1). One microlitre of cDNA was added to a 20 µl reaction volume containing 10 µl iQ SYBR Green Supermix (Bio-Rad), 10 pmol each of forward and reverse primers and 9.5 µl nuclease-free water. The PCR-amplification protocol consisted of 3 min at 95 °C, followed by 35 cycles of 10 s at 95 °C, 45 s at 50 °C and 45 s at 72 °C.

For the N-term and ORF3 regions (loci 1 and 3), a multiplex TaqMan real-time PCR was developed for discrimination between MNV-1 and WU20 based upon SNPs in the sequences targeted by fluorogenic TaqMan oligoprobes (Supplementary Table S1). One microlitre of cDNA was added to a 20 µl reaction volume containing 10 µl of iQ Supermix (Bio-Rad). Final concentrations of primers and probes are indicated in Supplementary Table S1. Amplification cycles were performed as follows: 5 min at 95 °C, followed by 30 cycles of 10 s at 95 °C and 40 s at 60 °C.

Bioinformatics. Sequence analyses and alignments were carried out in the BioEdit Sequence Editor software version 7.0.9.0 (Hall, 1999). Complete-genome sequence-similarity analysis was performed by using SimPlot software, available at http://sray.med.som.jhmi.edu/SCRoftware/simplot (Lole *et al.*, 1999). G+C content analysis was performed using CPGPLOT software (http://bioweb.pasteur.fr/docs/EMBOSS/cpgplot.html) (Larsen *et al.*, 1992).

One-step virus growth analysis and plaque-size determination. RAW cells cultured in 24-well plates were infected by the respective viruses at an m.o.i. of 5. After 1 h incubation on ice, the inoculum was removed and the cells were washed three times with PBS to remove unbound virus, followed by the addition of DMEMc. Plates were incubated at 37 °C for the stated length of time; time zero indicates the time at which the medium was added. After 0, 1, 4, 8, 12, 18 and 24 h incubation, an aliquot of the culture medium was removed and, together with infected cell monolayers, frozen at −80 °C. Virus titres were determined by plaque assay as described by Hyde *et al.* (2009). Plaque surfaces and diameters were determined with the ImageJ Java-based image-processing program (http://rsb.info.nih.gov/ij/).

Statistical analysis. The plaque sizes of Rec MNV were compared with the parental ones by the Kolmogorov–Smirnov statistic (Lilliefors, 1967; Muylkens *et al.*, 2006).

GenBank accession number. The consensus nucleotide sequence obtained for Rec MNV covering the ORF1–ORF2 junction was deposited in GenBank/EMBL/DDBJ under the accession no. HM044221.

ACKNOWLEDGEMENTS

We thank Professor Herbert Virgin and Dr Larissa Thackray (Washington University, St Louis, MO, USA) for providing the MNV isolates and RAW 264.7 cells; Professor Mieke Uyttendaele, Dr Leen Baert and Ambroos Stals for their help with MNV cell culture and virus production; and Professor Nadine Antoine for her contribution to plaque-size determination. This study was supported by grants from the Belgian Science Policy 'Science for a Sustainable Development' (SD/AF/01), the Fonds de la Recherche Scientifique (FRS-FNRS) (2.4624.09) and the University of Liège 'Fonds speciaux pour la Recherche-crédits classiques' 2008–2009 (C-09/60).

REFERENCES

Ambert-Balay, K., Bon, F., Le Guyader, F., Pothier, P. & Kohli, E. (2005). Characterization of new recombinant noroviruses. *J Clin Microbiol* **43**, 5179–5186.

Bruggink, L. D. & Marshall, J. A. (2009). Molecular and epidemiological features of GIIb norovirus outbreaks in Victoria, Australia, 2002–2005. *J Med Virol* **81**, 1652–1660.

Bull, R. A., Hansman, G. S., Clancy, L. E., Tanaka, M. M., Rawlinson, W. D. & White, P. A. (2005). Norovirus recombination in ORF1/ORF2 overlap. *Emerg Infect Dis* **11**, 1079–1085.

Bull, R. A., Tanaka, M. M. & White, P. A. (2007). Norovirus recombination. *J Gen Virol* **88**, 3347–3359.

Chuang, C. K. & Chen, W. J. (2009). Experimental evidence that RNA recombination occurs in the Japanese encephalitis virus. *Virology* **394**, 286–297.

Cooper, P. D. (1968). A genetic map of poliovirus temperature-sensitive mutants. *Virology* **35**, 584–596.

Coyne, K. P., Reed, F. C., Porter, C. J., Dawson, S., Gaskell, R. M. & Radford, A. D. (2006). Recombination of Feline calicivirus within an endemically infected cat colony. *J Gen Virol* **87**, 921–926.

Fan, J., Negroni, M. & Robertson, D. L. (2007). The distribution of HIV-1 recombination breakpoints. *Infect Genet Evol* **7**, 717–723.

Fukuda, S., Sasaki, Y., Takao, S. & Seno, M. (2008). Recombinant norovirus implicated in gastroenteritis outbreaks in Hiroshima Prefecture, Japan. *J Med Virol* **80**, 921–928.

Giraudo, A. T., Gomes, I., de Mello, P. A., Beck, E., La Torre, J. L., Scodeller, E. A. & Bergmann, I. E. (1988). Behavior of intertypic recombinants between virulent and attenuated aphthovirus strains in tissue culture and cattle. *J Virol* **62**, 3789–3794.

Gomes, K. A., Stupka, J. A., Gomez, J. & Parra, G. I. (2007). Molecular characterization of calicivirus strains detected in outbreaks of gastroenteritis in Argentina. *J Med Virol* **79**, 1703–1709.

Hall, T. A. (1999). BioEdit: a user friendly biological sequence alignment editor and analysis program for Windows 95/98/NT. *Nucleic Acids Symp Ser* **41**, 95–98.

Hansman, G. S., Takeda, N., Oka, T., Oseto, M., Hedlund, K. O. & Katayama, K. (2005). Intergenogroup recombination in sapoviruses. *Emerg Infect Dis* **11**, 1916–1920.

Hyde, J. L., Sosnovtsev, S. V., Green, K. Y., Wobus, C., Virgin, H. W., IV & Mackenzie, J. M. (2009). Mouse norovirus replication is associated with virus-induced vesicle clusters originating from membranes derived from the secretory pathway. *J Virol* **83**, 9709–9719.

Jiang, X., Espul, C., Zhong, W. M., Cuello, H. & Matson, D. O. (1999). Characterization of a novel human calicivirus that may be a naturally occurring recombinant. *Arch Virol* **144**, 2377–2387.

Karst, S. M., Wobus, C. E., Lay, M., Davidson, J. & Virgin, H. W., IV (2003). STAT1-dependent innate immunity to a Norwalk-like virus. *Science* **299**, 1575–1578.

Kirkegaard, K. & Baltimore, D. (1986). The mechanism of RNA recombination in poliovirus. *Cell* **47**, 433–443.

Lai, M. M. (1992). RNA recombination in animal and plant viruses. *Microbiol Rev* **56**, 61–79.

Larsen, F., Gundersen, G., Lopez, R. & Prydz, H. (1992). CpG islands as gene markers in the human genome. *Genomics* **13**, 1095–1107.

Lilliefors, H. W. (1967). On the Kolmogorov–Smirnov test for normality with mean and variance unknown. *J Am Stat Assoc* **62**, 399–402.

Lole, K. S., Bollinger, R. C., Paranjape, R. S., Gadkari, D., Kulkarni, S. S., Novak, N. G., Ingersoll, R., Sheppard, H. W. & Ray, S. C. (1999). Full-length human immunodeficiency virus type 1 genomes from subtype C-infected seroconverters in India, with evidence of intersubtype recombination. *J Virol* **73**, 152–160.

Martella, V., Campolo, M., Lorusso, E., Cavicchio, P., Camero, M., Bellacicco, A. L., Decaro, N., Elia, G., Greco, G. & other authors (2007). Norovirus in captive lion cub (*Panthera leo*). *Emerg Infect Dis* **13**, 1071–1073.

Martella, V., Lorusso, E., Decaro, N., Elia, G., Radogna, A., D'Abramo, M., Desario, C., Cavalli, A., Corrente, M. & other authors (2008). Detection and molecular characterization of a canine norovirus. *Emerg Infect Dis* **14**, 1306–1308.

Martella, V., Decaro, N., Lorusso, E., Radogna, A., Moschidou, P., Amorisco, F., Lucente, M. S., Desario, C., Mari, V. & other authors (2009). Genetic heterogeneity and recombination in canine noroviruses. *J Virol* **83**, 11391–11396.

Martin, D. P., van der Walt, E., Posada, D. & Rybicki, E. P. (2005). The evolutionary value of recombination is constrained by genome modularity. *PLoS Genet* **1**, e51.

Mauroy, A., Scipioni, A., Mathijs, E., Thys, C. & Thiry, E. (2009). Molecular detection of kobuviruses and recombinant noroviruses in cattle in continental Europe. *Arch Virol* **154**, 1841–1845.

McCahon, D. & Slade, W. R. (1981). A sensitive method for the detection and isolation of recombinants of foot-and-mouth disease virus. *J Gen Virol* **53**, 333–342.

Meurens, F., Keil, G. M., Muylkens, B., Gogev, S., Schynts, F., Negro, S., Wiggers, L. & Thiry, E. (2004). Interspecific recombination between two ruminant alphaherpesviruses, bovine herpesviruses 1 and 5. *J Virol* **78**, 9828–9836.

Muylkens, B., Meurens, F., Schynts, F., de Fays, K., Pourchet, A., Thiry, J., Vanderplasschen, A., Antoine, N. & Thiry, E. (2006). Biological characterization of bovine herpesvirus 1 recombinants possessing the vaccine glycoprotein E negative phenotype. *Vet Microbiol* **113**, 283–291.

Muylkens, B., Farnir, F., Meurens, F., Schynts, F., Vanderplasschen, A., Georges, M. & Thiry, E. (2009). Coinfection with two closely related alphaherpesviruses results in a highly diversified recombination mosaic displaying negative genetic interference. *J Virol* **83**, 3127–3137.

Nagy, P. D. & Simon, A. E. (1997). New insights into the mechanisms of RNA recombination. *Virology* **235**, 1–9.

Reuter, G., Vennema, H., Koopmans, M. & Szucs, G. (2006). Epidemic spread of recombinant noroviruses with four capsid types in Hungary. *J Clin Virol* **35**, 84–88.

Scipioni, A., Mauroy, A., Vinje, J. & Thiry, E. (2008). Animal noroviruses. *Vet J* **178**, 32–45.

Simmonds, P., Karakasiliotis, I., Bailey, D., Chaudhry, Y., Evans, D. J. & Goodfellow, I. G. (2008). Bioinformatic and functional analysis of RNA secondary structure elements among different genera of human and animal caliciviruses. *Nucleic Acids Res* **36**, 2530–2546.

Sosnovtsev, S. V., Belliot, G., Chang, K. O., Prikhodko, V. G., Thackray, L. B., Wobus, C. E., Karst, S. M., Virgin, H. W., IV & Green, K. Y. (2006). Cleavage map and proteolytic processing of the murine norovirus nonstructural polyprotein in infected cells. *J Virol* **80**, 7816–7831.

Spann, K. M., Collins, P. L. & Teng, M. N. (2003). Genetic recombination during coinfection of two mutants of human respiratory syncytial virus. *J Virol* **77**, 11201–11211.

Thackray, L. B., Wobus, C. E., Chachu, K. A., Liu, B., Alegre, E. R., Henderson, K. S., Kelley, S. T. & Virgin, H. W., IV (2007). Murine noroviruses comprising a single genogroup exhibit biological diversity despite limited sequence divergence. *J Virol* **81**, 10460–10473.

Thiry, E., Meurens, F., Muylkens, B., McVoy, M., Gogev, S., Thiry, J., Vanderplasschen, A., Epstein, A., Keil, G. & Schynts, F. (2005). Recombination in alphaherpesviruses. *Rev Med Virol* **15**, 89–103.

Tolskaya, E. A., Romanova, L. I., Blinov, V. M., Viktorova, E. G., Sinyakov, A. N., Kolesnikova, M. S. & Agol, V. I. (1987). Studies on the recombination between RNA genomes of poliovirus: the primary structure and nonrandom distribution of crossover regions in the genomes of intertypic poliovirus recombinants. *Virology* **161**, 54–61.

Vende, P., Le Gall, G. & Rasschaert, D. (1995). An alternative method for direct sequencing of PCR products, for epidemiological studies performed by nucleic sequence comparison. Application to rabbit haemorrhagic disease virus. *Vet Res* **26**, 174–179.

Wobus, C. E., Karst, S. M., Thackray, L. B., Chang, K. O., Sosnovtsev, S. V., Belliot, G., Krug, A., Mackenzie, J. M., Green, K. Y. & Virgin, H. W., IV (2004). Replication of *Norovirus* in cell culture reveals a tropism for dendritic cells and macrophages. *PLoS Biol* **2**, e432.

Wobus, C. E., Thackray, L. B. & Virgin, H. W., IV (2006). Murine norovirus: a model system to study norovirus biology and pathogenesis. *J Virol* **80**, 5104–5112.

Worobey, M. & Holmes, E. C. (1999). Evolutionary aspects of recombination in RNA viruses. *J Gen Virol* **80**, 2535–2543.

Zheng, D. P., Ando, T., Fankhauser, R. L., Beard, R. S., Glass, R. I. & Monroe, S. S. (2006). Norovirus classification and proposed strain nomenclature. *Virology* **346**, 312–323.

ALTERNATIVE ATTACHMENT FACTORS AND INTERNALISATION PATHWAYS FOR GIII.2 BOVINE NOROVIRUSES

Axel Mauroy[1], Laurent Gillet[2], Elisabeth Mathijs[1], Alain Vanderplasschen[2], Etienne Thiry[1,*].

[1] Virology and Viral Diseases, [2] Immunology, Department of Infectious and Parasitic Diseases, Faculty of Veterinary Medicine, University of Liège, 4000 Liège, Belgium

* Corresponding author. Tel.: +3243664250 ; fax: +3243664261

E-mail address: etienne.thiry@ulg.ac.be (E. Thiry)

Running title: Binding and entry pathways for bovine noroviruses

Summary: 156 words

Text: 5391 words

Figures: 5

Table: 1

Summary

Bovine noroviruses belong to the family *Caliciviridae,* genus *Norovirus*. Two genotypes are described and viruses genetically related to the Jena and Newbury-2 strains are classified into genotypes 1 and 2 respectively. In this study, virus-like particles (VLP) of the previously detected B309 Belgian strain, genetically related to genotype 2 bovine noroviruses, were used to investigate virus-host interactions *in vitro*. B309 VLP were shown to bind to several bovine cell lines. This binding was not affected by heparinase or chondroitinase treatment but was significantly inhibited by both sodium periodate, α-galactosidase, trypsin and phospholipase C treatment. Cell treatment by neuraminidase also moderately affected this binding. Taken together, these results show that, in addition to a galactosyl residue, sialic acid could also be involved in binding to susceptible cells. In addition, both the caveolae/lipid raft-associated pathway and macropinocytosis are used for B309 VLP internalisation by Madin-Darby Bovine Kidney cells. The data increase the knowledge on bovine norovirus cell interactions.

Keywords: norovirus, bovine, binding, ligand, receptor, internalisation,

Introduction

Norovirus (NoV)-like sequences and particles are found in several animal species (Mauroy *et al*., 2008; Scipioni *et al*., 2008) including the bovine species (Bridger *et al*., 1984;Woode & Bridger, 1978). They are non enveloped, single stranded RNA viruses belonging to the genus *Norovirus,* family *Caliciviridae,* in which four other genera (*Vesivirus, Lagovirus, Sapovirus* and *Nebovirus*) are also currently officially described (Green, 2007; http://www.ictvonline.org/virusTaxonomy.asp?version=2009). Animal NoV and human noroviruses (HuNoV), steadily reported as the main viral aetiology in an overwhelming proportion of human gastroenteritis cases and outbreaks, are divided into five genogroups (G) on the basis of phylogenetic analysis. All bovine noroviruses (BoNoV) sequences fall into GIII which is further divided into two genotypes. BoNoV genetically related to the reference strains Jena virus (JV) or Newbury2 (NB2) are classified into genotype 1 or 2, respectively (Liu *et al*., 1999; Oliver *et al*., 2007). To date, the large majority of NoV sequences detected in the bovine species have been genetically related to the NB2 genome and thus, this genotype seems to be the most prevalent worldwide (Han et *al*., 2004; Ike *et al*., 2007; Mauroy *et al*., 2009a, 2009b; Milnes *et al*., 2007; Park *et al*., 2007; Van Der Poel *et al*., 2003; Wise *et al*., 2004).

The study of NoV has been historically hampered by the lack of an efficient cell culture system (Duizer *et al.*, 2004) which is still not available for BoNoV. However, virus-like particles (VLP) can be rapidly obtained by different protein expression systems and these VLP have been shown to be morphologically and antigenically similar to the native strain (Han *et al*., 2005; Jiang *et al*., 1992).

Viral attachment can be facilitated by cell surface molecules recruiting viral particles into the extracellular compartment and facilitating their presentation to a cell-specific receptor (Smith

& Helenius, 2004). In this way, carbohydrates belonging to glycoaminoglycan chains of the cell surface proteoglycans and glycoproteins are often used by viruses (Vanderplasschen *et al.*, 1993). During co-evolution with their host, shift in receptor usage and capacity to exploit an alternative entry pathway may enhance the viral adaptation and modify their host range and their pathogenesis (Baranowski *et al.*, 2001). Several carbohydrate binding patterns are well described in the family *Caliciviridae*. Although junctional adhesion molecule 1 has been identified as a specific receptor for feline calicivirus (FCV) F9 strain (Makino *et al.*, 2006), this molecule was not implied in the binding of some other strains (Ossiboff and Parker, 2007) and α2,6-linked sialic acid has been shown to play the role of anchor in the primary binding steps (Stuart & Brown, 2007). Rabbit haemorrhagic disease virus (RHDV) mediates haemagglutination which has been explained by its ability to bind to carbohydrates structures related to the human blood group antigens (HBGA) expressed on human red blood cells (Ruvoen-Clouet *et al.*, 2000). These HBGA have been recognised for several years as candidate binding factors for HuNoV, with different binding patterns independent of the genotype classification (Tan & Jiang, 2005). Recently, Zhakour and collaborators (2009) identified the α-gal epitope (Galalpha1,3Galbeta1,4GlcNAc-R, known as Galili epitope), also related to the HBGA family (Macher & Galili, 2008), as a terminal residue involved in the binding of a Newbury2-related BoNoV. However, the concept of multi-receptors usage in the genus *Norovirus* was reinforced by the report of GII HuNoVLP binding to heparan sulphates by Tamura and collaborators (2004) and a recent outbreak caused by a GI.3 genetically related HuNoV affecting human regardless of their secretor-, Lewis- or ABO-status (Nordgren *et al.*, 2010). The use of sialic acid residues was also shown for the binding of some human and murine norovirus (MuNoV) MNV-1 strain (Rydell *et al.*, 2009; Taube *et al.*, 2009).

FCV entry pathway was shown to be dependent of clathrin-mediated endocytosis and acidification in endosomes (Stuart et al., 2006) meanwhile MuNoV endocytosis into permissive murine macrophages is mediated by a non-clatrhin, non caveolae, dynamin and cholesterol-dependent, pH-independent pathway (Gerondopoulos *et al*., 2010 ; Perry *et al*., 2009, 2010).

The aim of this study is to elucidate BoNoV-cell interactions during their binding and their internalisation. GIII.2 BoNoVLP from the B309 strain (Mauroy *et al*., 2009) were used in *in vitro* studies with different cell lines, in particular those of bovine origin, in order to characterize the cell surface recognition pattern and entry mechanisms.

Results

The structures involved in the binding of GIII.2 BoNoVLP are widely expressed and are related to carbohydrate structures

B309 VLP were incubated on monolayers of cell lines from different origins. Binding of B309 VLP was detected by immunofluorescence staining on all the bovine cell lines used in this study: Madin-Darby bovine kidney cells (MDBK), bovine turbinate cells (BT), embryonic bovine tracheal cells (EBTr), Georgia bovine kidney cells (GBK), embryonic bovine lung cells (EBL), Mac T cells (udder origin), bronchic cells, Bomac cells (macrophagic origin) and jejunocytes. No staining was shown when cells were pre-treated with sodium periodate ($NaIO_4$), a strong oxidizing agent opening saccharide rings (data only shown for MDBK cells). The specificity of this binding was controlled by the absence of fluorescence signals on cells incubated with either wild type baculovirus (*Autographa californica* multiple nucleocapsids polyhedrovirus, AcMNPV) antigens or heterologous

HuNoV Hawaii virus (HV) VLP (Figure 1A, B and C). Taken together, these results demonstrate that B309 VLP are able to bind cells originating from a wide range of tissues and that this primary binding is mediated by structures related to terminal carbohydrates residues.

Cell treatment by α-galactosidase, trypsin and phospholipase C drastically reduces B309 VLP binding and cell treatment by neuraminidase partially reduces the binding

MDBK were treated with different enzymes and then incubated with B309 VLP in experimental conditions decreasing internalisation (4 °C and use of sodium azide as cell metabolism inhibitor). Percentages of fluorescent cells and total fluorescence were quantified by flow cytometry. Cell treatment with different concentrations of $NaIO_4$ confirmed previous results obtained with immunofluorescence staining on cell layers. Mean fluorescence intensity drastically diminished with 50 mM $NaIO_4$ (note that this last concentration was severly toxic for cells). Among the various enzymes used in the study, binding of B309 VLP was significantly reduced (percentages of fluorescent cells reduced by up to 70%) by pre-treatment of MDBK cells with α-galactosidase (0.5 U), trypsine (1 mg) and phospholipase C. Both trypsin, chymotrypsin, Phospho-N-glycanase and neuraminidase activities were controlled as shown in supplementary data. Percentages of fluorescent cells and fluorescence intensities were 76% and 81%, 70% and 79%, 77% and 79%, 94% and 82% lower after treatment with respectively 0.5 U of α-galactosidase, 1 mg trypsin, 0.1 U phospholipase C and 0.5 U phospholipase C. Neuraminidase pre-treatment at 0.5 U partly reduced the binding of B309 VLP by 34% in both percentage of fluorescent cells and fluorescence intensity analysis (Figure 2A, C and E). When cells were treated with both α-galactosidase (0.5 U) and neuraminidase (0.5 U) or both trypsin (1 mg) and phospholipase C (0.5 U), binding was also significantly reduced, with a percentage of fluorescent cells similar to that of negative controls for the second combined treatment (Figure 2B and D). Taken together, these results

show that a galactosyl residue is deeply involved in the binding of the B309 VLP and that it is linked to both membrane glycoproteins and glycolipids. Sialic acid could either be a minor alternative binding factor or facilitate the attachment to the α-galactose residue. As combined α-galactosidase/neuraminidase treatment did not reduce completely the binding, another carbohydrate structure could be also involved.

Heparan or chondroitin sulphates are not implicated in the binding of GIII.2 BoNoVLP

B309 VLP binding was not significantly modified after heparinase II or chondroitinase ABC (activities controlled as shown in supplementary data) treatment of MDBK cells by flow cytometry analysis (Figure 3). Taken together, the results show that the heparan and chondroitin sulphates, widely used by some other viruses, are not alternative carbohydrate structures used in the binding of B309 VLP.

B309 VLP internalisation is temperature dependent

B309 VLP were incubated with both MDBK or bovine macrophage cells in experimental conditions allowing their internalisation. In this experiment, a fluorescence decrease reflected an internalisation of VLP. By comparison in flow cytometry analysis, fluorescence intensity was shown to be about 61% and 34% lower at 37 °C than at 4 °C or 21 °C respectively (Figure 4A and B) for MDBK cells, where internalisation was also confirmed by confocal microscopy (Figure 4C). In bovine macrophages, fluorescence intensity was shown to be about 51% lower at 37 °C than at 4 °C (Figure 4D and E). Taken together, the results show internalisation in both cell lines and that the internalisation rate of B309 VLP was higher at 37°C.

Internalisation of B309 VLP requires intact actin skeleton, is pH-dependent and involves both caveolae/lipid raft-mediated endocytosis and macropinocytosis

The internalisation pathway of B309 VLP was then tested in the same flow cytometry experiment. B309 VLP internalisation was allowed at optimal temperature (37 °C) and without the use of sodium azide. Before exposure to BoNoVLP, cells were incubated with different drugs known as endocytosis inhibitors. Optimum drug concentration to avoid cell toxicity was determined by the MTT test (the effect of the drugs on internalisation pathways and the concentrations used on MDBK cells in this study are shown in Table I). Among the drugs used, cytochalasin D (2 µM), chloroquine (600 µM) and amiloride hydrochloride (50 µM) were found to slightly increase the percentage of fluorescent cells (Figure 5A), and both cytochalasin D, chloroquine (600 µM) and nystatin (50 µM) increased cell fluorescence intensity after flow cytometry analysis (Figure 5B), inducing a reduction in B309 VLP internalisation. This result was confirmed in an immunofluorescent staining experiment where internalisation was reduced during incubation time in cytochalasin or chloroquine treated cells (Figure 5C). In the second experiment, upon increased concentrations of drugs and chlorpromazine, percentages of fluorescent cells and fluorescence intensity varied with amiloride hydrochloride and nystatin (Figure 5D and E) but not with chlorpromazine (chlorpromazine activity was controlled as shown in supplementary data). Taken together these results show that the actin skeleton is deeply involved in the internalisation of B309 VLP, that drugs interfering with endosomal pH decrease the internalisation and that B309 VLP entry is mediated both by the caveolae/lipid raft-associated pathway and by macropinocytosis.

Discussion

Genotype 2 BoNoV are widespread enteric viruses throughout the world, for which interactions with the host cell and the role in calf diarrhoea complex are poorly elucidated. Zoonotic transmission is suspected and discussed for these viruses. This study shows that carbohydrates structures, widely expressed on different bovine cells, but also on some other animal cells, are implicated in the binding of genotype 2 BoNoV (B309) VLP. Furthermore, it also shows that carbohydrate residues related to galactose are deeply involved in the binding of B309 VLP. Sialic acid could be also implicated but in a less important manner and heparan sulphates are not. By studying entry mechanisms, we demonstrated that B309 VLP internalisation mainly involves both the caveolae-associated pathway and macropinocytosis.

The proximity, in terms of receptors, between HuNoV and animal NoV, in particular BoNoV, is one of the risk factors that need to be studied in order to investigate the zoonotic issue. The zoonotic hypothesis is strengthened by the coexistence of these viruses in areas of high human and animal population density, by their usual faecal-oral route of infection, and by their resistance in the environment. Different molecules, often related to carbohydrates structures, can act as "hooks" specifically or non-specifically recruiting viral particles into the extracellular compartment. Recently, Zakhour and collaborators (2009) described the α-gal epitope as a molecular structure implied in the binding of NB2 VLP. The same authors also showed that NB2 VLP do not bind to carbohydrate structures classically described in the binding of HuNoV (H type1, H type 2, ABO antigens, Lewis antigens). These results and the loss during the evolution of Galili epitope expression by the human species (Macher & Galili, 2008) both suggest an absence of GIII.2 BoNoV cross-species transmission. The results of our flow cytometry study on binding inhibition showed that cell treatment with α-galactosidase drastically reduces the binding of B309 VLP. These results are in agreement with those obtained with VLP of the NB2 strain by Zhakour and collaborators (2009) and for VLP from another GIII.2-related BoNoV. In our study, B309 VLP binding capabilities to a

wide spectrum of bovine cells was also demonstrated. These results have shown the wide expression of the structure implicated in the binding and suggest a likely extended pathogenicity if the virus could be disseminated in the organism and if these cells could be permissive. Therefore, for the health and well-being of the calf, GIII.2 BoNoV could be considered as enteric pathogens as important as rotaviruses, for which associated viremia has been recently demonstrated (Crawford *et al.*, 2006).

Viruses can bind to alternative ligand for example when their primary target is occupied or inaccessible (Cilliers *et al.*, 2005; Harouse *et al.*, 1991; Jin *et al.*, 2010; Khan *et al.*, 2007; Negrete *et al.*, 2006; Yanagi *et al.*, 2009). Heparan sulphates are ubiquitous carbohydrates chains linked to core protein of all eukaryotic cells and are often reported to be primary binding structures for several viruses (Villanueva *et al.*, 2005). They have been shown to efficiently bind GII NoV (Tamura *et al.*, 2004). In our study, we tested the hypothesis that heparan or chondroitin sulphates could alternatively bind GIII.2 BoNoV. As no observed difference in the binding pattern was shown between non treated and heparinase or chondroitinase treated cells, we conclude that neither heparan nor chondroitin sulphates were involved in the binding of B309 VLP. Sialic acid moieties of gangliosides bind murine NoV during infection of murine macrophages (Taube *et al.*, 2009). As sialic acid is a common structure of the membrane of several animal cells and as it has been shown to be involved, even in a moderate way, in the binding of B309 VLP, it could enlarge the host spectrum of GIII.2 BoNoV or provide them with a minor alternative ligand. Alternatively, sialic acid could be involved in one of the sequential steps between binding and internalisation of the viral particle or facilitate the binding to the α-galactose residue.

In order to invade cells, viruses use all available endocytic pathways, including clathrin-mediated endocytosis, caveloae/lipid raft, macropinocytosis and novel non-clathrin non-caveolae pathways (Sieczkarski & Whittaker, 2002). In our study, we investigated the rate of

B309 VLP internalisation by evaluating the difference in fluorescence signal at the level of the cell membrane between drug-treated and non-treated cells by flow cytometry analysis. The optimal drug concentrations were in the range of those determined for FCV in CrFK cells (Stuart & Brown, 2006). When total fluorescence intensity on drug treated cells has been studied, in conditions compatible with the host cell metabolism, we found a significant difference with both chloroquine and cytochalasin D. The results obtained with chloroquine, known as an acidification inhibitor of the endosome, imply that B309 VLP entry could require a pH-dependent endocytic pathway. These results are in contrast with those that had previously shown MNV-1 entry to be pH-independent (Gerondopoulos *et al*., 2010; Perry *et al*., 2009). As internalisation pathways can be cell type-dependent (Miller & Hutt-Fletcher, 1992), we could explain these contrasting results with reference to the different cell lines used in the two experiments. From this perspective, it might be interesting to evaluate the GIII.2 BoNoV internalisation within bovine enterocyte as bovine kidney cells do not exactly reflect the main site of BoNoV infection. Another explanation could lie in the subtle differences in the internalisation pathways between BoNoV and MuNoV. The results obtained for cytochalasin D are explained by the fact that the actin skeleton can be involved in several cellular processes, in particular the endocytosis-associated ones (Girao *et al*., 2008). As even increasing concentrations of chlorpromazine did not affect the percentage of fluorescent cells, it can be concluded that, unlike in the case of FCV (Stuart & Brown, 2006), B309 VLP do not use clathrin-coated pits to enter MDBK cells. By contrast, increased concentrations of nystatin (by 50%) were shown to significantly increase both the percentage and fluorescence intensity of marked cells and these results imply that the caveolae/lipid-raft-associated pathways could be involved in the internalisation of B309 VLP. Nystatin is a sterol-binding drug that sequesters cholesterol, a prominent component of lipid rafts and it has already been demonstrated that some NoV (HuNoV and MuNoV) are capable of binding to

glycosphingolipids (Nilsson et al., 2009; Taube et al., 2009). Increasing concentrations by 50% of amiloride hydrochloride gave the same results. Macropinocytosis is considered to be a non-specific mechanism for internalisation as it does not require a specific ligand-receptor interaction and where the macropinosome is just the cell response to extracellular stimulations. On the other hand, macropinocytosis is widely and constitutively used by antigen-presenting cells. As these cells could be the easiest entry portal for enteric viruses such as NoV, further studies on the relationship between macropinocytosis, dendritic cells and NoV might be interesting.

Different studies on molecular prevalence and binding affinity seem to reveal that GIII.2 could not be at risk of transmission to human. However, the alternative use by viruses of different ligands or non-selective endocytic pathways could impair these preliminary data. Moreover, in order to further analyse the zoonotic potential of BoNoV, studies on receptors and the binding pattern of the GIII.1 BoNoV would also have to be performed as some motifs in the GIII.1 capsid protein, including the RGD integrin-binding motif (Tan *et al.*, 2003), seem to be more related to the GI HuNoV motifs. The binding possibilities offered to viruses by the diverse carbohydrates structures on the cell surface can be great and the viral adaptation to this ligand range, e.g. by mutations or recombination, is a part of their evolution. As for HuNoV, different carbohydrate binding patterns could be determined for both GIII.2 and GIII.1. Their respective specific receptors are as yet unknown, as are many other mechanisms of NoV cell invasion. Either the specific receptors or further steps could represent the real key-points in BoNoV cell/host tropism and permissivity.

Methods

Cell cultures

Spodoptera frugiperda insect cells (Sf9) were cultured at 28 °C with Sf900-II medium (Invitrogen). MDBK, BT, EBTr, GBK, EBL, Mac T, Bomac (kindly provided by Dr Donofrio, Parma University, Italy), and bovine bronchic cells were cultured at 37 °C with minimum Eagle's medium (MEM) (Invitrogen) supplemented with 10% heat inactivated foetal calf serum (FCS), 1% of a non essential amino acids preparation (NEAA) (Invitrogen) and 2% of a penicillin-streptomycin association (PS) (Invitrogen). Bovine jejunocytes (J8/13) (Loret *et al.*, 2009), kindly provided by Dr Rusu (University of Liège, Belgium), were cultured at 37 °C with Dulbecco's modified MEM (Invitrogen) supplemented with 20% FCS, 1% NEAA and 2% PS (Invitrogen).

Reagents and antibodies

Neuraminidase from *Clostridium perfringens* (cleavage specificity α-2-3, α-2-6, α-2-8), α-galactosidase, α-chymotrypsin, trypsin, phospholipase C, phospho-N-glycanase F, $NaIO_4$, heparinase II, chondroitinase ABC, chlorpromazine hydrochloride, nystatin, chloroquine diphosphate salt, amiloride hydrochloride hydrate, cytochalasin D and 7 actinomycin D were purchased from Sigma Aldrich. Endocytosis inhibiting drugs were all diluted at 10 mM in RNAse free water (Invitrogen) (chlorpromazine hydrochloride and chloroquine diphosphate salt) or in dimethyl sulphoxide (nystatin, amiloride hydrochloride hydrate and cytochalasin D). Alexa Fluor 488 goat anti-rabbit IgG monoclonal antibody (GAR-488) was purchased from Invitrogen.

GIII.2 BoNoV and Hawaii virus VLP

Virus-like particles of a GIII.2 genetically related BoNoV strain (B309), molecularly detected in a stool sample from a Belgian calf, were obtained as already mentioned elsewhere (Mauroy

304 *et al.*, 2009a). Briefly, the sequence coding for the single capsid protein (Genbank accession
305 number: EU794907, Bo/NoV/B309/2003/Be) was cloned into Bacmid (Bac-to-Bac system,
306 Invitrogen), which was thereafter transfected into Sf9 cells. The recombinant baculovirus was
307 used to infect Sf9 cells and the produced BoNoVLP were purified from supernatant by
308 ultracentrifugation in sucrose gradient. The presence of capsid protein and viral particles was
309 verified by both SDS-PAGE analysis and electron microscopy.

310 Virus-like particles of the HuNoV Hawaii virus were obtained in the same way from a
311 plasmid containing the HV ORF2 (kindly provided by Dr Vinjé, Centers for Disease Control,
312 USA). The presence of capsid protein and viral particles was verified by both SDS-PAGE
313 analysis and electron microscopy.

314 Antigens from an Sf9 cell culture infected by a wild-type baculovirus (AcMNPV) were also
315 produced and submitted to a similar procedure of purification. Protein concentration was
316 measured by BCA (Pierce) and on a NanoDrop1000 spectrophotometer (Thermo Scientific).

317

318 *Rabbit polyclonal serum against B309 VLP*

319 Three New Zealand rabbits were injected subcutaneously with 25 µg of antigen (B309 VLP,
320 HV VLP or PBS). Antigens were diluted in PBS with complete Freund adjuvant. Two
321 additional immunisations were carried out at intervals of 21 days with the same amount of
322 antigens diluted in PBS with incomplete Freund adjuvant. Rabbits were euthanised by
323 exsanguination 21 days after the last immunisation. Sera (called rabbit–αB309, rabbit-αHV,
324 rabbit-negative) were heat inactivated (30 min at 56 °C) and tested for reactivity and
325 specificity in an ELISA format. All experimental procedures were approved by the
326 Institutional Animal Care and Use Committee at the University of Liège (reference of the
327 protocol: 581).

Indirect immunofluorescence staining on cell culture binding assay

Confluent monolayers of MDBK, EBTr, Bomac, BT, EBL, MacT, bronchic cells and bovine jejunocytes were subcultured on coverslips in 24-wells plates (Greiner) the day before their use in the experiment. Following this, the medium was removed and cells were incubated for 30 min in PBS supplemented with heat inactivated horse serum at 10% v/v (PBS-HS). Some coverslips were pre-treated after a wash with PBS with 200 µl/well of a dilution of $NaIO_4$ (5 mM) for 45 min at 37 °C. $NaIO_4$ was then removed and coverslips were washed once with PBS and then incubated at 37 °C for 15 min with a 1% w/v solution of glycin. Coverslips were placed on ice and incubated with 200 µl of antigens solution in PBS at 1 ng/µl (B309 VLP, HV VLP or wild type AcMNPV) for 1h at 4 °C on a rocking platform. Antigens were removed and cells were then washed three times with PBS-HS and fixed for 45 min at 4 °C with a 2% solution of paraformaldehyde in PBS. Cells were washed three times with PBS and then blocked with PBS-HS for 1h at 37 °C. After three washes with PBS, cells were incubated with the 10,000-fold PBS diluted rabbit anti-B309 VLP serum for 1 h at 37 °C. Coverslips were washed three times with PBS-HS and then incubated for 1 h at 37 °C with an Alexa fluor 488 conjugated, 1,000-fold PBS diluted, goat anti-rabbit IgG. Cells were washed three times with PBS-HS and coverslips were mounted with ProLong gold antifade reagent (Invitrogen) before epifluorescent microscopy analysis, performed with a Nikon Eclipse TC2000 microscope equipped with an X-Cite120 Fluorescence Illumination System and a DC300F camera (Leica). The same assay was also performed on MDBK after treatment with cytochalasin D (2µM) or chloroquine (600 µM) for 1 h or 3 h.

Flow cytometry analysis on cell binding assay

MDBK were selected for flow cytometry analysis (FACS). Cells were grown at confluence and then seeded into 96-well plates (150,000 cells/well) and incubated for 1h at 37 °C. Cells were pelleted at 250g and then washed once with PBS-HS. Cells were then pelleted and incubated at 37 °C for 1h (or overnight for heparinase and chondroitiase treatment) with 100 µl of different reagent solutions: $NaIO_4$ at 50 and 5 mM ; phospho-N-glycanase F, fucosidase, galactosidase, neuraminidase, phospholipase A2 and phospholipase C at 5 and 1 U/ml ; heparinase and chondroitinase at 10 U/ml ; trypsin, and chymotrypsin at 10 and 1 mg/ml. After 45 min of incubation $NaIO_4$ solutions were removed, replaced with the same amount of 1% glycin w/v and incubated for 15 min at 37 °C. All cells were pelleted, washed once with ice-cold PBS-HS, pelleted and then incubated on ice with 100 µl of antigen (B309 VLP, HV VLP, PBS) at 0.5 ng/µl dilution in PBS-HS complemented with 1% azide w/v (PBS-HS-a). After incubation, cells were pelleted, washed twice for 5 min with PBS-HS-a and then incubated on ice for 45 min with a 5,000-fold diluted rabbit–αB309 in PBS-HS-a. Following this, cells were pelleted, washed twice for 5 min with PBS-HS-a and then incubated on ice for 30 min with a 10,000-fold diluted GAR-488 in PBS-HS-a. After incubation, cells were pelleted, washed three times for 5 min with PBS-HS-a, diluted in non-complemented ice-cold MEM and maintained on ice. Flow cytometry acquisitions and analyses were performed on a three-laser Becton Dickinson fluorescence-activated cell sorter (FACSAria) (Becton Dickinson, Erembodegem, Belgium).

Flow cytometry analysis on cell internalisation assay

The day before the internalisation experiment, MDBK cells were seeded into 96-well plates (150,000 cells/well). Cells were incubated with 100 µl of antigen (B309VLP, HV VLP, PBS) at 0.5 ng/µl dilution in PBS-HS at 4 °C for 1h. Unbound antigens were removed and cells were incubated in MEM at 4°C, 21 °C or 37 °C for 1h. After incubation, cells were pelleted,

377 washed twice for 5 min with ice-cold PBS-HS-a and then incubated on ice for 45 min with a
378 5,000-fold diluted rabbit–αB309 in PBS-HS-a. Following this, cells were pelleted, washed
379 twice for 5 min with ice-cold PBS-HS-a and then incubated on ice for 30 min with a 10,000-
380 fold diluted GAR-488 in PBS-HS-a. After incubation, cells were pelleted, washed three times
381 for 5 min with PBS-HS, diluted in non-complemented ice-cold MEM and maintained on ice.
382 Flow cytometry acquisitions and analyses were performed on a three-laser Becton Dickinson
383 fluorescence-activated cell sorter (FACSAria) (Becton Dickinson, Erembodegem, Belgium).
384 The same assay was then performed on Bomac cells at 4°C and 37°C. All conditions were
385 analysed in triplicates.

386 The same assay was also performed after drug treatment of the cells. A preliminary
387 experiment was performed on MDBK cells in 96 wells at 80% confluence in order to define
388 concentrations of the used drugs (cytochalasin, chloroquine, chlorpromazine, nystatin,
389 amiloride hydrochloride) compatible with cell metabolism. Briefly, cells were grown
390 overnight with different concentrations of drugs (the range was primarily defined following
391 the study of Stuart and Brown (2006) on the FCV. Cell viability and metabolism were
392 assessed by MTT and trypan blue tests to determine optimal drug concentration. The day
393 before the internalisation experiment, MDBK cells, grown at confluence, were seeded into
394 25 cm^2 culture flasks with complete MEM, with or without drugs diluted at the above defined
395 concentrations. The following tests were performed as already described above. All
396 conditions were analysed in triplicates. The same experiment was finally performed in
397 triplicates with MDBK cells previously treated with a 50% increased concentration of both
398 nystatin and amiloride hydrochloride.

399

400 *Confocal microscopy*

Confluent monolayer of MDBK was subcultured on coverslips in 24-wells plates (Greiner) the day before their use in the experiment. Following this, the medium was removed and cells were incubated for 30 min in PBS supplemented with heat inactivated horse serum at 10% v/v (PBS-HS). Coverslips were washed once with PBS and then incubated at 4 °C for 1h. Unbound antigens were removed and cells were incubated in MEM at 37 °C for 1h or directly fixed. MEM was then removed and cells were washed three times with PBS-HS. Cells were fixed for 45 min at 4 °C with a 2% solution of paraformaldehyde in PBS and then permeabilised with PBS-NP40 0.1% for 15 min. Cells were washed three times with PBS-HS and then incubated with the 5,000-fold PBS diluted rabbit anti-B309 VLP serum for 1 h at 37 °C. Coverslips were washed three times with PBS-HS and then incubated for 1 h at 37 °C with an Alexa fluor 488 conjugated, 1,000-fold PBS diluted, goat anti-rabbit IgG. Coverslips were washed three times with PBS-HS and then incubated for 1 h at 37 °C with a n Alexa fluor 488 conjugated, 1,000-fold dilution of 7 actinomycin D. Coverslips were washed three times with PBS-HS and then mounted with ProLong gold antifade reagent (Invitrogen) before confocal microscopy analyses, performed with a TCS SP confocal microscope (Leica, Heerbrugg, Switzerland).

Statistical analysis

Significance of the differences between means was assessed with the Wilcoxon-Mann-Whitney rank sum test ($p<0.05$).

Acknowledgements

This study was funded by the Belgian policy “Science for a Sustainable Development” (SD/AF/01), by the *Région Wallonne* (project 415701) and by “*Fonds Spéciaux pour la Recherche*” (University of Liège). L. Gillet is Research Associate of the ‘Fonds de la Recherche Scientifique – Fonds National Belge de la Recherche Scientifique’ (FRS-FNRS). The authors thank Dr Vinjé (Centers for Disease Control, USA) and Dr Rusu (University of Liège, Belgium) for their gifts, Dr Mast (CERVA, Belgium) for electron microscopy, Christine Thys and Daniel Mattina for their excellent technical assistance in molecular experiments, Lorène Dams for her expertise in cell culture, Cédric Delforge for his assistance in rabbit immunizations, Dominique Ziant and Dr Benjamin Dewals (FRS-FNRS) for their assistance in some of the flow cytometry experiments, and Angélique Zicola (Virology, University of Liège), professor M. Galleni and Dr M.-E. Dumez (Centre of Protein Engineering, University of Liège) for their valuable help in some control tests.

References

Baranowski, E., Ruiz-Jarabo, C. M. & Domingo, E. (2001). Evolution of cell recognition by viruses. *Science* **292**, 1102-1105.

Bridger, J. C., Hall, G. A. & Brown, J. F. (1984). Characterization of a calici-like virus (Newbury agent) found in association with astrovirus in bovine diarrhea. *Infect. Immun.* **43**, 133-138.

Cilliers, T., Willey, S., Sullivan, W. M., Patience, T., Pugach, P., Coetzer, M., Papathanasopoulos, M., Moore, J. P., Trkola, A., Clapham, P. & Morris, L. (2005). Use of alternate coreceptors on primary cells by two HIV-1 isolates. *Virology* **339**, 136-144.

Crawford, S. E., Patel, D. G., Cheng, E., Berkova, Z., Hyser, J. M., Ciarlet, M., Finegold, M. J., Conner, M. E. & Estes, M. K. (2006). Rotavirus viremia and extraintestinal viral infection in the neonatal rat model. *J. Virol.* **80**, 4820-4832.

Duizer, E., Schwab, K. J., Neill, F. H., Atmar, R. L., Koopmans, M. P. & Estes, M. K. (2004). Laboratory efforts to cultivate noroviruses. *J. Gen. Virol.* **85**, 79-87.

Gerondopoulos, A., Jackson, T., Monaghan, P., Doyle, N. & Roberts, L. O. (2010). Murine norovirus-1 cell entry is mediated through a non-clathrin, non-caveolae, dynamin and cholesterol dependent pathway. *J. Gen. Virol.*, **91**, 1428-1438.

Girao, H., Geli, M. I. & Idrissi, F. Z. (2008). Actin in the endocytic pathway: from yeast to mammals. *FEBS Lett.* **582**, 2112-2119.

Green, K. Y. (2007). *Caliciviridae* : The Noroviruses. In *Fields Virology*, fifth edition, pp. 949-979. Edited by D. M. Knipe. Philadelphia, USA: Lippinscott Williams & Wilkins.

Han, M. G., Smiley, J. R., Thomas, C. & Saif, L. J. (2004). Genetic recombination between two genotypes of genogroup III bovine noroviruses (BoNVs) and capsid sequence diversity among BoNVs and Nebraska-like bovine enteric caliciviruses. *J. Clin. Microbiol.* **42**, 5214-5224.

Han, M. G., Wang, Q., Smiley, J. R., Chang, K. O. & Saif, L. J. (2005). Self-assembly of the recombinant capsid protein of a bovine norovirus (BoNV) into virus-like particles and evaluation of cross-reactivity of BoNV with human noroviruses. *J. Clin. Microbiol.* **43**, 778-785.

Harouse, J. M., Laughlin, M. A., Pletcher, C., Friedman, H. M. & Gonzalez-Scarano, F. (1991). Entry of human immunodeficiency virus-1 into glial cells proceeds via an alternate, efficient pathway. *J. Leukoc. Biol.* **49**, 605-609.

Hewlett, L. J., Prescott, A. R. & Watts, C. (1994). The coated pit and macropinocytic pathways serve distinct endosome populations. *J. Cell. Biol.* **124**, 689-703.

Ike, A. C., Roth, B. N., Bohm, R., Pfitzner, A. J. & Marschang, R. E. (2007). Identification of bovine enteric Caliciviruses (BEC) from cattle in Baden-Wurttemberg. *Dtsch. Tierarztl. Wochenschr*. **114**, 12-15.

Jiang, X., Wang, M., Graham, D. Y. & Estes, M. K. (1992). Expression, self-assembly, and antigenicity of the Norwalk virus capsid protein. *J. Virol.* **66**, 6527-6532.

Jin, Q., Alkhatib, B., Cornetta, K. & Alkhatib, G. (2010) Alternate receptor usage of neuropilin-1 and glucose transporter protein 1 by the human T cell leukemia virus type 1. *Virology* **396**, 203-212.

Khan, A. G., Pichler, J., Rosemann, A. & Blaas, D. (2007). Human rhinovirus type 54 infection via heparan sulfate is less efficient and strictly dependent on low endosomal pH. *J. Virol.* **81**, 4625-4632.

Liu, B. L., Lambden, P. R., Gunther, H., Otto, P., Elschner, M. & Clarke, I. N. (1999). Molecular characterization of a bovine enteric calicivirus: relationship to the Norwalk-like viruses. *J. Virol.* **73**, 819-825.

Loret, S., Rusu, D., El Moualij, B., Taminiau, B., Heinen, E., Dandrifosse, G. & Mainil, J. (2009). Preliminary characterization of jejunocyte and colonocyte cell lines isolated by enzymatic digestion from adult and young cattle. *Res. Vet. Sci*. **87**, 123-132.

Macher, B. A. & Galili, U. (2008). The Galalpha1,3Galbeta1,4GlcNAc-R (alpha-Gal) epitope: a carbohydrate of unique evolution and clinical relevance. *Biochim. Biophys. Acta* **1780**, 75-88.

492 Makino, A., Shimojima, M., Miyazawa, T., Kato, K., Tohya, Y. & Akashi, H. (2006).
493 Junctional adhesion molecule 1 is a functional receptor for feline calicivirus. *J. Virol.*
494 **80**, 4482-4490.

495 Mauroy, A., Scipioni, A., Mathijs, E., Miry, C., Ziant, D., Thys, C. & Thiry, E. (2008).
496 Noroviruses and sapoviruses in pigs in Belgium. *Arch. Virol.* **153**, 1927-1931.

497 Mauroy, A., Scipioni, A., Mathijs, E., Saegerman, C., Mast, J., Bridger, J. C., Ziant, D., Thys,
498 C. & Thiry, E. (2009a). Epidemiological study of bovine norovirus infection by RT-
499 PCR and a VLP-based antibody ELISA. *Vet. Microbiol.* **137**, 243-251.

500 Mauroy, A., Scipioni, A., Mathijs, E., Thys, C. & Thiry, E. (2009b). Molecular detection of
501 kobuviruses and recombinant noroviruses in cattle in continental Europe. *Arch. Virol.*
502 **154**, 1841-1845.

503 Miller, N. & Hutt-Fletcher, L. M. (1992). Epstein-Barr virus enters B cells and epithelial cells
504 by different routes. *J. Virol.* **66**, 3409-3414.

505 Milnes, A. S., Binns, S. H., Oliver, S. L. & Bridger, J. C. (2007). Retrospective study of
506 noroviruses in samples of diarrhoea from cattle, using the Veterinary Laboratories
507 Agency's Farmfile database. *Vet. Rec.* **160**, 326-330.

508 Negrete, O. A., Wolf, M. C., Aguilar, H. C., Enterlein, S., Wang, W., Muhlberger, E., Su, S.
509 V., Bertolotti-Ciarlet, A., Flick, R. & Lee, B. (2006). Two key residues in ephrinB3
510 are critical for its use as an alternative receptor for Nipah virus. *PLoS Pathog.* **2**, e7.

511 Nilsson, J., Rydell, G. E., Le Pendu, J. & Larson, G. (2009). Norwalk virus-like particles bind
512 specifically to A, H and difucosylated Lewis but not to B histo-blood group active
513 glycosphingolipids. *Glycoconj. J.* **26**, 1171-1180.

514 Nordgren, J., Kindberg, E., Lindgren, P. E., Matussek, A. & Svensson, L. (2010). Norovirus
515 gastroenteritis outbreak with a secretor-independent susceptibility pattern, Sweden.
516 *Emerg. Infect. Dis.* **16**, 81-87.

517 Oliver, S. L., Asobayire, E., Charpilienne, A., Cohen, J. & Bridger, J. C. (2007). Complete
518 genomic characterization and antigenic relatedness of genogroup III, genotype 2
519 bovine noroviruses. *Arch. Virol.* **152**, 257-272.

520 Ossiboff, R. J., Parker, J. S. (2007). Identification of regions and residues in feline junctional
521 adhesion molecule required for feline calicivirus binding and infection. *J. Virol.*, **81,**
522 13608-13621.

523 Park, S. I., Jeong, C., Kim, H. H., Park, S. H., Park, S. J., Hyun, B. H., Yang, D. K., Kim, S.
524 K., Kang, M. I. & Cho, K. O. (2007). Molecular epidemiology of bovine noroviruses
525 in South Korea. *Vet. Microbiol.* **124**, 125-133.

526 Perry, J. W., Taube, S. & Wobus, C. E. (2009). Murine norovirus-1 entry into permissive
527 macrophages and dendritic cells is pH-independent. *Virus Res.* **143**, 125-129.

528 Perry, J. W., Wobus, C. E. (2010). Endocytosis of Murine Norovirus 1 into murine
529 macrophages is dependent of dynamin and cholesterol. *J. Virol.* **84**, 6163-6176.

530 Ruvoen-Clouet, N., Ganiere, J. P., Andre-Fontaine, G., Blanchard, D. & Le Pendu, J. (2000).
531 Binding of rabbit hemorrhagic disease virus to antigens of the ABH histo-blood group
532 family. *J. Virol.* **74**, 11950-11954.

533 Rydell, G. E., Nilsson, J., Rodriguez-Diaz, J., Ruvoen-Clouet, N., Svensson, L., Le Pendu, J.,
534 Larson, G. (2009). Human noroviruses recognize sialyl Lewis x neoglycoprotein.
535 *Glycobiology*, **19,** 309-320.

536 Scipioni, A., Mauroy, A., Vinje, J. & Thiry, E. (2008). Animal noroviruses. *Vet. J.* **178**, 32-
537 45.

538 Sieczkarski, S. B. & Whittaker, G. R. (2002). Dissecting virus entry via endocytosis. *J. Gen.*
539 *Virol*. **83**, 1535-1545.

540 Smith, A. E. & Helenius, A. (2004). How viruses enter animal cells. *Science* **304**, 237-242.

541 Stuart, A. D. & Brown, T. D. (2006). Entry of feline calicivirus is dependent on clathrin-
542 mediated endocytosis and acidification in endosomes. *J. Virol*. **80**, 7500-7509.

543 Stuart, A. D. & Brown, T. D. (2007). Alpha2,6-linked sialic acid acts as a receptor for Feline
544 calicivirus. *J. Gen. Virol*. **88**, 177-186.

545 Tamura, M., Natori, K., Kobayashi, M., Miyamura, T. & Takeda, N. (2004). Genogroup II
546 noroviruses efficiently bind to heparan sulfate proteoglycan associated with the
547 cellular membrane. *J. Virol*. **78**, 3817-3826.

548 Tan, M., Huang, P., Meller, J., Zhong, W., Farkas, T. & Jiang, X. (2003). Mutations within
549 the P2 domain of norovirus capsid affect binding to human histo-blood group
550 antigens: evidence for a binding pocket. *J.Virol.* **77**, 12562-12571.

551 Tan, M. & Jiang, X. (2005). Norovirus and its histo-blood group antigen receptors: an answer
552 to a historical puzzle. *Trends Microbiol*. **13**, 285-293.

553 Taube, S., Perry, J. W., Yetming, K., Patel, S. P., Auble, H., Shu, L., Nawar, H. F., Lee, C.
554 H., Connell, T. D., Shayman, J. A. & Wobus, C. E. (2009). Ganglioside-linked
555 terminal sialic acid moieties on murine macrophages function as attachment receptors
556 for murine noroviruses. *J. Virol*. **83**, 4092-4101.

557 Van Der Poel, W. H., van der Heide, R., Verschoor, F., Gelderblom, H., Vinje, J. &
558 Koopmans, M. P. (2003). Epidemiology of Norwalk-like virus infections in cattle in
559 The Netherlands. *Vet. Microbiol*. **92**, 297-309.

560 Vanderplasschen, A., Bublot, M., Dubuisson, J., Pastoret, P. P. & Thiry, E. (1993).
561 Attachment of the gammaherpesvirus bovine herpesvirus 4 is mediated by the

562 interaction of gp8 glycoprotein with heparinlike moieties on the cell surface. *Virology*
563 **196**, 232-240.

564 Villanueva, R. A., Rouille, Y. & Dubuisson, J. (2005). Interactions between virus proteins and
565 host cell membranes during the viral life cycle. *Int. Rev. Cytol.* **245**, 171-244.

566 White, L. J., Ball, J. M., Hardy, M. E., Tanaka, T. N., Kitamoto, N. & Estes, M. K. (1996).
567 Attachment and entry of recombinant Norwalk virus capsids to cultured human and
568 animal cell lines. *J. Virol.* **70**, 6589-6597.

569 Wise, A. G., Monroe, S. S., Hanson, L. E., Grooms, D. L., Sockett, D. & Maes, R. K. (2004).
570 Molecular characterization of noroviruses detected in diarrheic stools of Michigan and
571 Wisconsin dairy calves: circulation of two distinct subgroups. *Virus Res.* **100**, 165-
572 177.

573 Woode, G. N. & Bridger, J. C. (1978). Isolation of small viruses resembling astroviruses and
574 caliciviruses from acute enteritis of calves. *J. Med. Microbiol.* **11**, 441-452.

575 Yanagi, Y., Takeda, M., Ohno, S. & Hashiguchi, T. (2009). Measles virus receptors. *Curr.*
576 *Top. Microbiol. Immunol.* **329**, 13-30.

577 Zakhour, M., Ruvoen-Clouet, N., Charpilienne, A., Langpap, B., Poncet, D., Peters, T.,
578 Bovin, N. & Le Pendu, J. (2009). The alphaGal epitope of the histo-blood group
579 antigen family is a ligand for bovine norovirus Newbury2 expected to prevent cross-
580 species transmission. *PLoS Pathog.* **5**, e1000504.

581
582

583 **Tables**

584 Table I: Effects of drugs on endocytosis and drug concentration used in this study

Drug	Known effect on internalisation pathways	Concentration used in this study
Cytochalasin D	Prevents actin polymerisation, disrupts actin cytoskeleton	2 µM
Chloroquine	Inhibits acidification of endosomes	600 µM
Amiloride hydrochloride	Inhibits macropinocytosis	50 µM
Nystatin	Sterol-binding drug that sequesters cholesterol, inhibits endocytosis via lipid rafts/caveolae	50 µM
Chlorpromazine	Inhibits endocytosis via clathrin-coated pits, prevents (dis)assembly of clathrin lattices at cell surface and on endosomes	10 µM

585

586

587 **Figure legends**

588

589 Figure 1: Indirect immunofluorescence staining on binding assay with different bovine cell
590 cultures. A. Binding of B309 virus-like particles (VLP) (with or without sodium periodate
591 ($NaIO_4$) treatment), AcMNPV antigens and HV VLP on Madin-Darby Bovine Kidney cells.
592 The binding pattern of MDBK was representative of those of other cell lines. B. Binding of
593 B309 VLP to other bovine cell lines. $NaIO_4$: sodium periodate ; AcMNPV: wild type
594 baculovirus antigens ; HV: Hawaii NoVLP (human norovirus strain) ; MDBK: Madin-Darby
595 Bovine Kidney cells ; BoMac: bovine macrophages ; EBL: embryonic bovine lung cells ;
596 EBTr : embryonic bovine tracheal cells ; GBK: Georgia bovine kidney cells ; Mac T: bovine
597 cells from udder origin. C. Electron micrographs of B309 (left, bar: 200 nm) and HV VLP
598 (right, bar: 100 nm) on fractions of gradient purification after uranyl acetate negative staining
599 (courtesy of Dr Jan Mast).

600

601 Figure 2: Flow cytometry analysis performed after indirect staining on treated and non-treated
602 Madin-Darby Bovine Kidney cells (MDBK). Percentages (A, B) and fluorescence intensities
603 (C, D) of fluorescent cells after drug treatment and incubation with B309 VLP. Negative
604 samples were incubated with either phosphate buffer saline or heterologous VLP. In (B) and
605 (D), cells were treated with combined enzymes. Standard deviations are shown. E:
606 Logarithmic representation of fluorescence intensity by cell counts. Y axis is not standardised.
607 Non-treated MDBK incubated with B309 VLP (a) ; non-treated MDBK incubated with
608 heterologous VLP (human NoV Hawaii strain) (b) ; non-treated MDBK incubated with
609 phosphate buffer saline (c) ; MDBK treated with 50 mM $NaIO_4$ (d), 0.5 U α-galactosidase (e),
610 0.5 U neuraminidase (f), 0.5 U phospho-N-glycanase (g), 1 mg trypsin (h), 1 mg
611 chymotrypsin (i), 0.5 U phospholipase C (j), 0.5 U α-galactosidase and 0.5 U neuraminidase

612 (k), 1mg trypsin and 0.5 U phospholipase C (l) before incubation with B309 VLP. B309:
613 GIII.2 BoNoVLP ; HV: Hawaii NoVLP (human norovirus strain) ; $NaIO_4$: sodium periodate ;
614 PBS: phosphate buffer saline ; *: significant statistical difference ($p<0.05$).

615

616 Figure 3: Flow cytometry analysis performed after incubation with antigens (PBS, HV, B309)
617 and indirect staining on non-treated or treated (0.5 U of heparinase II or chondroitinase ABC)
618 Madin-Darby Bovine Kidney cells (MDBK). Standard deviations are shown. B309: GIII.2
619 BoNoVLP ; HV: Hawaii NoVLP (human norovirus strain) ; PBS: phosphate buffer saline.

620

621 Figure 4: B309 internalisation by Madin-Darby bovine kidney cells and bovine macrophages
622 Percentages (A) and fluorescence intensities (B) in flow cytometry analysis performed after
623 indirect staining on Madin-Darby Bovine Kidney cells (MDBK) incubated with antigens
624 (B309 VLP ; heterologous VLP, HV VLP ; phosphate buffer saline) at 4°C, 21°C and 37°C.
625 Standard deviations are shown. C: pictures of confocal microscopy on MDBK cells incubated
626 for 1h at 4°C with B309 VLP. Pictures were taken after 0 and 60 min of cell incubation at
627 37°C and indirect immunostaining of the VLP. Percentages (D) and fluorescence intensities
628 (E) in flow cytometry analysis performed after indirect staining on bovine macrophages
629 incubated with antigens (B309 VLP ; heterologous VLP, HV VLP ; phosphate buffer saline)
630 at 4°C, and 37°C. Standard deviations are shown. B309: GIII.2 BoNoVLP ; HV: Hawaii
631 NoVLP (human norovirus strain) ; PBS: phosphate buffer saline ; αB309: rabbit polyclonal
632 antibody against B309 VLP ; 7AAD : 7 aminoactinomycin D.

633

634 Figure 5: Inhibition of B309 internalisation by different substances inhibiting particular
635 internalisation pathways. Percentages (A) and fluorescence intensities (B) in flow cytometry

analysis performed after indirect staining on Madin-Darby Bovine Kidney cells (MDBK) treated with cytochalazin (2 µM), chloroquine (600 µM), amiloride hydrochloride (50 µM), nystatin (50 µM) and chlorpromazine (10 µM) and then incubated with antigens B309 VLP. Negative samples were incubated with either PBS or heterologous human NoVLP. Standard deviations are shown. C: Immunofluorescent staining after incubation of MDBK cells with B309 VLP. The staining was realised after 1 h or 3 h of incubation on both non treated cells, cytochalasin D- and chloroquine treated cells. Percentages (D) and fluorescence intensities (E) in flow cytometry analysis performed after indirect staining on Madin-Darby Bovine Kidney cells (MDBK) treated with cytochalazin, amiloride hydrochloride, nystatin and chlorpromazine (concentrations were increased by 50%, 75 µM, 75 µM and 15 µM respectively) and then incubated with antigens B309 VLP. Negative samples were incubated with either PBS or heterologous human NoVLP. Standard deviations are shown. B309: GIII.2 BoNoVLP ; HV: Hawaii NoVLP (human norovirus strain) ; PBS: phosphate buffer saline ; *: significant statistical difference ($p<0.05$).

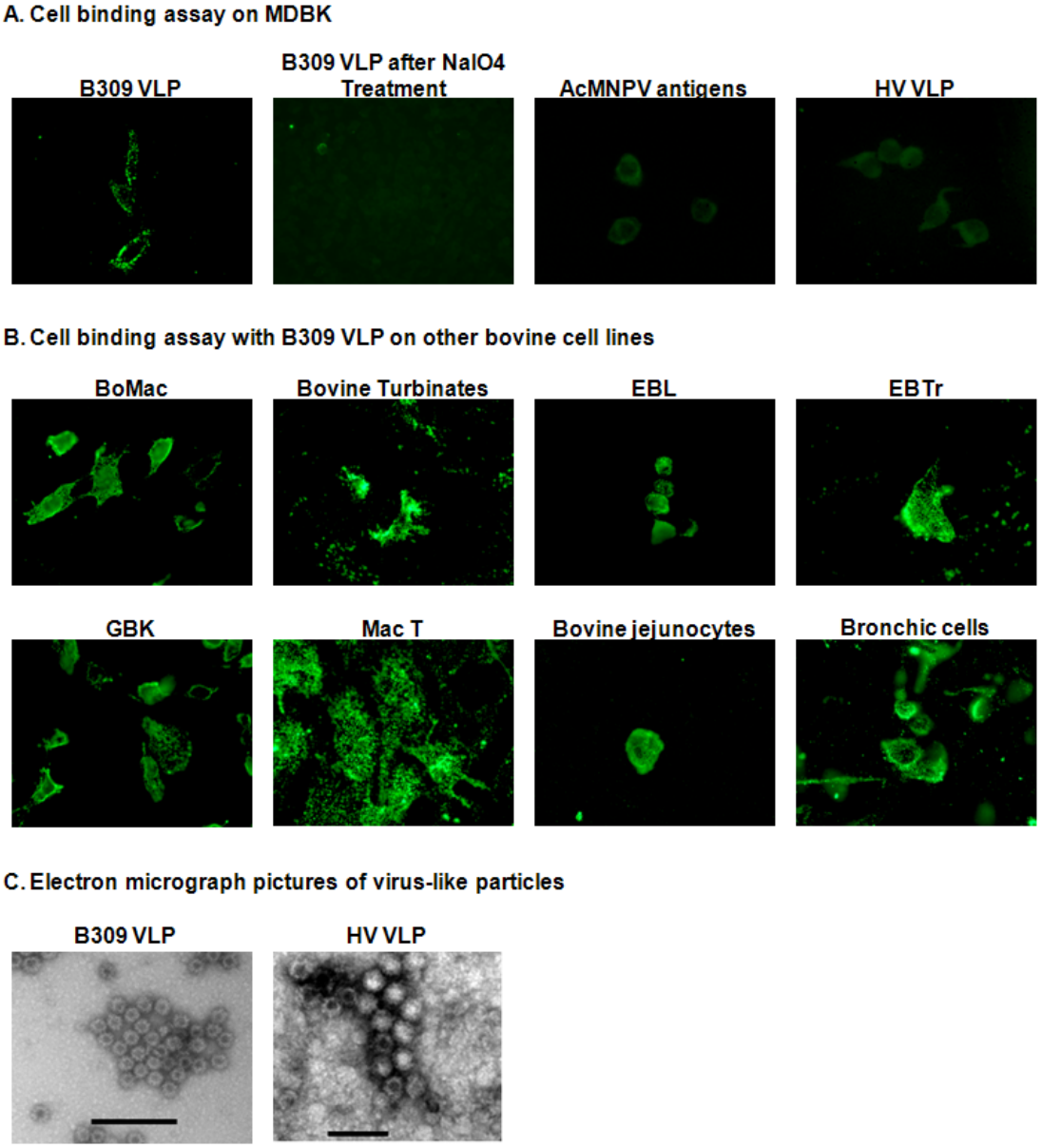

651

652 Fig. 1

653

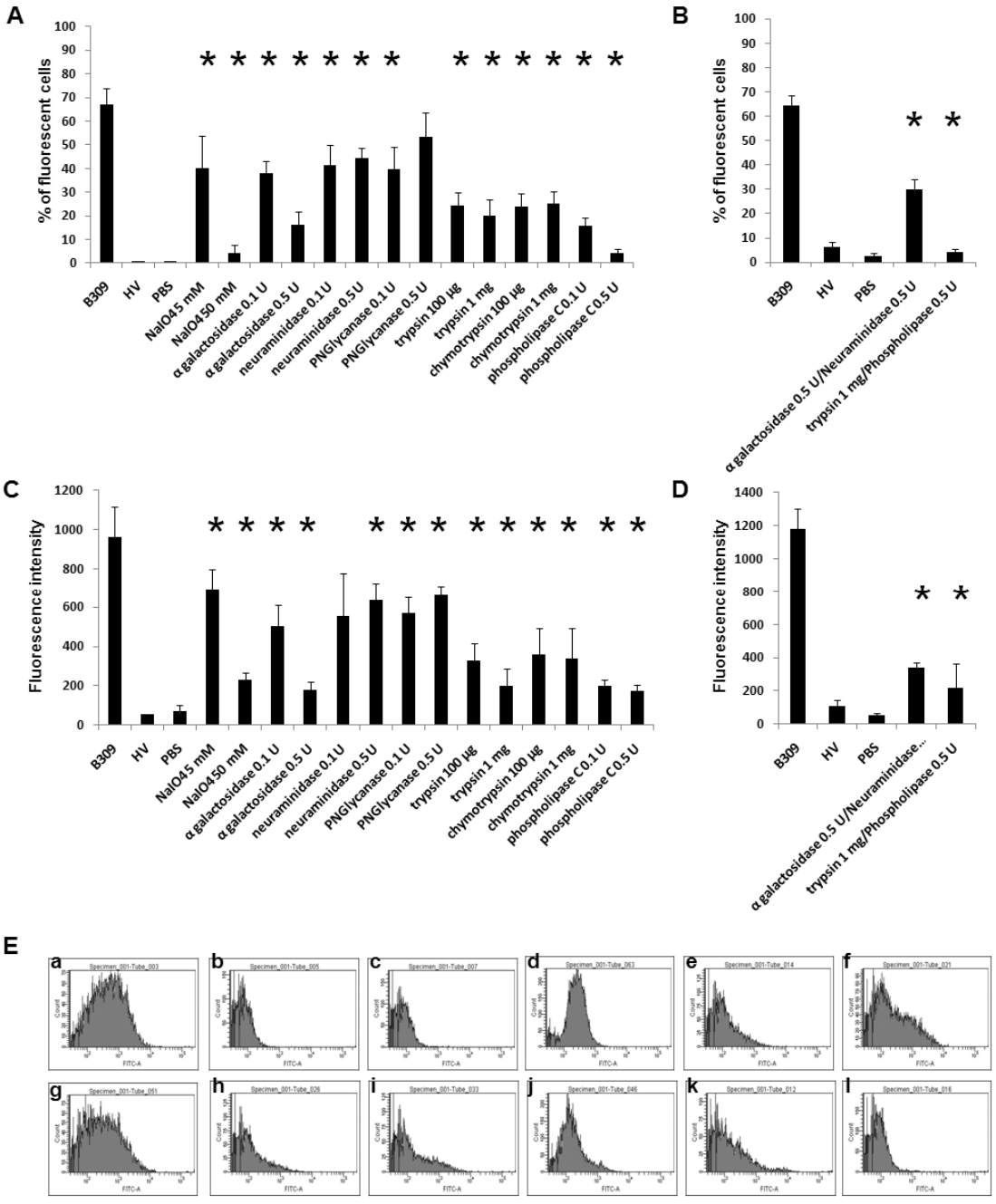

654

655 Fig. 2

656

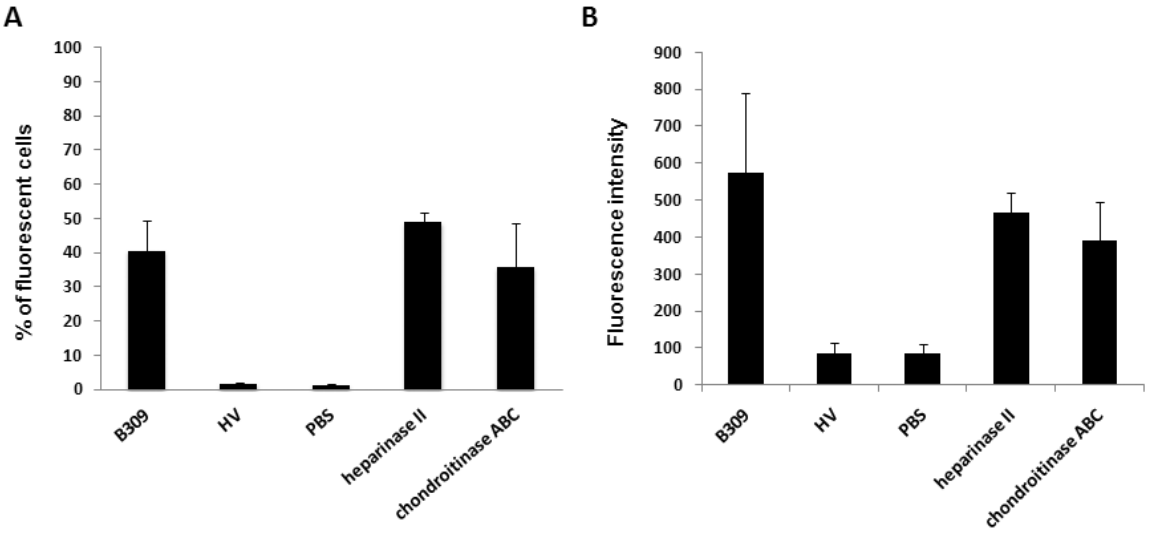

657

658 Fig. 3

659

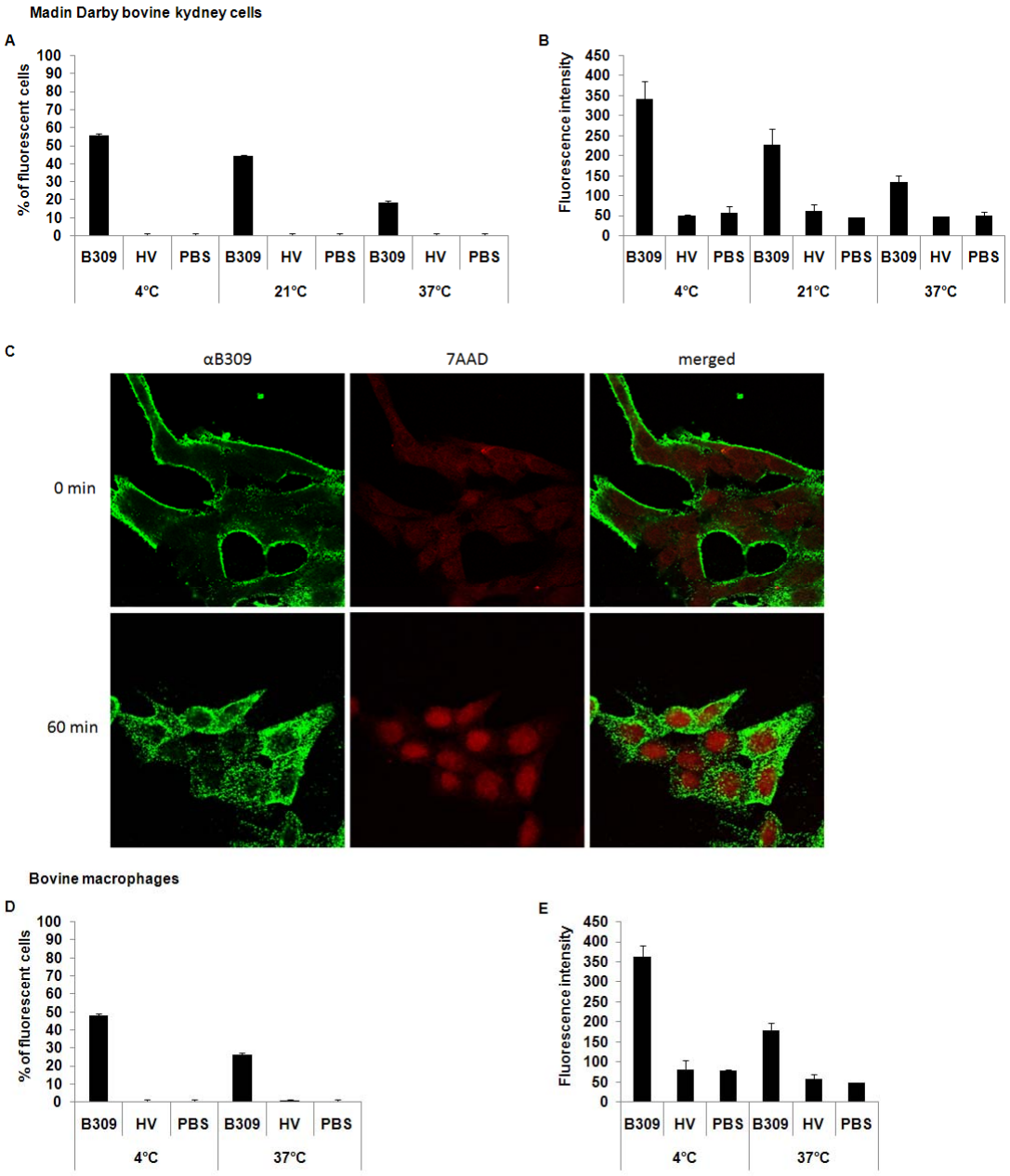

660

661 Fig. 4

662

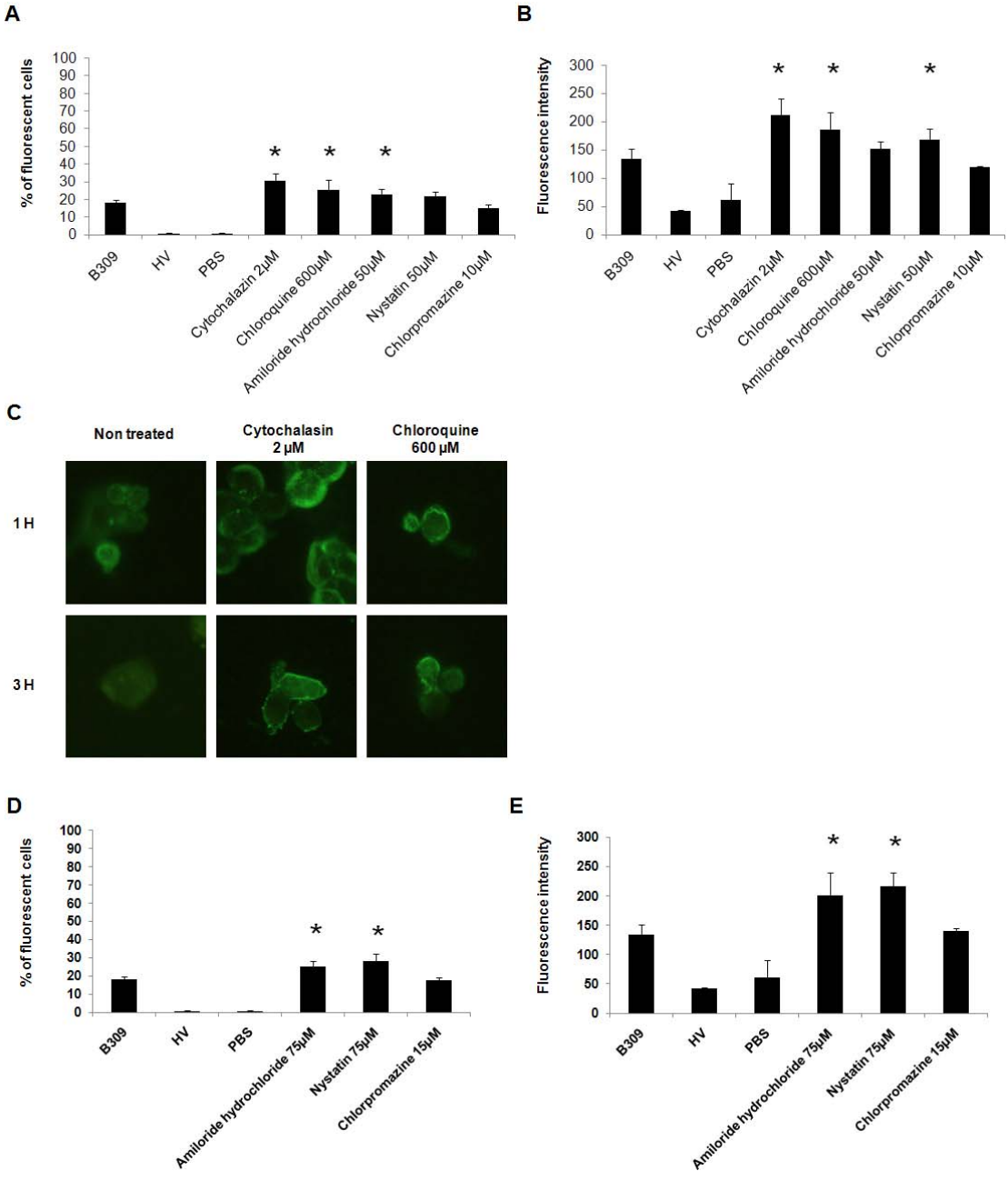
A
% of fluorescent cells
100
90
80
70
60
50
40
30
20
10
0
B309
HV
PBS
Cytochalazin 2µM
Chloroquine 600µM
Amiloride hydrochloride 50µM
Nystatin 50µM
Chlorpromazine 10µM
B
Fluorescence intensity
300
250
200
150
100
50
0
C
Non treated
Cytochalasin 2 µM
Chloroquine 600 µM
1 H
3 H
D
% of fluorescent cells
Amiloride hydrochloride 75µM
Nystatin 75µM
Chlorpromazine 15µM
E
Fluorescence intensity

663

664 Fig. 5

Food Microbiology 28 (2011) 52–58

Contents lists available at ScienceDirect

Food Microbiology

journal homepage: www.elsevier.com/locate/fm

Evaluation of a norovirus detection methodology for soft red fruits

Ambroos Stals [a,*], Leen Baert [a], Els Van Coillie [b], Mieke Uyttendaele [a]

[a] Ghent University, Faculty of Bioscience Engineering, Department of Food Safety and Food Quality, Laboratory of Food Microbiology and Food Preservation, Coupure Links 653, 9000 Ghent, Belgium
[b] Flemish Government, Institute for Agricultural and Fisheries Research, Technology and Food Sciences Unit, Brusselsesteenweg 370, 9090 Melle, Belgium

ARTICLE INFO

Article history:
Received 14 January 2010
Received in revised form
9 April 2010
Accepted 7 August 2010
Available online 14 August 2010

Keywords:
Norovirus
Murine norovirus-1
Detection methodology
Evaluation
Elution-concentration method
Real-time RT-PCR

ABSTRACT

In the present study, a proposed methodology for detection of GI and GII noroviruses (NoV) in soft red fruits was evaluated. The murine norovirus-1 (MNV-1), a recently described cultivable NoV surrogate was integrated in the detection methodology as full process control, reverse transcription control and real-time PCR internal amplification control.

Both the performance and robustness of the proposed methodology were analyzed.

Firstly, the performance of the method was examined by analysis of the recovery of MNV-1, GI and/or GII NoV inoculated on frozen raspberry crum samples. Results showed that the recovery of MNV-1 was not significantly influenced by the inoculum incubation time (30 min or overnight incubation) or the inoculum level (10^6 or 10^8 genomic MNV-1 copies/10 g of frozen raspberry crum sample). In contrast, a significant influence of the GI and GII NoV inoculum level (10^4 or 10^6 genomic MNV-1 copies/10 g of frozen raspberry crum sample) was noticed on the recovery of respectively GI and GII NoV from frozen raspberry crum samples.

Secondly, the robustness of the methodology was evaluated by subjecting three types of artificially MNV-1, GI and/or GII NoV contaminated soft red fruit products (deepfrozen forest fruit mix, fresh raspberries and fresh strawberry puree) to the method. Results showed a significant influence of the soft red fruit product type on the recovery efficiency of GI NoV and MNV-1, while no significant differences could be shown for GII NoV. In general, the recovery of GI and GII NoV in strawberry puree was more efficient from the strawberry puree compared to the two other soft red fruit types.

In conclusion, results show that this methodology can be used for detection of NoV in different soft red fruits, although NoV recovery efficiencies can be influenced by (1) the NoV concentration on the soft red fruit type and (2) the tested soft red fruit type.

1. Introduction

Noroviruses (NoV) are recognized as one of the leading causes of gastroenteritis in people of all age groups worldwide (Koopmans and Duizer, 2004). A number of reports have described these viruses as causative agents of food- and waterborne gastroenteritis outbreaks in Europe and in the USA. In 5 different European countries, 7–24% of viral (of which >90% NoV) gastroenteritis outbreaks were considered foodborne (Lopman et al., 2003b). Between 1994 and 2005, 6.6% of NoV outbreaks in the Netherlands were caused by ingestion of contaminated food (Svraka et al., 2007), while 5.2% of NoV outbreaks were caused by foodborne transmission in England and Wales between 1992 and 1999 (O'Brien et al., 2000). In the USA, contaminated food was the most reported vehicle of infection: it has been estimated that 40 to 57% of all NoV outbreaks were caused by this transmission type (Fankhauser et al., 2002; Mead et al., 1999). In a number of foodborne NoV outbreaks, fruits and vegetables were regarded as the causative agents. In particular, raspberries (Cotterelle et al., 2009; Falkenhorst et al., 2009; Le Guyader et al., 2004), tomatoes (Rutjes et al., 2006; Zomer et al., 2009), and salad vegetables (Lopman et al., 2003a) were considered as the causative food vehicle. Fruits and vegetables can be contaminated before harvesting by coming into contact with (sewage) water polluted with NoV (Horman et al., 2004; van den Berg et al., 2005). Postharvest contamination can occur during processing, storage, distribution or preparation and often the foodhandler plays a crucial role (Baert et al., 2009; Parashar et al., 1998).

Although efforts have been made recently (Asanaka et al., 2005; Straub et al., 2007), there is currently no reliable culture method available to detect NoV (Duizer et al., 2004). Therefore, detection of NoV relies solely on molecular methods, and real-time RT-PCR is currently considered as the gold standard for detection of NoV in

* Corresponding author. Tel.: +32 (0)9 264 99 02; fax: +32 (0)9 255 55 10.
E-mail address: ambroos.stals@ugent.be (A. Stals).

0740-0020/$ – see front matter © 2010 Elsevier Ltd. All rights reserved.
doi:10.1016/j.fm.2010.08.004

clinical, food and environmental samples (Jothikumar et al., 2005; Park et al., 2008; Wolf et al., 2007). Compared to clinical samples, detection of NoV on food samples is hardened due to the low concentration of virus particles and the presence of substances inhibiting molecular methods used for the detection and quantification of genomic material (Rijpens and Herman, 2002; Wilson, 1997; Escobar-Herrera et al., 2006). To address this problem, a number of elution-concentration methods for extraction of viral pathogens on fresh produce have been described (Baert et al., 2008a; Butot et al., 2007; Dubois et al., 2002; Love et al., 2008).

The current study describes the evaluation of a proposed NoV detection methodology consisting of (1) a NoV elution-concentration method described by Baert and colleagues (2008a) and (2) a multiplex real-time RT-PCR developed by Stals and colleagues (2009a). The performance of the method was determined on artificially contaminated frozen raspberry crum samples, while the robustness of the method was analyzed using a number of artificially contaminated soft red fruit products.

2. Methods

2.1. Soft red fruit products used for evaluation

Frozen raspberry crum samples were kindly provided by a local food manufacturer, while a frozen forest fruit mix, fresh strawberry puree and fresh raspberries were purchased at local food stores. Frozen raspberry crum samples were composed solely of raspberry pieces < 5 mm, while the fresh strawberry puree only contained mixed and homogenized strawberries. The frozen forest fruit mix contained strawberries, raspberries, blackberries, blueberries and black currants.

Raspberries, strawberries and all fruits present in the forest fruit mix consist mainly of water and carbohydrates, but are also a rich source of bioactive compounds such as phenolics, anthocyanins, organic acids, minerals and more (Tosun et al., 2009; Oszmianski and Wojdylo, 2009). All green parts were removed from the fresh raspberries before inoculation, and the strawberry puree contained strawberries solely with no added ingredients. The different fruit types in the frozen forest fruit mix did also not contain any green parts.

2.2. Artificial contamination of soft red fruit products

Soft red fruit products were artificially contaminated with GI and/or GII NoV and/or with MNV-1. For the GI and/or GII NoV inoculation, 2 stool samples containing GI.2 and GII.4 NoV, respectively, were friendly provided by the Rega Institute for Medical Research (Leuven, Belgium). Additionally, the soft red fruit samples were also artificially contaminated with diluted MNV-1 virus lysate. Tenfold serial dilutions of both faecal samples and of the MNV-1 virus lysate were prepared in PBS and stored at −80 °C until use. GI and/or GII NoV were incubated overnight, while the incubation times for MNV-1 inoculation were 30 min or overnight incubation. Concentrations of the GI and GII NoV genomic copies present in the diluted stool samples and of MNV-1 in the the diluted virus lysate were determined by real-time RT-PCR.

2.3. Virus extraction method

The virus extraction method was performed as described by Baert and colleagues (2008a). Briefly, 10 g of food product was washed with 30 ml of elution buffer (0.1 M Tris–HCl, 3% beef extract, 0.05 M glycine, pH 9.5 adjusted with 10 M NaOH) and 150 μl of pectinex 1XL (Novozymes, Dittingen, Switzerland) on a shaking platform during 20 min in a stomacher bag with filter compartment. The filtrate was transferred to a 50 ml centrifuge tube and centrifuged (10,000 × g, 15 min, 4 °C). The pH of the supernatant was adjusted to 7.2–7.4 with 0.1 M NaOH and 6 M HCl (Sigma, Steinheim, Switzerland). Subsequently, PEG 6000 (final concentration 10% wt/vol) and NaCl (final concentration 0.3 M) were added. The samples were placed overnight on a shaking platform (4 °C). The next day the samples were centrifuged (10,000 × g, 30 min, 4 °C) and the pellet was dissolved in 1 ml of PBS. The dissolved pellet was treated with one volume of chloroform/butanol (1:1 vol/vol) to remove inhibitory substances from the virus extract and centrifuged again (10,000 × g, 15 min, 4 °C). The aqueous phase (supernatans) was isolated and stored at −20 °C until RNA isolation.

2.4. RNA isolation

Hundred μl of the aqueous supernatans was used for RNA isolation with a RNeasy Mini kit (Qiagen, Hilden, Germany) according to the manufacturers' RNA Cleanup protocol (elution volume: 30 μl). All RNA isolations were stored at −20 °C until used.

2.5. Reverse transcription

A first pre-reaction mix consisting of 3 μl of extracted RNA and 1 μl of random hexamers (50 mM; Applied Biosystems, Foster City, CA, USA), in a final volume of 11.5 μl, was heated to 95 °C during 2 min, then cooled on ice during 2 min (thus avoiding the presence of secondary structures in the RNA and allowing the full hybridization of the RNA with the random hexamers). This first pre-reaction mix was then mixed with a second pre-reaction mix of 8.5 μl to obtain a final 20 μl RT-mastermix containing 2.5 μM random hexamers (Applied Biosystems), 25 U of Multiscribe reverse transcriptase (Applied Biosystems), 20 U of RNase inhibitor (Applied Biosystems), 5 mM $MgCl_2$ (Applied Biosystems), 1 × PCR buffer II (10 mM Tris HCl, pH 8.3, 50 mM KCl; Applied Biosystems), 0.1 mM dNTPs (GE Healthcare; Diegem, Belgium) and isolated RNA. Reverse transcription was carried out in a GeneAmp® PCR System 9700 (Applied Biosystems) with the following temperature profile: 22 °C for 10 min, 42 °C for 15 min, 99 °C for 5 min and 5 °C for 5 min. All cDNA was stored at −20 °C.

2.6. Quantitative real-time PCR

Quantitative multiplex real-time PCR for simultaneous detection of GI and GII NoV and for MNV-1 was carried out as described before by Stals et al. (2009a). Briefly, the 25 μl reaction mix consisted of 5 μl template DNA, 12.5 μl of TaqMan Universal PCR Master Mix (Applied Biosystems) containing dUTP and uracyl N-glycosylase (UNG), primers and hydrolysis probes. For GI NoV detection, primers QNIF4 (500 nM), NV1LCR (900 nM) and hydrolysis probe NVGGIp (100 nM) were used, while for GII NoV detection, primers QNIF2 (500 nM), COG2R (900 nM) and hydrolysis probe QNIFS (250 nM) were used. Finally, for detection of MNV-1, primers FW-ORF1/ORF2, RV-ORF1/ORF2 and fluorescent minor groove binding TaqMan® probe MGB-ORF1/ORF2 were all used in a final concentration of 200 nM. All primers and hydrolysis probes were purchased from Eurogentec (Liège, Belgium), except the minor groove binding TaqMan® probe, which was purchased from Applied Biosystems. Real-time quantification was performed on the Lightcycler® 480II real-time PCR instrument (Roche Diagnostics, Mannheim, Germany) under the following conditions: incubation at 50 °C for 2 min to activate UNG, initial denaturation/activation at 95 °C for 10 min, followed by 50 cycles of amplification with denaturation at 95 °C for 15 s and annealing and extension at 60 °C for 1 min. Amplification data were collected and analysed with the Lightcycler® 480II instruments' software. In some cases, primers and hydrolysis probes for detection

of MNV-1 were used as a singleplex real-time PCR assay. All real-time PCR reactions were duplicated except when mentioned.

Analysis of the standard curves of the GI/GII NoV and MNV-1 multiplex assay showed PCR efficiencies of 92.9%, 84.7% and 87.0%, respectively, while the MNV-1 singleplex assay had a 86.0% PCR efficiency. Intercepts of the multiplex assay were situated at 43.3, 43.7 and 39.7, respectively, while the MNV-1 singleplex assay showed an intercept of 42.8. All R^2 values were at least 0.997.

2.7. Overview detection strategy (Fig. 1)

Twenty grams of a soft red fruit product was split in 2 subsamples of each 10 g. Except for the negative control samples, both subsamples were subsequently artificially contaminated with GI and/or GII NoV and incubated at 4 °C overnight. The first subsample (10 g) was additionally spiked with 1 ml of an MNV-1 solution containing 10^6–10^7 genomic MNV-1 copies/ml, which functioned as full detection process control (MNV-1 PC). The MNV-1 PC was incubated during 30 min at room temperature. After virus extraction, RNA cleanup and reverse transcription (RT), the recovery efficiency of the MNV-1 PC was determined in the subsample by singleplex real-time RT-PCR for detection of MNV-1 (The presence of GI/GII NoV was not analyzed in this subsample).

Viral RNA of the second subsample (10 g) of the food product was extracted in parallel with the first subsample and RT of the isolated RNA was performed in duplicate. One µl of MNV-1 RNA (containing 10^3–10^4 RNA copies) was added to the RT reaction mix of 1 of the duplicate RT reactions as RT control (MNV-1 RTC). Finally, GI/GII NoV and MNV-1 cDNA was detected by multiplex real-time PCR as described above. One µl (containing ca. 10^2 plasmid copies) of plasmid p20.3 containing a full MNV-1 genome (Sosnovtsev et al., 2006) was added to the real-time PCR reaction mix of the cDNA preparation without MNV-1 RTC as real-time PCR internal amplification control (MNV-1 IAC). All real-time PCR reactions were duplicated.

Thus, 2 singleplex real-time PCR reactions for detection of the MNV-1 PC were performed in the first 10 g food subsample (inoculated with the MNV-1 PC). In the second 10 g food subsample (inoculated with GI and/or GII NoV), 4 multiplex real-time PCR reactions were executed for the detection of GI and GII NoV (2 reactions with the MNV-1 RTC and 2 reactions with the MNV-1 IAC).

The recovery of GI and GII NoV and MNV-1 PC were both quantitatively and qualitatively analyzed. Quantitative analysis was performed by comparing the mean recovered number of GI/GII NoV or MNV-1PC genomic copies with the mean inoculated number of GI/GII NoV or MNV-1 PC genomic copies. Qualitative analysis of the recovery of GI/GII NoV and MNV-1 PC was calculated by comparison of the number of positive real-time PCR signals to the number of performed real-time PCR reactions. The quantitative and qualitative analyses were expressed respectively as the "recovery efficiency" and "recovery success rate" in Tables 1 and 2.

Finally, the theoretical detection limit (100% recovery efficiency) of this method was determined at 400 genomic NoV copies per 10 g of soft red fruit food product.

2.8. Statistical analysis

For the Quantitative analyses, a two-way analysis of variance (2-way ANOVA) was used to investigate (1) the effect of incubation time and inoculation concentration on the recovery efficiency of MNV-1 from frozen raspberry crum and (2) the effect of the presence of different concentrations of GI and GII NoV on the recovery efficiencies of GI and GII NoV from raspberries. In addition, a one-way analysis of variance (1-way ANOVA) was used to investigate the effect of the GI or GII NoV inoculation concentrations on the recovery efficiencies of GI or GII NoV, respectively. As the assumptions for a 1-way ANOVA analysis were not fulfilled for the data describing the influence of the soft red fruit type (deep frozen forest fruit mix, fresh raspberries or strawberry puree) on the recovery efficiencies of GI and GII NoV and MNV-1, a non-parametric Kruskal–Wallis test (KW test) was applied.

All statistical analyses were performed using the statistical package R (version 2.10.1; R Foundation for Statistical Computing).

3. Results

3.1. Effect of the incubation time and inoculum level on the MNV-1 recovery

The effect of the incubation time and inoculum level on the MNV-1 recovery efficiency was analyzed by inoculating 2 different levels of MNV-1 on not GI/GII NoV inoculated soft red fruit samples

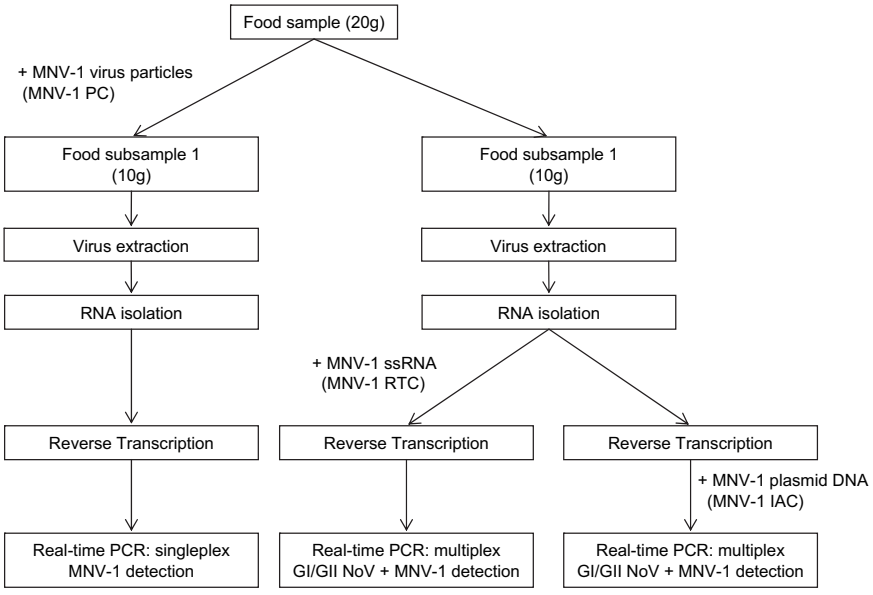

Fig. 1. Overview of the strategy used for detection of NoV in soft red fruit products.

Table 1
Influence of NoV inoculum level on NoV extraction efficiencies from 10 g of artificially contaminated deepfrozen raspberry crum samples. Every inoculation (combination) was duplicated.

Inoculum	GI NoV Inoculum level (genomic copies/10 g)	GII NoV Inoculum level (genomic copies/10 g)	Recovery efficiency[a] GI NoV ± stdev (success rate)[b]	Recovery efficiency[a] GII NoV ± stdev (success rate)[b]	Recovery efficiency[a] MNV-1 PC ± stdev (success rate)[b]
GI NoV	1.47×10^7	/[c]	28.44 ± 3.09% (4/8)	Negative	12.79 ± 2.10% (4/4)
	1.95×10^5	/	6.41 ± 4.64% (8/8)	Negative	14.34 ± 1.94% (4/4)
GII NoV	/	7.09×10^7	Negative	12.79 ± 2.93% (8/8)	12.40 ± 0.42% (4/4)
	/	2.32×10^6	Negative	5.70 ± 1.47 % (8/8)	13.63 ± 2.04 % (4/4)
GI + GII NoV	1.47×10^7	7.09×10^7	22.05 ± 8.31 % (8/8)	15.18 ± 5.39 % (8/8)	15.99 ± 5.84 % (4/4)
	1.47×10^7	2.32×10^6	19.26 ± 4.64% (8/8)	2.93 ± 0.93 % (8/8)	14.18 ± 6.32 % (4/4)
	1.95×10^5	7.09×10^7	9.71 % (1/8)	12.28 ± 1.09 % (7/8)	20.49 ± 1.29 % (4/4)
	1.95×10^5	2.32×10^6	11.79 ± 7.30 % (5/8)	7.00 ± 1.38 % (5/8)	19.61 ± 1.71 % (4/4)
Negative control	/	/	Negative	Negative	15.69 ± 7.06 % (4/4)

[a] ((Mean number GI/GII NoV or MNV-1 genomic copies recovered from 10 g of inoculated fruit sample)/(Number GI/GII NoV or MNV-1 genomic copies inoculated on 10 g of fruit sample)) × 100%.
[b] # Positive real-time PCR reactions/# performed real-time PCR reactions.
[c] Not added.

during 2 incubation periods: thirty minutes or overnight (both at 4 °C). In detail, high (2.66×10^8 genomic copies) and lower (2.66×10^6 genomic copies) levels of MNV-1 were inoculated on 10 g of frozen raspberry crum. Since no GI or GII NoV were inoculated, the detection strategy presented in Fig. 1 was not applied. Every combination of incubation time/inoculum level was triplicated, while real-time PCR reactions were not duplicated. Additionally, two not inoculated samples were analyzed as negative control.

The recovery efficiency of MNV-1 from raspberries was not significantly influenced by either the MNV-1inoculum levels (2-way ANOVA; $p = 0.8$) or the incubation time (2-way ANOVA; $p = 0.36$). In detail, High and low level MNV-1 inoculum levels were recovered with mean efficiencies of 28.75 ± 14.40% and 16.00 ± 14.58%, respectively. MNV-1 could be recovered with mean efficiencies of 19.30 ± 15.98% and 25.45 ± 17.87% after a thirty minute or overnight incubation period, respectively. Since no significant differences were found, an MNV-1 concentration resembling the lower MNV-1 inoculum level (ca. 10^6 MNV-1 genomic copies) in combination with a 30 min incubation time was chosen as MNV-1 PC in the NoV detection strategy (Fig. 1).

3.2. Determination GI and GII NoV recovery efficiency

To examine the recovery of GI and GII NoV from soft red fruits, 2 different inoculum levels of GI and/or GII NoV were spiked onto both frozen raspberry crum subsamples (each 10 g) as described in the detection strategy (Fig. 1) and incubated over night at 4 °C, resulting in 8 different inoculation(s) (combinations) (Table 1). Every inoculation (combination) was performed in duplicate. Additionally, two not GI or GII NoV inoculated samples were analyzed as negative control samples.

Quantitative analysis showed that the recovery efficiencies of GI and GII NoV solely from the frozen raspberry crum samples were influenced significantly by their inoculum level (1-way ANOVA; $p = 0.002$ and $p = 0.0001$, respectively). In addition, the presence of GI or GII NoV did not significantly influence the recovery of GII or GI NoV (2-way ANOVA; $p = 0.65$ and $p = 0.36$, respectively).

In detail, GI NoV genomic copies were recovered with a mean efficiency of 28.44 ± 3.09% (high inoculum level) and 6.41 ± 4.62% (low inoculum level) without the presence of GII NoV. In combination with the high and low level GII NoV inoculum, the high level GI NoV inoculum was recovered with mean efficiencies of

Table 2
Influence of soft red fruit type on NoV extraction efficiencies from artificially contaminated soft red fruit products. Inoculation(s) (combinations) were not duplicated.

Food type	GI NoV Inoculum level (genomic copies/10 g)	GII NoV Inoculum level (genomic copies/10 g)	Recovery efficiency[a] GI NoV ± stdev (recovery success rate)[b]	Recovery efficiency[a] GII NoV ± stdev (recovery success rate)[b]	Recovery efficiency[a] MNV-1 PC (recovery success rate)[b]
Deepfrozen forest fruit mix	3.99×10^4	/[c]	7.42 ± 2.65 % (2/4)		23.65% (2/2)
	/	9.63×10^4		Negative (0/4)	7.78% (2/2)
	3.99×10^4	9.63×10^4	13.47 ± 7.72 % (4/4)	20.68 ± 18.27 % (4/4)	28.78% (2/2)
	/	/	Negative	Negative	32.78% (2/2)
Fresh raspberries	3.99×10^4	/	21.50 ± 6.74 % (4/4)		8.29% (2/2)
	/	9.63×10^4		35.20 ± 31.54 % (2/4)	25.76% (2/2)
	3.99×10^4	9.63×10^4	Negative (0/4)	Negative (0/4)	21.10% (2/2)
	/	/	Negative	Negative	12.87% (2/2)
Fresh strawberry puree	3.99×10^4	/	51.13 ± 38.24 % (4/4)		52.05% (2/2)
	/	9.63×10^4		47.72 ± 25.43 % (4/4)	39.64% (2/2)
	3.99×10^4	9.63×10^4	61.06 ± 40.11 % (4/4)	25.26 ± 19.08 % (3/4)	75.65% (2/2)
	/	/	Negative	Negative	42.23% (2/2)

[a] ((Mean number GI/GII NoV or MNV-1 genomic copies recovered from 10 g of inoculated fruit sample)/(Number GI/GII NoV or MNV-1 genomic copies inoculated on 10 g of fruit sample)) × 100 %.
[b] # Positive real-time PCR reactions/# performed real-time PCR reactions.
[c] Not added.

22.05 ± 8.31% and 19.26 ± 4.64%, respectively. Similarly, 9.71% and 11.79 ± 7.30% of the low level GI NoV inoculum could be recovered in the presence of the high and low level GII NoV inoculum, respectively.

GII NoV genomic copies were recovered with mean efficiencies of 12.79 ± 2.93% (high inoculum level) and 5.70 ± 1.47% (low inoculum level) without the presence of GI NoV. In combination with the high and low level GI NoV inoculum, the high level GII NoV inoculum was recovered with mean efficiencies of 15.18 ± 5.39% and 12.28 ± 1.09%, respectively. Similarly, 2.93 ± 0.93% and 7.00 ± 1.38% of the low level GI NoV inoculum could be recovered in the presence of the high and low level GI NoV inoculum, respectively.

Finally, no inhibition of the reverse transcription reactions or real-time PCR was noticed for any of the samples. The MNV-1 RTC and MNV-1 IAC were detected without matrix at Ct values of 23.61 and 30.34, respectively and were in all samples detected at Ct values of 24.06 ± 0.32 and 30.11 ± 0.41. The MNV-1 PC could be recovered in all samples with a mean efficiency of 15.46 ± 4.00%.

Qualitative analysis showed that the high level GI NoV inoculum could be recovered with success rates of 4/8, 8/8 and 8/8 when solely inoculated and in combination with a low and high level GII NoV inoculum, respectively. In contrast, while the low level GI NoV inoculum could be recovered solely with a success rate of 8/8, success rates of 5/8 and 1/8 were noticed in combination with the low and high level GII NoV inoculum. The high level GII NoV inoculum could be recovered with success rates of 8/8,7/8 and 8/8 when solely inoculated and in combination with a low and high level GI NoV inoculum respectively. Finally, while the low level GII NoV inoculum could be recovered solely with a success rate of 8/8, success rates of 5/8 and 8/8 were observed in combination with a high and low level level GI NoV inoculum, respectively.

3.3. Evaluation NoV detection methodology on various soft red fruit products (Table 2)

To examine the robustness of the NoV detection methodology on a range of soft red fruit products, low levels of GI and/or GII NoV were inoculated onto both 10 g soft red fruit subsamples (deep frozen forest fruit mix, fresh raspberries or strawberry puree) as described in the detection strategy (Fig. 1). Inoculation(s) (combinations) were not duplicated. For each soft red fruit type, a not GI or GII NoV inoculated sample (10 grams) was analyzed as negative control.

Quantitative analysis showed that the recovery efficieny of GI NoV and MNV-1 inocula differed significantly according to the fruit type tested (KW test; $p = 0.037$ for GI; $p = 0.021$ for MNV-1). No such significant influences were noticed for the recovery of the GII NoV inoculum (KW test; $p = 0.21$).

In detail, the GI NoV inoculum was recovered in the deepfrozen forest fruit mix with mean efficiencies of 7.42 ± 2.65% and 13.47 ± 7.72%, respectively solely inoculated and in combination with the GII NoV inoculum. In contrast, the GII NoV inoculum could only be recovered in combination with the GI NoV inoculum with a mean efficiency of 20.68 ± 18.27% in the deepfrozen forest fruit mix, while no recovery was noticed when inoculated solely (it should also be noted that the MNV-1 PC was in this sample recovered with a low efficiency (7.78%)). In the fresh raspberries, the GI and GII NoV inocula were recovered with mean efficiencies of 21.50 ± 6.74% and 35.20 ± 31.54% when inoculated solely. Recovery of the combined GI and GII NoV inoculum was not possible from this fruit product. In the fresh strawberry puree, the GI NoV inoculum was recovered with mean efficiencies of 51.13 ± 38.24% and 61.06 ± 40.11%, respectively solely inoculated and in combination with the GII NoV inoculum. Similarly, the GII NoV inoculum could be recovered with mean efficiencies of 47.72 ± 25.43% and 25.26 ± 19.08%, respectively solely inoculated and in combination with the GI NoV inoculum. The mean recovery efficiencies of the MNV-1 PC in all deepfrozen forest fruit, fresh raspberry and fresh strawberry puree samples were 17.01 ± 7.89%, 23.25 ± 10.97% and 52.39 ± 16.40%, respectively. No inhibition of the reverse transcription reactions or real-time PCR was noticed for any of the samples: the MNV-1 RTC and MNV-1 IAC were detected without matrix at respective Ct values of 27.53 and 28.89 and were in all samples detected at Ct values of 29.24 ± 0.70 and 29.01 ± 0.39.

Qualitative analysis showed that, while recovery success rates of 2/4 and 0/4 were noticed in the deepfrozen forest fruit mix when GI and GII NoV were solely inoculated, a recovery success rate of 4/4 was noticed for both GI and GII NoV inocula when simultaneously inoculated on the deepfrozen forest fruit mix. While GI and GII NoV could be recovered with success rates of respectively 4/4 and 2/4 when inoculated solely on fresh raspberries, no recovery was noticed when GI and GII NoV were inoculated simultaneously (recovery success rates: 0/4). In addition, a recovery success rate of 4/4 was noticed in the fresh strawberry puree for GI when solely inoculated and or simultaneously with the GII NoV inoculum. For the GII NoV inoculum, recovery success rates of 4/4 and 3/4 were noticed in the fresh strawberry puree, respectively solely inoculated and in combination with the GI NoV inoculum. Finally, recovery of the MNV-1 PC was successful in all soft red fruit types.

4. Discussion

In the presented study, a methodological approach for the detection and quantification of noroviruses (NoV) in soft red fruit products is proposed and evaluated. The proposed NoV detection method is the combination of (1) a viral RNA extraction method developed by Baert et al. (2008a) and (2) a multiplex real-time RT-PCR assay for simultaneous detection of genogroup I (GI) and II (GII) NoV and the murine norovirus-1 (MNV-1) as described by Stals et al. (2009a). The described NoV detection strategy was based on the use of controls at different steps throughout the procedure that are considered critical for correct quantification: the reverse transcription of the extracted and isolated RNA and the real-time PCR reaction. Genomic MNV-1 RNA was used as reverse transcription control (MNV-1 RTC) and a plasmid containing a full genome of MNV-1 was used as real-time PCR internal amplification control (MNV-1 IAC) to detect possible inhibition of the reverse transcription reaction or real-time PCR, respectively. In parallel, the full NoV detection procedure was controlled using MNV-1 virus particles as process control (MNV-1 PC).

Costafreda and colleagues (2006) have described a similar approach for detection of (HAV) in shellfish. However, the latter study differed from the current study in two points: the protocol only included a reverse transcription control (RTC) and a full detection procedure process control (PC). The RTC consisted of a ssRNA fragment containing the primer-probe binding sites of the developed HAV real-time RT-PCR assay in the study. A genetically modified mengovirus (a HAV surrogate virus) was added to the artificially contaminated sample as PC. In contrast to other studies (Escobar-Herrera et al., 2006; Trujillo et al., 2006), the MNV-1 RTC in the current study was not based on synthetic run-off RNA transcripts, since such short nucleic acid fragments can easily cause laboratory contamination, leading to false-positive results (Stals et al., 2009b). The use of MNV-1 as process control in NoV detection protocols has been proposed due to its genetic similarities towards the NoV genome (Baert et al., 2008b; Wobus et al., 2006).

Although a number of methods have been published for detection of NoV in fruits and vegetables, no standardized method has been approved yet. Therefore, most labs are restricted to their

in-house developed methods. A possible reason for this lack of standardization is the limited attention spent on the evaluation and validation of such existing methods, resulting in the unawareness of inter-lab robustness of proposed methods. However, recent efforts have been made within various EU projects, between reference laboratories and within the European Committee for Standardization/Technical Committee/Working Group 6/Task Group 4 on virus detection in foods (CEN/TC275/WG6/TAG4), to stimulate the acceptance of a standardized method (Croci et al., 2008; Rodriguez-Lazaro et al., 2007).

The performance of the NoV detection method was investigated by analysis of the influence of (1) the GI and GII NoV and MNV-1 inoculum levels and (2) the inoculum incubation time of MNV-1 on the recovery efficiencies and recovery success rates. In general, GI and GII NoV could be recovered in frozen raspberry crum samples with mean efficiencies varying between 6 and 28% and 3 to 15%, respectively.

A similar NoV elution-concentration protocol designed by Butot et al. (2007) recovered 2160 RT-PCR units of GI.4 NoV per 60 g of food product with efficiencies of 1.7%, 2.6%, 17.9% and 19.6% in fresh strawberries, frozen raspberries, frozen blueberries and fresh raspberries, respectively. In a recent study, GI and GII NoV were extracted from artificially contaminated strawberries by combining a similar NoV elution-concentration method with an immunomagnetic separation technique (Park et al. 2008). In the latter study, 4×10^3–10^4 RT-PCR units GI and GII NoV RT-PCR units could be recovered with efficiencies of 29.50% and 14.14%, respectively.

A recent study comparing different aspects of the NoV elution – PEG concentration method (using conventional RT-PCR) showed that 85% recovery of 4×10^4 GII.4 NoV RT-PCR units from fresh strawberries was possible when combining a 3% beef extraction buffer as elution buffer with 8% (w/v) PEG8000 precipitation (Kim et al., 2008). Finally, Cheong et al. (2009) obtained 3.9% to 50% recoveries when extracting 4.8×10^0–10^3 GII NoV RT-PCR units from 5 g of strawberries by comparing different elution buffers in a similar elution-concentration detection protocol.

Results showed that, although the inoculum level had a significant influence on the recovery efficiency of GI and GII NoV in frozen raspberry crum samples, no significant effect of the presence of GI and GII NoV was noticed on the recovery of GII and GI NoV, respectively. Additionally, no significant influence of the inoculum time and inoculum level was noticed on the recovery efficiency of MNV-1. In concordance with these results, a recent analysis of naturally contaminated shellfish samples artificially contaminated with a genetically modified mengovirus process control showed that there were no differences in extraction efficiencies of the process control when GI and GII NoV were separate or simultaneously present (Le Guyader et al., 2009). The influence of the NoV concentration NoV on the recovery efficiency has been investigated by several authors, yet no consensus could be found. Fumian et al. (2009) found that high levels (pure and 10% PBS diluted fecal samples) of GI NoV on lettuce caused lower extraction efficiencies (approximately 1 log) compared to lower levels (1% and 0.1% PBS diluted fecal samples). Such results were not noticed in our study. However, the authors did not include an inhibition control in the detection method, hence possible inhibition of the reverse transcription reaction or real-time PCR could not be excluded. In contrast, a recent study showed that the recovery of NoV in lettuce was more successful at higher concentrations, both in small and high volumes of tested food samples (Cheong et al., 2009).

Finally, the robustness of the proposed NoV detection methodology was investigating by inoculating low levels (approximately 10^4–10^5 genomic copies/10 g soft red fruit product) of GI and/or GII NoV on various soft red fruit products. In general, a significant influence of the soft red fruit product type was noticeable: extraction of GI NoV and of the MNV-1 PC was more efficient in fresh strawberry puree samples compared to deepfrozen forest fruit samples or fresh raspberries, while no such effect was noticed for GII NoV. The effect of different food matrices on the quantification of NoV in food products has only been investigated by a limited number of authors. A recent study combining carbohydrate-coated magnetic beads with conventional RT-PCR showed that the recovery of NoV from lettuce and green onions had a higher success rate compared to the recovery of NoV from fresh strawberries (Morton et al., 2009). Results obtained in the current study were in contrast to a very similar extraction method developed by Dubois et al. (2002). The latter study showed a tenfold less efficient recovery of the NoV elution-concentration method when tested on mashed strawberries compared to frozen raspberries and fresh strawberries.

In conclusion, a NoV detection methododology has been succesfully evaluated, consisting of (1) a described NoV virus extraction method and RNA isolation (Baert et al., 2008a,b) and (2) two (multiplex) real-time RT-PCR assays for detection of GI and GII NoV and/or MNV-1. Additionally, a quantitative NoV detection strategy was proposed in which the murine norovirus-1 was successfully included as full detection procedure process control, reverse transcription control and real-time PCR internal amplification control. Results showed that the proposed NoV detection method is able to detect high and low NoV concentrations on a range of soft red fruit products. This NoV detection methodology therefore provides a reliable means for detection of human noroviruses in soft red fruit products.

Acknowledgements

This work was supported by Belgian Science Policy – Science for a Sustainable Development (SSD – NORISK – SD/AF/01). Clinical norovirus samples were kindly provided by Prof. Marc Van Ranst and Dr. Elke Wollants of the Rega Institute for Medical Research (Leuven, Belgium).

References

Asanaka, M., Atmar, R.L., Ruvolo, V., Crawford, S.E., Neill, F.H., Estes, M.K., 2005. Replication and packaging of Norwalk virus RNA in cultured mammalian cells. Proc. Natl. Acad. Sci. U.S.A. 102, 10327–10332.

Baert, L., Uyttendaele, M., Debevere, J., 2008a. Evaluation of viral extraction methods on a broad range of Ready-To-Eat foods with conventional and real-time RT-PCR for Norovirus GII detection. Int. J. Food Microbiol. 123, 101–108.

Baert, L., Wobus, C.E., Van Coillie, E., Thackray, L.B., Debevere, J., Uyttendaele, M., 2008b. Detection of murine norovirus 1 by using plaque assay, transfection assay, and real-time reverse transcription-PCR before and after heat exposure. Appl. Environ. Microbiol. 74, 543–546.

Baert, L., Uyttendaele, M., Stals, A., Van Coillie, E., Dierick, K., Debevere, J., Botteldoorn, N., 2009. Reported foodborne outbreaks due to noroviruses in Belgium: the link between food and patient investigations in an international context. Epidemiol. Infect. 137, 316–325.

Butot, S., Putallaz, T., Sanchez, G., 2007. Procedure for rapid concentration and detection of enteric viruses from berries and vegetables. Appl. Environ. Microbiol. 73, 186–192.

Cheong, S., Lee, C., Choi, W.C., Lee, C.H., Kim, S.J., 2009. Concentration method for the detection of enteric viruses from large volumes of foods. J. Food Prot. 72, 2001–2005.

Costafreda, M.I., Bosch, A., Pinto, R.M., 2006. Development, evaluation, and standardization of a real-time TaqMan reverse transcription-PCR assay for quantification of hepatitis A virus in clinical and shellfish samples. Appl. Environ. Microbiol. 72, 3846–3855.

Cotterelle, B., Drougard, C., Rolland, J., Becamel, M., Boudon, M., Pinede, S., Traoré, O., Balay, K., Pothier, P., Espié, E., 2009. Outbreak of norovirus infection associated with the consumption of frozen raspberries, France, March 2005. Euro. Surveill. 10 (17).

Croci, L., Dubois, E., Cook, N., De Medici, D., Schultz, A.C., China, B., Rutjes, S.A., Hoorfar, J., van der Poel, W.H.M., 2008. Current methods for extraction and concentration of enteric viruses from fresh fruit and vegetables: towards international standards. Food Anal. Methods 1, 73–84.

Dubois, E., Agier, C., Traore, O., Hennechart, C., Merle, G., Cruciere, C., Laveran, H., 2002. Modified concentration method for the detection of enteric viruses on

fruits and vegetables by reverse transcriptase-polymerase chain reaction or cell culture. J. Food Prot. 65, 1962–1969.
Duizer, E., Schwab, K.J., Neill, F.H., Atmar, R.L., Koopmans, M.P.G., Estes, M.K., 2004. Laboratory efforts to cultivate noroviruses. J. Gen. Virol. 85, 79–87.
Escobar-Herrera, J., Cancio, C., Guzman, G.I., Villegas-Sepulveda, N., Estrada-Garcia, T., Garcia-Lozano, H., Gomez-Santiago, F., Gutierrez-Escolano, A.L., 2006. Construction of an internal RT-PCR standard control for the detection of human caliciviruses in stool. J. Virol. Methods 137, 334–338.
Falkenhorst, G., Krussell, L., Lisby, M., Bo Madsen, S., Böttiger, B., Molbak, K., 2009. Imported frozen raspberries cause a series of norovirus outbreaks in Denmark, 2005. Euro. Surveill. 10 (38).
Fankhauser, R.L., Monroe, S.S., Noel, J.S., Humphrey, C.D., Bresee, J.S., Parashar, U.D., Ando, T., Glass, R.I., 2002. Epidemiologic and molecular trends of "Norwalk-like viruses" associated with outbreaks of gastroenteritis in the United States. J. Infect. 186, 1–7.
Fumian, T.M., Leite, J.P.G., Marin, V.A., Miagostovich, M.P., 2009. A rapid procedure for detecting noroviruses from cheese and fresh lettuce. J. Virol. Methods 155, 39–43.
Horman, A., Rimhanen-Finne, R., Maunula, L., von Bonsdorff, C.H., Torvela, N., Heikinheimo, A., Hanninen, M.L., 2004. Campylobacter spp., Giardia spp., Cryptosporidium noroviruses and indicator organisms in surface water in southwestern Finland, 2000–2001. Appl. Environ. Microbiol. 70, 87–95.
Jothikumar, N., Lowther, J.A., Henshilwood, K., Lees, D.N., Hill, V.R., Vinje, J., 2005. Rapid and sensitive detection of noroviruses by using TaqMan-based one-step reverse transcription-PCR assays and application to naturally contaminated shellfish samples. Appl. Environ. Microbiol. 71, 1870–1875.
Kim, H.Y., Kwak, I.S., Hwang, I.G., Ko, G., 2008. Optimization of methods for detecting norovirus on various fruit. J. Virol. Methods 153, 104–110.
Koopmans, M., Duizer, E., 2004. Foodborne viruses: an emerging problem. Int. J. Food Microbiol. 90, 23–41.
Le Guyader, F.S., Mittelholzer, C., Haugarreau, L., Hedlund, K.O., Alsterlund, R., Pommepuy, M., Svensson, L., 2004. Detection of noroviruses in raspberries associated with a gastroenteritis outbreak. Int. J. Food Microbiol. 97, 179–186.
Le Guyader, F.S., Parnaudeau, S., Schaeffer, J., Bosch, A., Loisy, F., Pommepuy, M., Atmar, R.L., 2009. Detection and quantification of noroviruses in shellfish. Appl. Environ. Microbiol. 75, 618–624.
Lopman, B.A., Adak, G.K., Reacher, M.H., Brown, D.W.G., 2003a. Two epidemiologic patterns of Norovirus outbreaks: Surveillance in England and Wales, 1992–2000. Emerg. Infect. Dis. 9, 71–77.
Lopman, B.A., Reacher, M.H., van, D.Y., Hanon, F.X., Brown, D., Koopmans, M., 2003b. Viral gastroenteritis outbreaks in Europe, 1995–2000. Emerg. Infect. Dis. 9, 90–96.
Love, D.C., Casteel, M.J., Meschke, J.S., Sobsey, M.D., 2008. Methods for recovery of hepatitis A virus (HAV) and other viruses from processed foods and detection of HAV by nested RT-PCR and TaqMan RT-PCR. Int. J. Food Microbiol. 126, 221–226.
Mead, P.S., Slutsker, L., Dietz, V., Mccaig, L.F., Bresee, J.S., Shapiro, C., Griffin, P.M., Tauxe, R.V., 1999. Food-related illness and death in the United States. Emerg. Infect. Dis. 5, 607–625.
Morton, V., Jean, J., Farber, J., Mattison, K., 2009. Detection of noroviruses in ready-to-eat foods by using carbohydrate-coated magnetic beads. Appl. Environ. Microbiol. 75, 4641–4643.
O'Brien, S.J., Mitchell, R.T., Gillespie, I.A., Adak, G.K., 2000. Microbiological status of ready-to-eat fruit and vegetables. Discussion paper: advisory committee on the microbiological of food. ACM 476, 1–34.
Oszmianski, J., Wojdylo, A., 2009. Comparative study of phenolic content and antioxidant activity of strawberry puree, clear, and cloudy juices. Eur. Food Res. Technol. 4, 623–631.
Parashar, U.D., Dow, L., Fankhauser, R.L., Humphrey, C.D., Miller, J., Ando, T., Williams, K.S., Eddy, C.R., Noel, J.S., Ingram, T., Bresee, J.S., Monroe, S.S., Glass, R.I., 1998. An outbreak of viral gastroenteritis associated with consumption of sandwiches: implications for the control of transmission by food handlers. Epidemiol. Infect. 121, 615–621.
Park, Y., Cho, Y.H., Jee, Y., Ko, G., 2008. Immunomagnetic separation combined with real-time reverse transcriptase PCR assays for detection of norovirus in contaminated food. Appl. Environ. Microbiol. 74, 4226–4230.
Rijpens, N.P., Herman, L.M.F., 2002. Molecular methods for identification and detection of bacterial food pathogens. J. AOAC Int. 85, 984–995.
Rodriguez-Lazaro, D., Lombard, B., Smith, H., Rzezutka, A., D'Agostino, M., Helmuth, R., Schroeter, A., Malorny, B., Miko, A., Guerra, B., Davison, J., Kobilinsky, A., Hernandez, M., Bertheau, Y., Cook, N., 2007. Trends in analytical methodology in food safety and quality: monitoring microorganisms and genetically modified organisms. Trends Food Sci. Technol. 18, 306–319.
Rutjes, S.A., Lodder-Verschoor, F., van der Poel, W.H.M., van Duijnhoven, Y.T.H.P., Husman, A.M.D., 2006. Detection of noroviruses in foods: a study on virus extraction procedures in foods implicated in outbreaks of human gastroenteritis. J. Food Prot. 69, 1949–1956.
Sosnovtsev, S.V., Belliot, G., Chang, K.O., Prikhodko, V.G., Thackray, L.B., Wobus, C.E., Karst, S.M., Virgin, H.W., Green, K.Y., 2006. Cleavage map and proteolytic processing of the murine norovirus nonstructural polyprotein in infected cells. J. Virol. 80, 7816–7831.
Stals, A., Baert, L., Botteldoorn, N., Werbrouck, H., Herman, L., Uyttendaele, M., Van Coillie, E., 2009a. Multiplex real-time RT-PCR for simultaneous detection of GI/GII Noroviruses and murine norovirus 1. J.Virol. Methods 161, 247–253.
Stals, A., Werbrouck, H., Baert, L., Botteldoorn, N., Herman, L., Uyttendaele, M., Van Coillie, E., 2009b. Laboratory efforts to eliminate contamination problems in the real-time RT-PCR detection of noroviruses. J. Microbiol. Methods 77, 72–76.
Straub, T.M., Bentrup, K.H.Z., Orosz-Coghlan, P., Dohnalkova, A., Mayer, B.K., Bartholomew, R.A., Valdez, C.O., Bruckner-Lea, C.J., Gerba, C.P., Abbaszadegan, M.A., Nickerson, C.A., 2007. Cell culture assay for human noroviruses – response. Emerg. Infect. Dis. 13, 1117–1118.
Svraka, S., Duizer, E., Vennema, H., de Bruin, E., van der Veer, B., Dorresteijn, B., Koopmans, M., 2007. Etiological role of viruses in outbreaks of acute gastroenteritis in the Netherlands from 1994 through 2005. J. Clin. Microbiol. 45, 1389–1394.
Tosun, M., Ercisli, S., Karlidag, H., Sengul, M., 2009. Characterization of red raspberry (Rubus idaeus L.) genotypes for their physicochemical properties. J. Food Sci. 74 (7), C575–C579.
Trujillo, A.A., McCaustland, K.A., Zheng, D.P., Hadley, L.A., Vaughn, G., Adams, S.M., Ando, T., Glass, R.I., Monroe, S.S., 2006. Use of TaqMan real-time reverse transcription-PCR for rapid detection, quantification, and typing of norovirus. J. Clin. Microbiol. 44, 1405–1412.
van den Berg, H., Lodder, W., van der Poel, W., Vennema, H., Husman, A.M.D., 2005. Genetic diversity of noroviruses in raw and treated sewage water. Res. Microbiol. 156, 532–540.
Wilson, I.G., 1997. Inhibition and facilitation of nucleic acid amplification. Appl. Environ. Microbiol. 63, 3741–3751.
Wobus, C.E., Thackray, L.B., Virgin, H.W., 2006. Murine norovirus: a model system to study norovirus biology and pathogenesis. J. Virol. 80, 5104–5112.
Wolf, S., Williamson, W.M., Hewitt, J., Rivera-Aban, M., Lin, S., Ball, A., Scholes, P., Greening, G.E., 2007. Sensitive multiplex real-time reverse transcription-PCR assay for the detection of human and animal noroviruses in clinical and environmental samples. Appl. Environ. Microbiol. 73, 5464–5470.
Zomer, T.P., De Jong, B., Kühlmann-Berenzon, S., Nyrén, O., Svenungsson, B., Hedlund, K.O., Ancker, C., Wahl, T., Andersson, Y., 2009. A foodborne norovirus outbreak at a manufacturing company. Epidemiol. Infect. 21, 1–6.

Journal of Food Protection, Vol. 000, No. 000, 0000, Pages 000–000
doi:10.4315/0362-028X.JFP-10-209

Screening of Fruit Products for Norovirus and the Difficulty of Interpreting Positive PCR Results

AMBROOS STALS,[1]* LEEN BAERT,[1] VICKY JASSON,[1] ELS VAN COILLIE,[2] AND MIEKE UYTTENDAELE[1]

[1]*Laboratory of Food Microbiology and Food Preservation, Department of Food Safety and Food Quality, Faculty of Bioscience Engineering, Ghent University, Coupure Links 653, 9000 Ghent, Belgium; and* [2]*Technology and Food Science Unit, Institute for Agricultural and Fisheries Research, Flemish Government, Brusselsesteenweg 370, 9090 Melle, Belgium*

MS 10-209: Received 20 May 2010/Accepted 8 November 2010

ABSTRACT

Despite recent norovirus (NoV) outbreaks related to consumption of fruit products, little is known regarding the NoV load on these foods. Therefore, 75 fruit products were screened for NoV presence by using an evaluated in-house NoV detection methodology consisting of a NoV extraction method and a reverse transcription quantitative PCR assay. Additionally, the fruit samples were screened for bacterial pathogens and bacterial hygiene indicators. Results of the NoV screening showed that 18 of 75 samples tested positive for GI and/or GII NoV despite a good bacteriological quality. The recovery of murine norovirus 1 virus particles acting as process control was successful in 31 of 75 samples with a mean recovery efficiency of 11.32% ± 6.08%. The level of detected NoV genomic copies ranged between 2.5 and 5.0 log per 10 g. NoV GI and/or GII were found in 4 of 10, 7 of 30, 6 of 20, and 1 of 15 of the tested raspberries, cherry tomatoes, strawberries, and fruit salad samples, respectively. However, confirmation of the positive quantitative PCR results by sequencing genotyping regions in the NoV genome was not possible. Due to the nature of the method used (reverse transcription quantitative PCR) for detection of genomic material, no differentiation was possible between infectious and noninfectious viral particles. No Nov outbreaks related to the tested fruit product types were reported during the screening period, which hampers a conclusion as to whether or not these unexpected high numbers of NoV-positive results should be perceived as a public health threat. These results, however, may indicate a prior NoV contamination of the tested food samples throughout the fresh produce chain.

Due to the beneficial effects of fruits and vegetables on the consumer's health, efforts have been made recently to promote the inclusion of these food products into daily diets, and a minimum daily consumption of 400 g is recommended *(17, 37)*. However, the increased consumption of fruits and vegetables has also been linked to an increased number of foodborne outbreaks associated with these food types *(14)*. In particular, a number of acute bacterial and nonbacterial gastroenteritis foodborne outbreaks have been linked to consumption of fresh fruit products and have been summarized in various review articles *(31, 33)*.

Foodborne outbreaks related to fruit products are probably mainly caused via two transmission routes. The fruit product can be contaminated by preharvest manipulations such as the use of contaminated irrigation water *(15, 26)*, and a second possible cause of these foodborne outbreaks is by (post-) harvest contamination of the fruit product. In the latter contamination type, often an infected food handler or the use of contaminated equipment and/or process water is involved *(5, 32)*.

* Author for correspondence. Tel: 00 32 (0)9 264 99 02; Fax: 00 32 (0)9 255 55 10; E-mail: Ambroos.Stals@ugent.be.

To investigate whether these transmission routes might introduce NoV in the food chain, data are needed regarding NoV prevalence on fresh produce.

The goal of the present study was therefore twofold: first, the presence of noroviruses (NoV) was determined on a total of 75 raspberry, cherry tomato, strawberry, and mixed-fruit salad samples by using an in-house–developed and evaluated NoV detection methodology for fruit products *(36)*. The use of (genomic material of) murine norovirus 1 (MNV-1), a cultivable NoV surrogate virus, was applied as a control at different crucial steps in the NoV analysis. Secondly, the presence of three bacterial pathogens (*Escherichia coli* O157:H7, *Salmonella, Listeria* spp., and *Listeria monocytogenes*) and enumerations of *Enterobacteriaceae* and *E. coli* were analyzed in all tested fruit samples.

MATERIALS AND METHODS

Overview of analyzed samples. A total of 75 fruit samples that might pose a risk for NoV contamination (raspberries, cherry tomatoes, strawberries, and fruit salads) were analyzed for NoV and bacteriological pathogens and indicators. For raspberries, two lots (originating from Serbia and Poland) containing five samples originating from five different farms were tested. For cherry tomatoes and strawberries, three and two lots (originating from Spain), respectively, containing 10 samples each were analyzed. Finally, 15 mixed-fruit salads (prepared in Belgium) were

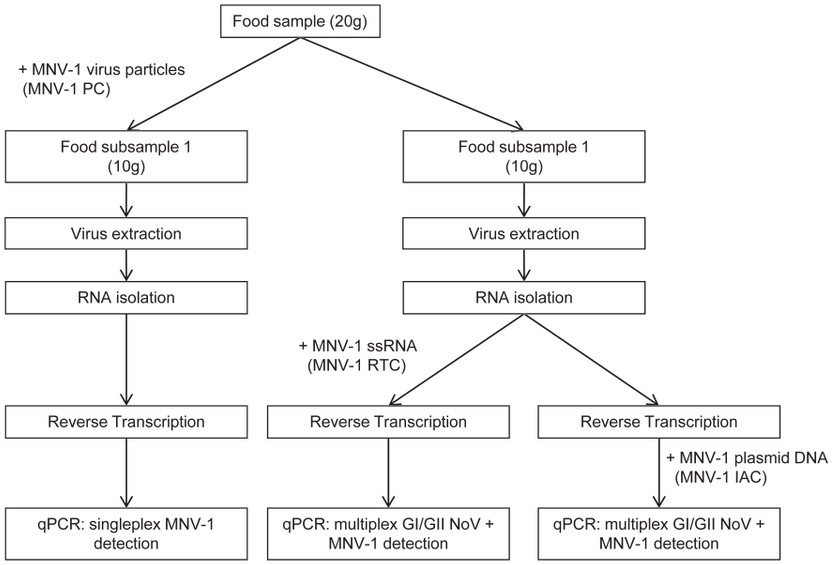

FIGURE 1. *Overview of the strategy used for detection of NoV in the fruit products.*

examined. All samples were kindly provided by local manufacturers and distributors. Bacteriological analysis was performed within 24 h of arrival of the samples, while aliquots of the samples were stored at 4°C for NoV analysis (all samples were analyzed for NoV within a maximum of 48 h).

Norovirus analysis: overview of NoV detection strategy. Twenty grams of fruit product was split into two subsamples of 10 g each (Fig. 1). The first subsample was inoculated with 1 ml of an MNV-1 solution containing 10^3 to 10^4 MNV-1 genomic copies/ml, functioning as process control (MNV-1 PC). The MNV-1 PC was incubated for 30 min at room temperature. After virus extraction, RNA purification and reverse transcription (RT), the recovery of the MNV-1 PC was determined quantitatively and qualitatively in this subsample by singleplex RT-quantitative PCR (RT-qPCR) for detection of MNV-1.

Virus extraction and RNA purification of the second food subsample (10 g) of the fruit sample were performed in parallel with the first subsample, and RT of the purified RNA was performed twice. One microliter of MNV-1 genomic RNA (containing 10^3 to 10^4 copies) was added to one of the two RT reaction mixes as RT control (MNV-1 RTC). One microliter ($\sim 10^2$ copies) of plasmid p20.3 containing a full MNV-1 genome *(34)* was added to the qPCR mix of the cDNA preparation without MNV-1 RTC as qPCR internal amplification control (MNV-1 IAC). Finally, GI and GII NoV and MNV-1 ~~plasmid DNA/MNV-1~~ RTC were detected by multiplex qPCR as described previously *(35)*.

Thus, four multiplex qPCRs were performed for the detection of GI and GII NoV and MNV-1 (two reactions with the MNV-1 RTC and two reactions with the MNV-1 IAC).

Data analysis. The recovery of the MNV-1 PC from the first subsample was both qualitatively and quantitatively analyzed. First, qualitative analysis of the recovery of MNV-1 PC was calculated as the ratio of the number of samples (per fruit type) with successful recovery of the MNV-1 PC to the total number of samples (per fruit type). The recovery of the MNV-1 PC was defined as successful when at least one of the singleplex real-time PCR duplicates was positive. This qualitative analysis was defined as ''recovery success rate'' in Table 1. Secondly, quantitative analysis of the recovery of the MNV-1 PC was performed per individual sample as follows: (mean recovered number of MNV-1 PC genomic copies per individual sample/mean inoculated number

TABLE 1. *Quantitative and qualitative analysis of the performance of MNV-1 as process control (MNV-1 PC), reverse transcription control (MNV-1 RTC), and qPCR internal amplification control (MNV-1 IAC)*

		MNV-1 PC		MNV-1 RTC	MNV-1 IAC
Fruit type	*N*	% Mean recovery efficiency[a] ± SD (recovery success rate)[b]	Recovery efficiency range (%)	% Recovery efficiency ± SD (recovery success rate)	% Recovery efficiency ± SD (recovery success rate)
Raspberries	10	12.94 ± 9.3 (8/10)	2.79–27.27	46.17 ± 17.70 (9/10)	100.93 ± 9.55 (9/10)
Cherry tomatoes	30	11.17 ± 8.22 (2/30)	2.57–19.78	56.13 ± 12.31 (30/30)	117.76 ± 9.22 (30/30)
Strawberries	20	12.80 ± 5.60 (19/20)	5.35–19.68	46.54 ± 29.75 (20/20)	114.27 ± 19.03 (20/20)
Mixed-fruit salad	15	8.39 ± 1.18 (2/15)	7.56–9.23	63.81 ± 15.72 (15/15)	119.32 ± 28.32 (15/15)
Total	75	11.32 ± 6.08 (31/75)	2.57–27.27	53.16 ± 18.87 (74/75)	114.75 ± 15.70 (74/75)

[a] Recovery efficiency: [(mean level of MNV-1 genomic/RNA/plasmid copies inoculated)/(mean level of MNV-1 genomic/RNA/plasmid copies recovered)] × 100%.

[b] Recovery success rate: (no. of samples per fruit type with successful recovery of the MNV-1 PC/RTC/IAC)/(no. of samples per fruit type).

TABLE 2. *Overview of NoV genomic presence on tested fruit samples*

Type of fruit	Sample name	GI NoV presence[a] (~~Cq~~ Ct value[s])	GII NoV presence[a] (~~Cq~~ Ct value[s])
Raspberries ($n = 10$)	RB P03 20090421	ND[b]	3.05 (39.98)
	RB P05 20090421	2.61 (40.81)	3.70 (37.66)
	RB S01 20090421	2.45 (41.24; 41.47)	3.60 (38.03)
	RB S02 20090421	3.21 (38.74)	ND
Cherry tomatoes ($n = 30$)	CT 07 20090423	ND	3.91 (38.66)
	CT 09 20090423	4.11 (40.67)	ND
	CT 10 20090423	4.33 (39.98)	ND
	CT 01 20090429	4.08 (38.54; 38.30)	ND
	CT 04 20090429	ND	4.19 (41.31)
	CT 06 20090429	4.07 (37.39; 39.53)	5.04 (38.38)
	CT 03 20090513	4.38 (39.38)	4.67 (37.15)
Strawberries ($n = 20$)	SB 01 20090506	4.10 (39.27)	3.28 (39.75)
	SB 04 20090506	ND	3.05 (40.58)
	SB 06 20090506	ND	3.77 (38.01)
	SB 03 20090520	2.29 (41.97)	ND
	SB 04 20090520	2.86 (40.02)	ND
	SB 07 20090520	3.40 (38.20)	ND
Fruit salads ($n = 15$)	FS 01 20090504	ND	4.64 (40.92; 40.19)

[a] Number of detected genomic NoV copies per 10 g of fruit product sample (expressed in log scale).
[b] ND, not detected.

of MNV-1 PC genomic copies per individual sample) × 100%. Only samples with a successful recovery of the MNV-1 PC were used in the quantitative analysis of the MNV-1 PC recovery. This quantitative analysis was defined as ''recovery efficiency'' in Tables 1 and 2. NoV genomic copy levels expressed in Table 2 were not corrected ~~and correspond~~ to the recovery efficiency of the MNV-1 PC.

Virus extraction method. The virus extraction method was based on a previously reported method *(3)*. Briefly, 10 g of food product was washed with 30 ml of elution buffer (0.1 M Tris-HCl, 3% beef extract, 0.05 M glycine, pH 9.5, adjusted with 10 M NaOH) and 150 μl of pectinex 1XL (Novozymes, Dittingen, Switzerland) on a shaking platform for 20 min in a stomacher bag with a filter compartment. The filtrate was transferred to a 50-ml centrifuge tube and centrifuged (10,000 × *g,* 15 min, 4°C). The pH of the supernatant was adjusted to 7.2 to 7.4 with 0.1 M NaOH and 6 M HCl (Sigma, Steinheim, Switzerland). Subsequently, PEG 6000 and NaCl were added to obtain final concentrations of 10% (wt/vol) and 0.3 M, respectively. The samples were placed overnight on a shaking platform (4°C). The next day, the samples were centrifuged (10,000 × *g,* 30 min, 4°C) and the pellet was dissolved in 1 ml of phosphate-buffered saline. The dissolved pellet was treated with 1 volume of chloroform-butanol (1:1, vol/vol; Sigma) and centrifuged again (10,000 × *g,* 15 min, 4°C).

RNA purification. One hundred microliters of the aqueous phase was kept separately and stored at −20°C until it was used for RNA purification with an RNeasy Mini kit (Qiagen, Hilden, Germany) according to the manufacturers' RNA cleanup protocol (elution volume, 30 μl).

RT. A prereaction mix consisting of 3 μl of purified RNA, 1 μl of random hexamers (50 mM; Applied Biosystems, Foster City, CA) and nuclease-free water in a final volume of 11.5 μl was heated to 95°C for 2 min followed by 2 min of cooling on ice. In accordance to the NoV detection strategy (Fig. 1), 1 μl of MNV-1 RNA obtained from diluted MNV-1 lysate was added to specific RT reactions as MNV-1 RTC. This first prereaction mix was then mixed with a second prereaction mix of 8.5 μl to obtain a final 20-μl RT reaction mix containing 2.5 ~~m~~M random hexamers (Applied Biosystems), 25 U of Multiscribe reverse transcriptase (Applied Biosystems), 20 U of RNase inhibitor (Applied Biosystems), 5 mM $MgCl_2$ (Applied Biosystems), 1× PCR buffer II (10 mM Tris-HCl, pH 8.3, 50 mM KCl; Applied Biosystems), ~~0.~~1 mM deoxynucleoside triphosphates (GE Healthcare; Diegem, Belgium), and extracted RNA. RT was carried out in a GeneAmp PCR System 9700 (Applied Biosystems) with the following temperature profile: 22°C for 10 min, 42°C for 15 min, 99°C for 5 min, and 5°C for 5 min. All cDNA preparations were stored at −20°C.

qPCR. qPCR was carried out as described before *(35)*. Briefly, the 25-μl reaction mix consisted of 5 μl of template DNA, 12.5 μl of TaqMan Universal PCR Master Mix (Applied Biosystems) containing dUTP, uracyl *N*-glycosylase, and primers and hydrolysis probes. In accordance with the NoV detection strategy (Fig. 1), 1 μl (~10^2 copies) of plasmid p20.3 *(34)* was added as MNV-1 IAC to the qPCR mix without MNV-1 RTC. Real-time quantification was performed on the Lightcycler LC480II qPCR instrument (Roche Diagnostics, Mannheim, Germany) under the following conditions: incubation at 50°C for 2 min to activate uracyl *N*-glycosylase and initial denaturation and activation at 95°C for 10 min, followed by 50 cycles of amplification with denaturation at 95°C for 15 s and annealing and extension at 60°C for 1 min. Amplification data were collected and analyzed with the LC480II instruments' software.

All qPCR terminology and data were described according to the ''minimum information for publication of quantitative real-time PCR experiments'' guidelines *(8)*.

Bacteriological analysis: *Enterobacteriaceae* and *E. coli* enumeration. For quantitative *Enterobacteriaceae* and *E. coli* enumerations, 25 g of the fruit sample was homogenized in 225 ml of buffered peptone water (BioMérieux, Marcy-l'Etoile, France). Subsequently, 1.0 ml of this primary dilution of the fruit samples was analyzed by using the TEMPO BC (*Enterobacteriaceae* enumeration) or TEMPO EC (*E. coli* enumeration) automated

most-probable-number methods (BioMérieux), according to the manufacturer's instructions.

***Listeria* spp. and *L. monocytogenes*.** For detection of *Listeria* spp. and *L. monocytogenes,* 25 g of the soft red fruit sample was diluted in 225 ml of Half-Fraser Broth (BioMérieux) and subsequently homogenized by using the Seward Laboratory blender 400 (UAC House). After 20 to 26 h of incubation at 30°C, 1 ml of this primary enrichment culture was transferred to a 10-ml Fraser Broth tube (Biomérieux) and subsequently incubated for 20 to 26 h at 30°C. Analysis of the second enrichment culture was performed with the VIDAS LIS method (BioMérieux), according to the manufacturer's instructions.

Salmonella spp. The presence of *Salmonella* spp. was analyzed with the iQ-Check *Salmonella* II kit (Bio-Rad, Nazareth Eke, Belgium) as described by the manufacturer. Briefly, 25 g of the fruit sample was diluted in 225 ml of buffered peptone water (BioMérieux) and homogenized using the Seward Laboratory blender 400 (UAC House). After 8 h of incubation at 37°C, 1 ml of the enriched sample was centrifuged (10,000 × *g,* 10 min, room temperature), and the supernatant was discarded. DNA was extracted by adding 200 μl of the lysis reagent followed by a short vortexing step at room temperature. Subsequently, the samples were heated for 10 min at 95 to 100°C and after a centrifugation step (10,000 × *g,* 5 min, room temperature), 5 μl of the obtained DNA suspension was used for the amplification reaction (45 μl of PCR mixture). Real-time quantification was performed on the SDS 7300 qPCR instrument (Applied Biosystems) with the following temperature protocol: 50°C for 2 min, initial denaturation and activation at 95°C for 10 min, followed by 50 cycles of amplification with denaturation at 95°C for 20 s, annealing at 55°C for 30 s, and extension for 30 s at 72°C. Amplification data were collected and analyzed with the SDS 7300 instruments' software.

***E. coli* 0157:H7.** For detection of *E. coli* 0157:H7, 25 g of the fruit sample was diluted in 225 ml of buffered peptone water (BioMérieux) and homogenized by using the Seward Laboratory blender 400 (UAC House). After 8 h of incubation at 41°C, the presence of *E. coli* O157:H7 was analyzed by using the iQ-Check *E. coli* O157:H7 kit (Bio-Rad) as described by the manufacturer. Briefly, 200 μl of the complete lysis reagent was added to 100 μl of the enriched samples followed by a short vortexing step at room temperature. Subsequently, the samples were heated for 10 min at 95 to 100°C, and after a centrifugation step (10,000 × *g,* 5 min, room temperature), 5 μl of the obtained DNA suspension was used for the amplification reaction (45 μl of PCR mixture). Real-time quantification was performed on the SDS 7300 qPCR instrument (Applied Biosystems) under the following conditions: initial denaturation and activation at 95°C for 10 min, followed by 50 cycles of amplification with denaturation at 95°C for 15 s, annealing at 58°C for 30 s, and extension for 30 s at 72°C. Amplification data were collected and analyzed with the SDS 7300 instruments' software.

RESULTS

MNV-1 controls. The recoveries of the MNV-1 PC, MNV-1 RTC, and MNV-1 IAC were analyzed both quantitatively (''recovery efficiency'') and qualitatively (''recovery success rate'') (Table 1). Qualitative analysis showed that the recovery of the MNV-1 PC was dependent on the fruit type tested: while recovery success rates of 8/10 and 19/20 were noticed in raspberries and strawberries, respectively, recovery success rates of 2/30 and 2/15 were noticed in cherry tomatoes and mixed-fruit salads, respectively. Quantitative analysis showed that the mean recovery efficiency of the successfully recovered MNV-1 PCs was similar in all tested fruit types as mean recovery efficiencies ranged between 8.38% ± 1.18% and 12.94% ± 9.33%.

Qualitative analysis of the recovery of the MNV-1 RTC and MNV-1 IAC showed that recovery success rates of 30/30, 20/20, and 15/15 were obtained in cherry tomatoes, strawberries, and fruit salads, respectively, while a recovery success rate of 9/10 in raspberries was noted. Additionally, quantitative analysis of the recovery of the MNV-1 RTC and MNV-1 IAC showed the MNV-1 RTC was recovered with mean recovery efficiencies ranging between 46.17% ± 17.70% and 63.81% ± 15.72% , while the MNV-1 IAC was recovered with mean recovery efficiencies ranging between 100.93% ± 9.55% and 119.32% ± 28.32%. The rather low recovery of the MNV-1 RTC indicated limited inhibition of the RT step in some samples.

NoV analysis: raspberries. Four of 10 raspberry samples tested positive for GI and/or GII NoV with genomic NoV levels in the positive samples ranging between 2.45 and 3.70 log per 10 g of raspberry sample. However, only one of four RT-qPCRs was positive for GI or GII NoV genomic material in these samples, except for one sample (Table 2). It should be noted that in one NoV-positive sample the MNV-1 PC could not be recovered, although the MNV-1 RTC and MNV-1 IAC did not indicate inhibition of either the RT step or qPCR in this sample. Inhibition of all RT-qPCRs was observed in another sample; therefore, no conclusions could be drawn for this sample regarding the presence or absence of NoV genomic copies.

Cherry tomatoes. Seven of 30 cherry tomato samples tested positive for GI and/or GII NoV. The genomic NoV levels detected were generally higher than those in other ~~soft red~~ fruit samples and ranged between 3.91 and 5.04 log per 10 g of cherry tomato sample. However, only one of four RT-qPCRs was positive for GI and/or GII NoV in these samples, except for a single sample (Table 2). It should be noted that the MNV-1 PC could be recovered in only one positive sample, although the MNV-1 RTC and MNV-1 IAC did not indicate inhibition of either the RT step or qPCR in all samples. A remark regarding the qPCR results of the cherry tomato samples is that a higher background fluorescence was noticed in the GI NoV and GII NoV assays within the multiplex qPCR assay than that observed with other fruit types. While this led to a shifted standard curve and thus to corresponding higher ~~Cq~~ values for positive samples, this did not interfere with the quantitative properties of the qPCR assay.

Strawberries. Six of 20 strawberry samples tested positive for GI and/or GII NoV with levels in the positive samples ranging between 2.29 and 4.10 genomic NoV copies per 10 g of strawberry sample. However, only one of four RT-qPCRs was positive for GI and/or GII NoV in all

TABLE 3. *Overview of bacteriological analysis of tested fruit samples*

Fruit type (25 g)	*N*	*Enterobacteriaceae* No. of positive samples (mean load[a])	*E. coli* No. of positive samples (mean load[a])	*Salmonella*[b]	*E. coli* O157:H7[b]	*Listeria* spp. and *L. monocytogenes*[b] No. of positive samples (specification)
Raspberries	10	2 (2.38)	0 (<1)	ND	ND	1 (*Listeria* spp.)
Cherry tomatoes	30	1 (1.51)	0 (<1)	ND	ND	ND
Strawberries	20	0 (<1)	0 (<1)	ND	ND	ND
Mixed-fruit salad	15	10 (2.88)	0 (<1)	ND	ND	3 (*Listeria* spp.)
Total	75	13 (2.70)	0 (<1)	ND	ND	4 (*Listeria* spp.)

[a] Values are expressed in log scale.
[b] ND, not detected.

C3

positive samples. It should be noted that in the single NoV-positive sample where the MNV-1 PC could not be recovered, a low recovery efficiency (21.27%) of the MNV-1 RTC was noticed, suggesting a possible inhibition of the RT.

Fruit salad samples. A single fruit salad sample of 15 tested samples tested positive for GII NoV, while no GI NoV were detected. A genomic NoV level of 4.64 log was observed in the positive sample with two of four RT-qPCRs being positive. A remark regarding the qPCR results of the fruit salad samples, similar to the cherry tomato results, is that a higher background fluorescence was noticed in the GII NoV assay within the multiplex qPCR assay than for other fruit types. While this led to a shifted standard curve and thus to corresponding higher ~~Cq~~ Cq values for positive samples, this did not interfere with the quantitative properties of the qPCR assay.

Bacteriological analysis: *Enterobacteriaceae* and *E. coli* enumeration. The presence of *Enterobacteriaceae* varied per sample type: 3 (5.0%) of 60 raspberry, cherry tomato, and strawberry samples were positive, with a mean load ranging between 1.51 and 2.38 log, while 10 (66.7%) of 15 mixed-fruit salad samples were positive with a mean load of 2.88 log (Table 3). *E. coli* was not detected in any of the samples.

***E. coli* O157, *Salmonella,* and *Listeria* spp. and *L. monocytogenes*.** Neither *E. coli* O157 nor *Salmonella* could be shown to be present in any of the tested samples, while one raspberry sample and three mixed-fruit salad samples tested positive for *Listeria* spp.

DISCUSSION

Various nonbacterial acute gastroenteritis outbreaks have been caused by intake of virally contaminated raspberries *(10, 12, 20, 30),* strawberries *(16, 31),* tomatoes *(41),* and mixed-fruit salads *(33).* In addition, a number of bacterial foodborne outbreaks have been linked to consumption of similar fruit and vegetable products *(5, 11, 13).*

In spite of these outbreaks linked to consumption of contaminated fruit products, only a number of authors have investigated the microbiological quality of these fruit products. In particular, the presence of enteric viruses in these food products has not been thoroughly investigated due to the lack of sensitive detection methods. Therefore, the present study was undertaken after the development and evaluation of a NoV detection methodology that could reliably detect 10^4 genomic copies per 10 g of fruit product *(36).* MNV-1, a cultivable NoV surrogate, was integrated in this detection methodology as full process control (MNV-1 PC), RT control (MNV-1 RTC), and ~~real-time~~ PCR (qPCR) internal amplification control (MNV-1 IAC).

The inclusion of MNV-1 in the NoV detection strategy was partially successful. While the MNV-1 RTC and IAC could successfully be recovered in 74 of 75 samples, the MNV-1 PC could only successfully be recovered in 31 of 75 samples. Quantitative analysis of the successful MNV-1 PC recoveries showed variable recovery efficiencies. It is therefore recommended that an MNV-1 PC with a higher level of genomic copies ($\geq 10^5$ genomic copies per 10 g of food product) should be used in further studies and when routinely screening fruit products for NoV in order to correctly interpret the recovery of this MNV-1 PC.

The present study showed an unexpected high prevalence of NoV detected by RT-qPCR on the tested fruit samples. In total, 18 of 75 tested fruit samples tested positive for GI and/or GII NoV, with levels between 2.5 and 5.0 log per 10 g of food product. It should be noted that maximally two of four performed qPCRs per sample gave a positive signal in samples where NoV genomic presence was detected, which can be explained by the fact that most detected NoV levels were close to the presumed detection limit of the methodology. Since the observed ~~Cq~~ Cq values of the positive samples ranged between 37 and 42, it is important to mention that all negative template controls were negative, thus excluding positive qPCR signals due to PCR contamination. Contamination-preventing measures such as the use of dedicated environmental conditions (separate working areas, UV and hypochlorite decontamination, and dedicated pipettes) and the use of uracil DNA-glycosylase containing real-time PCR mastermixes were respected at all time.

Due to the high number of qPCR-positive results, confirmation of the results was attempted by subjecting NoV-positive cDNA preparations, RNA preparations, and virus extracts to three conventional RT-PCR assays used for

genotyping NoV. Primer sets described by Vennema et al. *(38),* Kojima et al. *(19),* and Vinje et al. *(39),* targeting genotyping regions A, C, and D, respectively, were applied *(23).* However, no NoV sequences could be obtained despite intensive efforts.

In a majority of the NoV-positive samples, cloning of a (weak to very weak) PCR band of correct height failed, most likely due to insufficient material. The successfully cloned PCR bands from two cherry tomato samples and from the fruit salad sample could not confirm NoV presence by sequencing (data not shown). Most likely, the degenerated primer sets allowed aspecific amplification of genomic material of the food matrix.

It has been shown that RT-qPCR is 10^2- to 10^4-fold more sensitive than conventional RT-PCR *(6, 28),* which may explain the failed confirmation, since only 1 to 20 NoV genomic copies were detected by RT-qPCR in the cDNA of most positive samples.

Confirmation by obtaining sequences of fruits and vegetables samples that tested positive by real-time PCR has been tried by several research groups, but most of them were unsuccessful *(2, 22, 40).* A recent study investigating a cluster of NoV foodborne outbreaks was able to confirm NoV presence in raspberries by conventional RT-PCR and subsequent sequencing *(25).*

Only a limited number of authors have investigated the presence of enteric viruses on fruit products not related to foodborne outbreaks. Recently, Mattison et al. *(24)* found NoV presence in 148 of 275 tested packaged leafy greens. Similar to our results, confirmation was also difficult, although sequencing confirmed NoV presence in 16 of 148 positive samples. A similar study examining the presence of GI and GII NoV, adenoviruses, enteroviruses, and rotaviruses in irrigated vegetables was performed by Cheong et al. *(9).* However, only 2 of 30 samples (lettuce and chicory) tested positive for adenoviruses, while a single spinach sample contained adenoviruses as well as NoV.

It should be noted that the real-time PCR assay performed in the present study used primers and hydrolysis probes recommended by the ~~CEN/TC275/WG6/TAG4 workgroup,~~ which does not recommend confirmation because use of the hydrolysis probes should ensure the specific detection of NoV genomic material.

Ideally, only infectious NoV virus particles should be detected, and the use of propidium monoazide in combination with RT-qPCR has been suggested for this purpose. Although this has been successfully tested for heat-inactivated poliovirus, heat-inactivated NoV was still detectable by this approach *(29).* Another approach for the specific amplification of infectious NoV is the treatment of virus extracts with RNase, but varying results have been reported. While RNase treatment has been shown to prevent RT-PCR amplification of heat-inactivated feline calicivirus, poliovirus, and hepatitis A virus, MNV-1 and human-infective NoV could still be detected after a heat treatment and a hand sanitizer treatment *(4, 21, 27).*

Regarding the bacteriological quality of the tested fruit samples, analysis for *Enterobacteriaceae* on mixed-fruit salad samples has been performed by Abadias et al. *(1),* and a presence of 3.0 log was observed, which is similar to the results presented here. The presence of *E. coli* O157:H7 and *Salmonella* on various fruit products has been investigated by several authors, and as in the present study, no presence of this pathogen has been reported *(7, 18).* In contrast to a single study wherein the presence of *L. monocytogenes* has been reported on a strawberry sample *(18),* our results were in concordance with those of Abadias et al. *(1)* showing the absence of this pathogen.

Despite the good bacteriological quality, an unexpected high prevalence of NoV was observed by RT-qPCR in particular in raspberries, strawberries, and cherry tomatoes. However, it should clearly be noted that these positive qPCR results do not provide direct evidence for the presence of infectious NoV particles on the contaminated food products, since (q)PCR can only detect genomic material and thus cannot distinguish infectious and noninfectious NoV particles. For MNV-1, a $1{:}10^2$ ratio of infectious virus particles to genomic copies has been noticed before on an untreated MNV-1 lysate solution, while a $1{:}10^8$ ratio of the same was noticed when submitting this MNV-1 lysate to a heat treatment *(4).* Therefore, development of methods able to discriminate infectious and noninfectious NoV particles in foods may be able to clarify this matter.

In conclusion, the results of the present study show the difficulty of expressing positive (q)PCR results in terms of public health threat if no associated diseases or outbreaks are reported. Although these low NoV levels might indicate virus contamination at some point during the fresh produce chain, care should be taken before translating these results as a significant risk to public health. However, a possible risk for foodborne transmission of NoV from these food products cannot be excluded either.

ACKNOWLEDGMENTS

This work was supported by Belgian Science Policy—Science for a Sustainable Development (SSD–NORISK–SD/AF/01). The authors thank Andrew Muhame and Bram Vonck for laboratory assistance in the bacteriological analysis of the fruit samples.

REFERENCES

1. Abadias, M., J. Usall, M. Anguera, C. Solsona, and I. Vinas. 2008. Microbiological quality of fresh, minimally-processed fruit and vegetables, and sprouts from retail establishments. *Int. J. Food Microbiol.* 123:121–129.
2. Anderson, A. D., V. D. Garrett, J. Sobel, S. S. Monroe, R. L. Fankhauser, K. J. Schwab, J. S. Bresee, P. S. Mead, C. Higgins, J. Campana, and R. I. Glass. 2001. Multistate outbreak of Norwalk-like virus gastroenteritis associated with a common caterer. *Am. J. Epidemiol.* 154:1013–1019.
3. Baert, L., M. Uyttendaele, and J. Debevere. 2008. Evaluation of viral extraction methods on a broad range of Ready-To-Eat foods with conventional and real-time RT-PCR for Norovirus GII detection. *Int. J. Food Microbiol.* 123:101–108.
4. Baert, L., C. E. Wobus, E. Van Coillie, L. B. Thackray, J. Debevere, and M. Uyttendaele. 2008. Detection of murine norovirus 1 by using plaque assay, transfection assay, and real-time reverse transcription-PCR before and after heat exposure. *Appl. Environ. Microbiol.* 74: 543–546.
5. Beuchat, L. R. 1996. Pathogenic microorganisms associated with fresh produce. *J. Food Prot.* 59:204–216.
6. Beuret, C. 2004. Simultaneous detection of enteric viruses by multiplex real-time RT-PCR. *J. Virol. Methods* 115:1–8.

7. Bohaychuk, V. M., G. E. Gensler, R. K. King, K. I. Manninen, O. Sorensen, J. T. Wu, M. E. Stiles, and L. M. McMullen. 2006. Occurrence of pathogens in raw and ready-to-eat meat and poultry products collected from the retail marketplace in Edmonton, Alberta, Canada. *J. Food Prot.* 69:2176–2182.
8. Bustin, S. A., V. Benes, J. A. Garson, J. Hellemans, J. Huggett, M. Kubista, R. Mueller, T. Nolan, M. W. Pfaffl, G. L. Shipley, J. Vandesompele, and C. T. Wittwer. 2009. The MIQE guidelines: minimum information for publication of quantitative real-time PCR experiments. *Clin. Chem.* 55:611–622.
9. Cheong, S., C. Lee, S. W. Song, W. C. Choi, C. H. Lee, and S. J. Kim. 2009. Enteric viruses in raw vegetables and groundwater used for irrigation in South Korea. *Appl. Environ. Microbiol.* 75:7745–7751.
10. Cotterelle, B., C. Drougard, J. Rolland, M. Becamel, M. Boudon, S. Pinede, O. Traoré, K. Balay, P. Pothier, and E. Espié. 2009. Outbreak of norovirus infection associated with the consumption of frozen raspberries, France, March 2005. *Euro. Surveill.* 10(4):E050428.1.
11. Doyle, M. P., and M. C. Erickson. 2008. Summer meeting 2007—the problems with fresh produce: an overview. *J. Appl. Microbiol.* 105: 317–330.
12. Falkenhorst, G., L. Krusell, M. Lisby, S. B. Madsen, B. Bottiger, and K. Molbak. 2005. Imported frozen raspberries cause a series of norovirus outbreaks in Denmark, 2005. *Euro Surveill.* 10(9): E050922.2.
13. Hanning, I. B., J. D. Nutt, and S. C. Ricke. 2009. Salmonellosis outbreaks in the United States due to fresh produce: sources and potential intervention measures. *Foodborne Pathog. Dis.* 6:635–648.
14. Hedberg, C. W., K. L. MacDonald, and M. T. Osterholm. 1994. Changing epidemiology of food-borne disease—a Minnesota perspective. *Clin. Infect. Dis.* 18:671–682.
15. Hernandez, F., R. Monge, C. Jimenez, and L. Taylor. 1997. Rotavirus and hepatitis A virus in market lettuce (Latuca sativa) in Costa Rica. *Int. J. Food Microbiol.* 37:221–223.
16. Hutin, Y. J. F., V. Pool, E. H. Cramer, O. V. Nainan, J. Weth, I. T. Williams, S. T. Goldstein, K. F. Gensheimer, B. P. Bell, C. N. Shapiro, M. J. Alter, and H. S. Margolis. 1999. A multistate, foodborne outbreak of hepatitis A. *N. Engl. J. Med.* 340:595–602.
17. Joffe, M., and A. Robertson. 2001. The potential contribution of increased vegetable and fruit consumption to health gain in the European Union. *Public Health Nutr.* 4:893–901.
18. Johannessen, G. S., S. Loncarevic, and H. Kruse. 2002. Bacteriological analysis of fresh produce in Norway. *Int. J. Food Microbiol.* 77: 199–204.
19. Kojima, S., T. Kageyama, S. Fukushi, F. B. Hoshino, M. Shinohara, K. Uchida, K. Natori, N. Takeda, and K. Katayama. 2002. Genogroup-specific PCR primers for detection of Norwalk-like viruses. *J. Virol. Methods* 100:107–114.
20. Le Guyader, F. S., C. Mittelholzer, L. Haugarreau, K. O. Hedlund, R. Alsterlund, M. Pommepuy, and L. Svensson. 2004. Detection of noroviruses in raspberries associated with a gastroenteritis outbreak. *Int. J. Food Microbiol.* 97:179–186.
21. Liu, P. B., Y. W. Chien, E. Papafragkou, H. M. Hsiao, L. A. Jaykus, and C. Moe. 2009. Persistence of human noroviruses on food preparation surfaces and human hands. *Food Environ. Virol.* 1:141–147.
22. Makary, P., L. Maunula, T. Niskanen, M. Kuusi, M. Virtanen, S. Pajunen, J. Ollgren, and N. N. T. Minh. 2009. Multiple norovirus outbreaks among workplace canteen users in Finland, July 2006. *Epidemiol. Infect.* 137:402–407.
23. Mattison, K., E. Grudeski, B. Auk, H. Charest, S. J. Drews, A. Fritzinger, N. Gregoricus, S. Hayward, A. Houde, and B. E. Lee. 2009. Multicenter comparison of two norovirus ORF2-based genotyping protocols. *J. Clin. Microbiol.* 47:3927–3932.
24. Mattison, K., J. Harlow, V. Morton, A. Cook, F. Pollari, and S. Bidawid. 2010. Enteric viruses in ready-to-eat packaged leafy greens. *Emerg. Infect. Dis.* 16:1815–1817.
25. Maunula, L., M. Roivainen, M. Keranen, S. Makela, K. Soderberg, M. Summa, C. H. von Bonsdorff, M. Lappalainen, T. Korhonen, M. Kuusi, and T. Niskanen. 2009. Detection of human norovirus from frozen raspberries in a cluster of gastroenteritis outbreaks. *Euro Surveill.* 14:16–18.
26. Mukherjee, A., D. Speh, E. Dyck, and F. Diez-Gonzalez. 2004. Preharvest evaluation of coliforms, *Escherichia coli, Salmonella,* and *Escherichia coli* O157:H7 in organic and conventional produce grown by Minnesota farmers. *J. Food Prot.* 67:894–900.
27. Nuanualsuwan, S., and D. O. Cliver. 2002. Pretreatment to avoid positive RT-PCR results with inactivated viruses. *J. Virol. Methods* 104:217–225.
28. Pang, X. L., B. Lee, L. Chui, J. K. Preiksaitis, and S. S. Monroe. 2004. Evaluation and validation of real-time reverse transcription-PCR assay using the LightCycler system for detection and quantitation of norovirus. *J. Clin. Microbiol.* 42:4679–4685.
29. Parshionikar, S., I. Laseke, and G. S. Fout. 2010. Use of propidium monoazide in reverse transcriptase PCR to distinguish between infectious and noninfectious enteric viruses in water samples. *Appl. Environ. Microbiol.* 76:4318–4326.
30. Ponka, A., L. Maunula, C. H. von Bonsdorff, and O. Lyytikainen. 1999. An outbreak of calicivirus associated with consumption of frozen raspberries. *Epidemiol. Infect.* 123:469–474.
31. Rutjes, S. A., F. Lodder-Verschoor, W. H. M. van der Poel, Y. T. H. P. van Duijnhoven, and A. M. D. Husman. 2006. Detection of noroviruses in foods: a study on virus extraction procedures in foods implicated in outbreaks of human gastroenteritis. *J. Food Prot.* 69: 1949–1956.
32. Sair, A. I., D. H. D'Souza, C. L. Moe, and L. A. Jaykus. 2002. Improved detection of human enteric viruses in foods by RT-PCR. *J. Virol. Methods* 100:57–69.
33. Sivapalasingam, S., C. R. Friedman, L. Cohen, and R. V. Tauxe. 2004. Fresh produce: a growing cause of outbreaks of foodborne illness in the United States, 1973 through 1997. *J. Food Prot.* 67: 2342–2353.
34. Sosnovtsev, S. V., G. Belliot, K. O. Chang, V. G. Prikhodko, L. B. Thackray, C. E. Wobus, S. M. Karst, H. W. Virgin, and K. Y. Green. 2006. Cleavage map and proteolytic processing of the murine norovirus nonstructural polyprotein in infected cells. *J. Virol.* 80: 7816–7831.
35. Stals, A., L. Baert, N. Botteldoorn, H. Werbrouck, L. Herman, M. Uyttendaele, and E. Van Coillie. 2009. Multiplex real-time RT-PCR for simultaneous detection of GI/GII noroviruses and murine norovirus 1. *J. Virol. Methods* 161:247–253.
36. Stals, A., L. Baert, E. Van Coillie, and M. Uyttendaele. 2011. Evaluation of a norovirus detection methodology for soft red fruits. *Food Microbiol.* 28:52–58.
37. Van Duyn, M. S., and E. Pivonka. 2000. Overview of the health benefits of fruit and vegetable consumption for the dietetics professional: selected literature. *J. Am. Diet. Assoc.* 100:1511–1521.
38. Vennema, H., E. de Bruin, and M. Koopmans. 2002. Rational optimization of generic primers used for Norwalk-like virus detection by reverse transcriptase polymerase chain reaction. *J. Clin. Virol.* 25: 233–235.
39. Vinje, J., R. A. Hamidjaja, and M. D. Sobsey. 2004. Development and application of a capsid VP1 (region D) based reverse transcription PCR assay for genotyping of genogroup I and II noroviruses. *J. Virol. Methods* 116:109–117.
40. Wadl, M., K. Scherer, S. Nielsen, S. Diedrich, L. Ellerbroek, C. Frank, R. Gatzer, M. Hoehne, R. Johne, G. Klein, J. Koch, J. Schulenburg, U. Thielbein, K. Stark, and H. Bernard. 2010. Foodborne norovirus-outbreak at a military base, Germany, 2009. *BMC Infect. Dis.* 10:30.
41. Zomer, T. P., B. De Jong, S. Kühlmann-Berenzon, O. Nyrén, B. Svenungsson, K. O. Hedlund, C. Ancker, T. Wahl, and Y. Andersson. 2009. A norovirus outbreak at a manufacturing company. *Epidemiol. Infect.* 138:501–506.

Authors Queries

Journal: **Journal of Food Protection**
Paper: **food-74-03-05**
Title: **Screening of Fruit Products for Norovirus and the Difficulty of Interpreting Positive PCR Results**

Dear Author
During the preparation of your manuscript for publication, the questions listed below have arisen. Please attend to these matters and return this form with your proof. Many thanks for your assistance

Query Reference	Query	Remarks
1	Author: This article has been edited for grammar, style, and usage. Please compare it with your original document and make corrections on these pages. Please limit your corrections to substantive changes that affect meaning. If no change is required in response to a question, please write ''OK as set'' in the margin. Copy editor	
2	Author: Keywords: [norovirus presence, fruit products, detection methodology, MNV-1, positive PCR results]. Key words are used for indexing, please approve or edit as needed. Copy editor	
3	Author: References have been renumbered per style for alphabetic order; please check references and in-text citations carefully. Copy editor	Ok as set
4	Author: Please check sentence beginning with ''NoV genomic copy levels expressed in Table 2.'' If not as meant, please clarify what ''corresponding to'' refers to. Copy editor	Answer: "and correspond" was removed from this sentence
5	Author: Please check sentence beginning with ''Primer sets described by…'' to ensure that all reference citations in this sentence are correctly placed. Copy editor	Ok as set

AUTHORS: THE FOLLOWING QUERIES/COMMENTS ARE FOR EDITORIAL STAFF FROM PROOFREADERS. The editorial staff will contact you if they have any questions regarding these queries and comments.

EDITORIAL STAFF: Query markers appear in boxes in the margins as a question mark followed by a number. Please respond to each query in the margin of the corresponding proof page. Comment markers are suggested corrections that will also appear in the margin, but as a "C" followed by a number. If you wish to implement the suggested correction, please transfer the correction to the margin and text of the corresponding proof page.

C1: Authors: In author line is van set properly? Thanks PR
C2: In Table 1, please make 2nd and 3rd straddle rules lightface. PR
C3: In Table 3, in 7th column, please center 1, 3, and 4 (Listeria spp.) under head as blocked. PR